JAERI TANDEM & V.D.G.
ANNUAL REPORT
1997
(April 1, 1997 – March 31, 1998)

October 1998

Department of Materials Science

日 本 原 子 力 研 究 所
Japan Atomic Energy Research Institute

JAERI TANDEM & V.D.G.
Annual Report
1997
April 1, 1997 – March 31, 1998

Department of Materials Science※

Tokai Research Establishment
Japan Atomic Energy Research Institute
Tokai-mura, Naka-gun, Ibaraki-ken

This annual report describes research activities which have been performed with the JAERI tandem accelerator and the Van de Graaff accelerator from April 1, 1997 to March 31, 1998. Summary reports of 40 papers, and lists of publication, personnel and cooperative researches with universities are contained.

※Editors: Suehiro TAKEUCHI, Hiroshi IKEZOE, Satoshi CHIBA, Masao SATAKA, Yuichiro NAGAME, Satoshi TAKEMORI and Akira IWAMOTO

原研タンデム、バンデグラフ加速器
１９９７年度年次報告

日本原子力研究所東海研究所
物質科学研究部※

　本年次報告書は、東海研の原研タンデム及びバンデグラフ加速器で、１９９７年４月１日から１９９８年３月３１日までの間に行われた研究活動をとりまとめたものである。
　(1) 加速器の運転と開発研究　(2) 核構造　(3) 核反応　(4) 核理論　(5)原子分子物理・固体物理及び材料の放射線効果の５部門にまたがる ４０編の研究報告、公表された文献、関与した職員及び大学等との協力研究のリストを収録している。
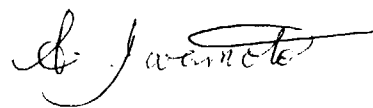
東海研究所：〒319-1195　茨城県那珂郡東海村白方白根２－４
※（編集者）竹内末広・池添　博・千葉　敏・左高正雄・永目論一郎
　　　　　　竹森聡司・岩本　昭

PREFACE

This report covers research and development activities using the tandem accelerator and its superconducting booster at JAERI, Tokai, for the period from April 1, 1997 to March 31, 1998. During this period, the tandem accelerator was operated over 4,300 hours and delivered stable beams to the experiments in the fields of accelerator developments, nuclear structure, nuclear reactions, atomic physics, solid state physics and radiation effects in materials. The superconducting booster was utilized for 36 days on 12 experimental subjects. Fourteen research programs have been carried out in collaborations with a hundred researchers from universities and national research institutes.

A compact electron cyclotron resonance (ECR) ion source was installed in the high voltage terminal of the tandem accelerator in place of the duoplasmatron ion source at the end of FY 1997. The ECR ion source makes it possible to use noble gas ions like Xe and also metallic ions like Pb in the tandem accelerator with enough intensities and energies and to inject these beams into the booster.

By utilizing an array of gamma-ray anti-Compton detectors, experiments on nuclear structure study of high spin states in A=130 and 160 regions have been performed with emphasis on their electromagnetic properties. Further development of the detector system is underway to facilitate more efficient spectroscopic studies.

Akira Iwamoto
Deputy Director
Department of Materials Science

This is a blank page.

Contents

This is a blank page.

1. Accelerator Operation and Development

This is a blank page.

1.1 TANDEM ACCELERATOR AND BOOSTER OPERATION

ACCELERATORS OPERATION GROUP

<u>Tandem Accelerator and Booster</u>: The operations of the tandem accelerator for experiments were performed as scheduled in the past one year. There were three short periods of scheduled maintenance. The running time was 4277 hours. The summary of the operation from April 1, 1997 to March 31, 1998 is as follows.

1) Time distribution in terms of terminal voltages (Tandem accelerator)

>16 MV	30 days	16.4 %
15-16	91	49.7
14-15	28	15.3
13-14	2	1.1
12-13	0	0
11-12	8	4.4
10-11	17	9.3
9-10	2	1.1
8-9	2	1.1
<8	3	1.8

Booster operation

^{58}Ni	270-290 MeV	6 days
^{76}Ge	635	9
^{82}Se	730	4
^{90}Zr	360-390	5
^{127}I	580-600	9
^{197}Au	823	3

The tandem accelerator had an unexpected tank opening at the middle of November due to a trouble of the cotrol system in a shorted section. After 4 days long cancellation of the scheduled-experiments, the accelerator was operated until 13th in February 1998 except year-end holidays. The tandem booster and its helium refrigeration systems were operated 3 periods during 2 scheduled machine time periods. At the time of holidays, the helium refrigerators were stopped for 4 weeks to keep the safety and save the power.

The helium refrigeration systems were in operation for 70 days from June 30, 58 days from October 27 and 26 days from January 19 in 1998. During these times, the super-conducting booster was utilized for 36 days for 12 experimental subjects. The booster ran steadily at field gradients between 3MV/m and 4.5MV/m.

1.2 UTILIZATION OF TANDEM ACCELERATOR AND BOOSTER

T. YOSHIDA and S. KANDA

The utilization of the tandem accelerator facility was carried out for 183 days for various experiments in two scheduled machine times in the 1997 fiscal year(FY). The collaboration research system between JAERI and universities had been handed over to the division of Office of Planning in JAERI from Research Center for Nuclear Science and Technology in University of Tokyo from the 1997 FY. Research programs are determined by the 2 program advisory committee, Nuclear physics and Nuclear chemistry committee and Atomic and Solid-state physics committee once a year. The collaboration research programs for the 1997 FY were examined at late November in 1996, and the 8 and 6 subjects were accepted by the respective committees. These programs accounted for approximately 75% of the whole machine time. Fifteen ion species were utilized in the 2 experimental periods as follows.

1) Time distribution in terms of projectile

^{1}H(^{2}H)	7 days	^{63}Cu	2 days
^{6,7}Li	24	^{76}Ge	9
^{12,13}C	7	^{82}Se	7
^{16,18}O	2	^{90}Zr	6
^{28,30}Si	24	^{107}Ag	2
^{32,33}S	22	^{127}I	16
^{35,37}Cl	8	^{197}Au	19
^{58,60}Ni	30		

The experimental terms allotted in the three periods were 10 days in April 1 to April 10, 82 days in June 2 to September 4 and 91 days in October 13 to February 13 in 1998. The first term was extended from the last term of the 1996 FY. The summary of allotted time to various experimental subjects is as follows. The number of subjects were 5 subjects for the extended period, 22 subjects for the 1st period and 25 subjects for the 2nd period.

Research field	allotted days	total number of subjects
Nuclear physics	123	36
Atomic and Solid-state physics	39	33
Nuclear chemistry	14	3
Material research	5	4
Detector development	2	2

1.3 STATUS OF THE SUPERCONDUCTING BOOSTER

S. TAKEUCHI, M. MATSUDA, N. ISHIZAKI, H. TAYAMA and I. OHUCHI

The superconducting booster for the JAERI tandem accelerator was running as well without troubles as before, in the FY of 1997. Total beam time of energy boosting for user's experiments was 36 days, which corresponded to about 20 % of the whole beam time of the tandem accelerator. Accelerated ions are shown in Table 1. The booster played an additional role of a beam transport line without acceleration to the booster target room for 49 days.

Table 1. Accelerated ions in the FY of 1997

Ion	Beam time(day)	Energy in/out(MeV)	Field Gradient(MV/m)
$^{58}Ni^{11+,13+}$	6	180-215 / 270-290	3.0-3.7
$^{76}Ge^{22+}$	9	195 / 635	3.8-4.0
$^{82}Se^{24+}$	4	195 / 750	3.2-5.4
$^{90}Zr^{12+}$	5	205 / 260-390	3.8-3.9
$^{127}I^{28+}$	9	205 / 580-630	3.0-4.0
$^{197}Au^{25+}$	3	340 / 823-900	3.3-5.6

Out-of-phase-lock still occasionally happened to several resonators. The problem was settled mainly by re-tuning the resonator control circuits. We were, however, partly concerned with a resonator problem such as a momentary growth of electron field emission or frequency instability due to a helium pressure change. Another significant problem was the weak and unstable beam intensity for very heavy ions. This problem was due to foil strippers which were very short lived against very heavy ions. As a solution for it, we have a plan of using an ECR ion source in the high voltage terminal to directly accelerate highly charged positive ions with high intensity. The installation work was being carried out at the end of the FY 1997 and should be reported elsewhere in this annual report.

The booster includes some resonators, in the first four cryo-modules, suffering from Q-*disease*(resonator Q degradation due to an increase of RF surface resistance with niobium hydride precipitation). It is effective in recovering high Q values to precool the resonators fast over the precipitation temperature zone of 130K to 90K. A three step sequential precooling was carried out in the last FY 1996. And, the average cooling rate was increased to 28.5 K/h from 12K/h of the normal case. There was a Q recovery to 74% of the values obtained from the off-line resonator testing. This method was applied to the resonators in the FY 1997 also when high acceleration voltages were required during the operation period. Figure 1 shows Q values measured in July 1997 as well as in June 1995 and in the off-line tests done before 1993. Field gradients measured at RF input of 4 W in July, 1997 are shown in Fig. 2. Their average, 5.4 MV/m, is satisfactorily high.
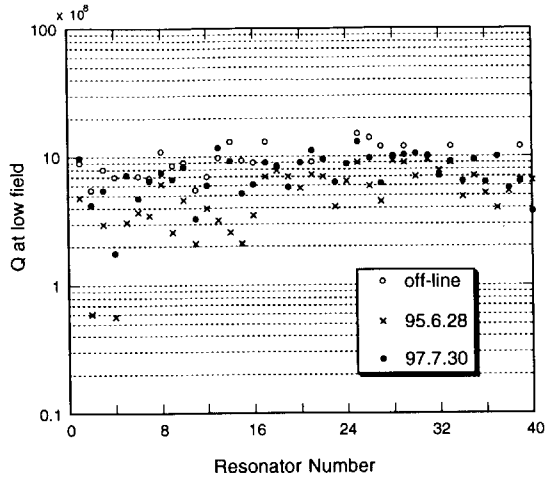
Fig.1. Q values measured at low fields
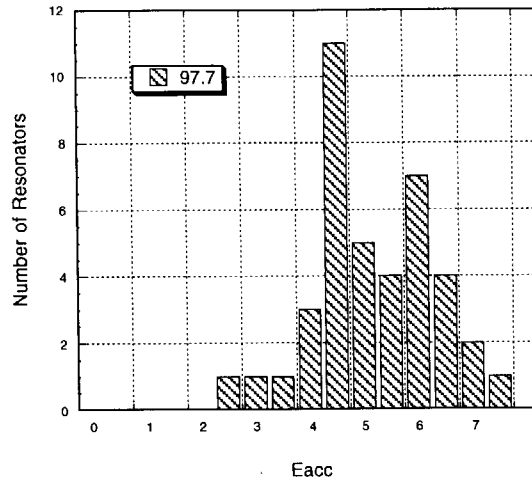
Fig.2. Histogram of resonator field gradients at the RF input of 4 W (July, 1997).

The ideal method of curing the Q-disease is to extract hydrogen out of the niobium. High temperature heat treatment in a vacuum furnace is, however, not applicable to the resonators of which outer cans are made of niobium-clad copper. All our trials to extract hydrogen from hydrogen polluted niobium without heating have resulted in no effect. In the FY 1997, we tried to heat only the center conductor part, which is purely made of niobium, to about 600 C in vacuum without heating the outer can, using a spare resonators and setting a 1.5 kW heater inside the center conductor. The Q was recovered from 13 % to 30% for the condition of a slow precooling(10-12K/h) over the precipitation zone. The accelerating field gradient at an rf input of 4 watts was increased from 2.7 MV/m to 4.0 MV/m. This partial outgassing method can be effective on the resonators heavily polluted with hydrogen.

RF power amplifiers were moved from the RF control room to the sides of the cryomodules. Forwarding RF power into every resonator was increased a lot by the tune-up from 100 watts to 150 watts done before and shortening the rf power cable done this time. As an additional benefit, phonic noise from the amplifier's electric cooling fans vanished from the RF control room where operators worked.

The cryogenic system and RF control stations were routinely cared and running well. The helium compressors were overhauled. There were no serious troubles to report. A satellite control station of the tandem accelerator developed by S. Hanashima was placed next to the resonator control stations. It now allows us to control all accelerator components from the RF control room.

1.4 STUDY OF ACCELERATION
OVER THE TRANSITION VELOCITY

S. TAKEUCHI

The superconducting quarter wave resonators used in the tandem booster linac have two acceleration gaps and can accelerate heavy ions over a wide range of incident velocity grater than 0.05c. The transit time factor that characterizes the acceleration efficiency for different incident velocities crosses zero at the velocity of 0.05c and has a small negative peak below the velocity(Fig.1). The negative peak implies that an acceleration can take place if the synchronous phase is reversed. It is interesting to know whether it is possible to accelerate ions over the zero-cross-point of the transit time factor. This work showed that it is theoretically possible.

The energy gain from a resonator is usually given as

$$\Delta E = q\, E_{acc}\, L\, TTF(\beta)\, \cos \phi_s$$

where q is the charge state of incident ions, E_{acc} the mean field gradient in the resonator, L the acceleration length, TTF the transit time factor, β the beam velocity and ϕ_s the synchronous phase. This formula is valid only for the case that velocity changes in the resonator are negligible. For the present case, it is quite necessary to take into account of the velocity changes, because acceleration and deceleration take place alternatively in the alternating electric field although the resultant velocity change after the resonator is very small.

Fig.1. Transit time factor of a $\beta_{opt} = 0.1$ quarter wave resonator.

The calculation was carried out by solving the equation of motion using the Runge-Kutta method. In the calculation, Cl^{10+} ions and the shape of the quarter wave resonators of $b_{opt}=0.1$ in the JAERI Tandem Superconducting Booster were chosen.

In Fig. 2, velocity increases/decreases from several incident velocities calculated for a field gradient of 5 MV/m are shown as a function of synchronous phase. The transition velocities that give no energy gain were found to move up in the negative side of synchronous phases and to move down in the positive side.   One finds phases giving small velocity increases not only in the normal acceleration phase span between -90 and +90 but also in the normal deceleration phase span between +90 and -90 through ±180. And one can see that an acceleration over the transition zone is possible if we take a path on velocity increasing phases as shown by arrows in the figure. Figure 3 presents the energy growth as well as energy gains calculated for an acceleration of Cl^{10+} (30MeV) by 40 resonators with a field gradient of 5MV/m. In the JAERI Tandem Booster, this unusual acceleration mode is not necessary for medium heavy ions like Cl but potentially worth applying for very heavy ions like Pb or Bi of which injection velocities are lower than 0.05c in the normal accelerating mode of the tandem accelerator with single stage electron stripping at the terminal. A result of calculation for Bi^{36+} is shown in Fig. 4.

Fig. 2. Velocity increases/decreases of Cl^{10+}
ions as a function of synchronous
phase from several injection
velocities. Thick arrows indicate the
accelerations on the path taken in the
calculation of Fig.3.
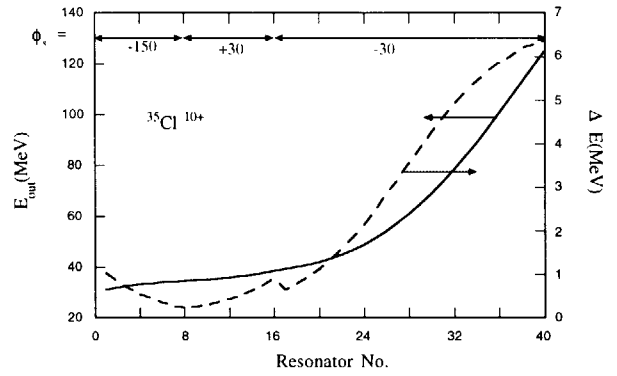
Fig.3. Energy growth(solid) and energy gain
(broken) of Cl^{10+} as a function of
resonator number.
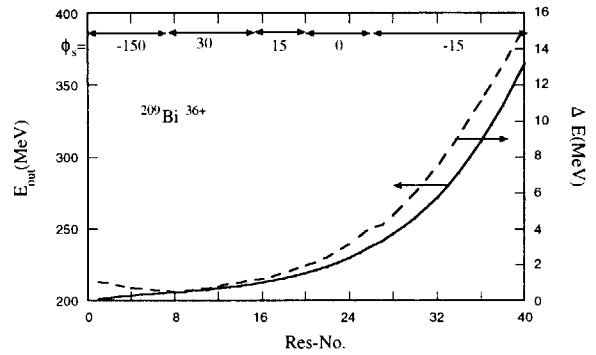
Fig. 4. Energy growth(solid) and energy gain
(broken) of Bi^{36+} as a function of
resonator number.

1.5 CONTROL SYSTEM FOR THE JAERI TANDEM ACCELERATOR

S.HANASHIMA

JAERI tandem accelerator facility has several bending magnets in its beam lines. They were activated by current stabilized sources. There is a problem in such a magnet system, that the field is not uniquely defined by the current, because there are hysteresis and temperature instability of the magnet yoke. Usually we precisely measure the field by an NMR field meter. In the present fiscal year, we have introduced field feedback control systems to two of the bending magnets. Figure 1 shows a configuration of the system. The magnetic field is measured by an NMR field meter. The device controller reads the field value through a GPIB bus and uses the value to correct the field to a target value. It controls a current power source through 18-bit DAC. The device controller is a subsystem of the tandem control system[1,2,3] and the control system handles the subsystem like other devices of the accelerator.

Figure 2 shows a basic concept of the feedback control. There are two signal paths controlling the current power source. The one is an open loop control path from the target field value. The target value from the upstream of the control system is converted to an approximated value of current associated to the target field value. And it is fed forward to the current source setting. The other is a field feedback path, which corrects the generated field to the target value. The difference between the target value and the measured value is fed to a loop filter. The filter is an integral type low pass filter modified to limit both output value and a through rate. When the target value is changed, contribution from the open loop control changes immediately. In the case of the field measurement failures, the amount of correction from the feedback loop is maintained until newly measured field value is obtained or some timeout period has elapsed. This two-path scheme enables both rapid response to a large change of the target value and keeping lock-in condition of the NMR

Fig.1 : A configuration of field feedback control system.
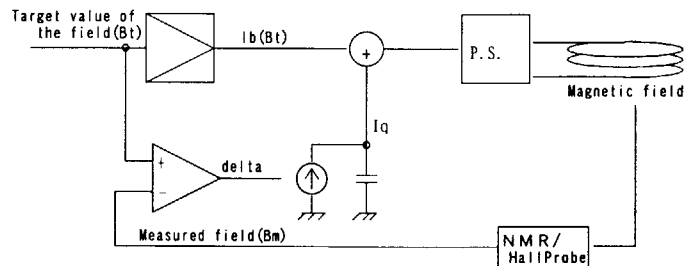
Fig.2 : A scheme of field control

signal in case of small change. The filter operation is made by a software of the device controller. The NMR field meter measures the field in every 0.5S. But the filter calculation is made in every 3.2 mS. The stability and the accuracy of the field are very good after some settling time.

In actual operation of the system, we have recognized a few points to be improved. The first point is that a break of NMR locking in condition causes disorder of the system response in the manual beam tuning. The second is a delay of the locking in, near the field regions where ranges of the field meter are switched. The last is that interference appears infrequently between the field control and a control of a slide transformer in the power source. We intend to improve the above points and to apply the system to the other bending magnets in the accelerator system.

References
1)Hanashima S.: JAERI TANDEM & V.D.G. Annual Report 1993 pp7-8.
2)Hanashima S. et al.: Transputer/Occam Japan 5 IOS Press,   1993 pp69-81.
3)Hanashima S.: JAERI TANDEM & V.D.G. Annual Report 1996 pp9.

1.6 INSTALLATION OF ECR ION SOURCE INTO THE TANDEM ACCELERATOR

M. MATSUDA, S. TAKEUCHI and C. KOBAYASHI*

We have been pushing a plan to install a compact ECR ion source in the high voltage terminal of the tandem accelerator in order to increase beam intensity, beam energy and beam species. Since the ion source is placed in the severe environment; i.e. in the high pressure gas and under attack from occasional electric discharges in the accelerator, we made conceivable preparation. We experimentally accumulated operational data on the ion source and found optimum operational conditions. Some less sensitive parameters can be fixed at optimum conditions to reduce the remote-control parameters to the least and to increase the operational safety. After high pressure tests of various devices and the development of the injection system, the ion source was finally set in the tandem accelerator during the regular maintenance period starting from February.

Since the tandem accelerator is tightly scheduled to supply ion beams to the users, we have to keep damage to the main accelerator system minimum if some troubles occurred in the ECR ion source or the injection system; especially, we should avoid fatal damage that result in opening the high pressure vessel in the period of scheduled machine time. For this reason, the simplest injection system of the ion source with a minimum function was initially set, and further improvement of the performance will be made at a next step after confirming the reliability of the injection system. With regard to the ECR ion source, only three parameters were included in the operational system, which were opening and closing of a gas valve, bias voltage and RF power. Although the adjustment of the flow of the source gas is quite important to supply highly charged and intense beams, a constant leak source was used. This method was quite effective for easy handling.
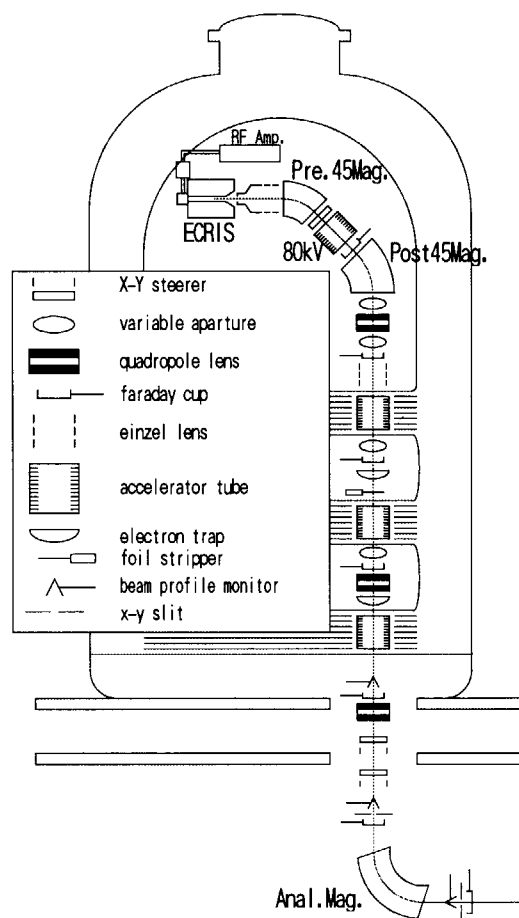
Fig. 1. Terminal ion source handling system

---

* Nihon Advanced Technology. Co.

The beam handling system of the terminal ion injector is shown in Fig.1. The ion beams are extracted by a 30 kV(max) potential gap from the ion source, focused by an Einzel lens, and then the mass and charge of them are roughly selected by the 45° pre-analyzing magnet. The pre-analyzing magnet is used to reduce the load to pre-acceleration tube, since the beams from the ion source amount to 2mA. The horizontal beam direction is corrected by an electrostatic steerer placed just after the analyzing magnet. After an acceleration by an 80kV pre-acceleration tube, desired ions are selected by the 45° post-analyzing magnet. Finally ion beams are focused by an electrostatic quadrupole triplet lens, and injected into the main acceleration tube.

Power supplies and the control circuits of the terminal injector system are grounded to the terminal electric potential(0kV Deck) or high voltage deck(80 and 110kV Deck). The source gas control circuit and bias power supply are mounted in the 110kV Deck, and the 30kV power supply for extraction, Einzel lens, 45° pre-analyzing magnet and steerer are set in 80kV Deck. All devices in the high voltage deck are controlled in communication with the 0kV Deck using the light-link system and electric power is provided by an insulating transformer. The RF generator, the 45° post-analyzing magnet, cooling system, 80kV high voltage power supply for pre-acceleration and communication circuits for the control are installed in the 0kV Deck.

The installation of the ECR ion source was carried out in the period of the regular maintenance of the tandem accelerator starting from the middle of February in 1998. The ECR ion source, beam line components, their control circuits, power supplies, RF generator and cooling systems were installed and the data to the ACCELL (the control system of the tandem accelerator) were amended. Large devices were brought in through the top hatch by crane. The construction work was done as previously scheduled. The final configuration of the equipment is shown in Fig.2.

① ECR "NANOGAN"
② einzel lens
③ 45° pre-magnet & probe
④ x-steerer
⑤ lens & pre-acc. tube
⑥ faraday cup
⑦ ion pump
⑧ 45° magnet & probe
⑨ electric quadropole

1000mm

acc. tube
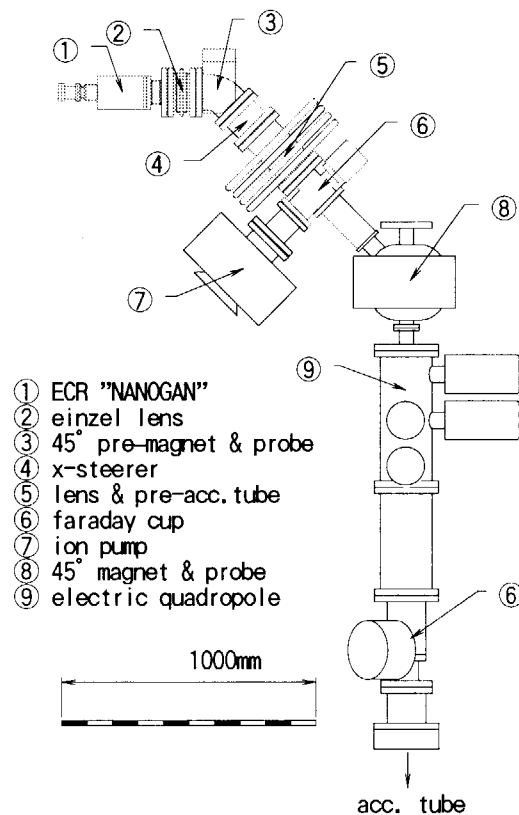
Fig.2. Installation arrangement of the ECR ion source

Although all devices worked well in the beam extraction test under atmospheric pressure, some troubles were found in the power supplies, which were due to pressurized insulating gas and electric discharges, in the actual operation of the tandem accelerator. Some filters were not effective against electric surges. The power supplies were replaced or repaired twice opening the high pressure vessel. At the end of this installation period, H^+ and Ar^{8+} beams could be accelerated at a terminal voltage of 13MV and reached to the Faraday cup after the analyzing magnet of the tandem accelerator. In this experiment, the beams of Ar^{8+} and N^{3+} which were closed in magnetic rigidity were perfectly resolved at the entrance of the acceleration tube of the tandem accelerator. This is the first successful experiment in the world with use of an ECR ion source as a terminal ion source in a tandem accelerator. The loading in the acceleration tube due to large emittance, which is initially considered to be a serious problem, was solved by the insertion of several apertures in the injector beam line.

In the next step, the troubles by the high pressure gas and electric discharges will be studied and solved, and we will obtain much improved performance of Ar ion acceleration from the in-terminal ECR ion source.

Reference
[1] P. Sortais et al., Proc. 12th Int. Workshop on ECR ion sources, RIKEN, 1995, p.44.
[2] D. K. Olsen et al., Proc. 10th Int. Workshop on ECR ion sources, Oak Ridge, 1990, p.1.

2. Nuclear Structure

This is a blank page.

2.1 BETA-DECAY HALF-LIFE OF THE NEW ISOTOPE ^{167}Tb

M. ASAI, S. ICHIKAWA, K. TSUKADA, M. SAKAMA[1], Y. KOJIMA[2],
T. HIROSE[2], M. SHIBATA[2], A. OSA, I. NISHINAKA, Y. NAGAME,
Y. HATSUKAWA, N. SHINOHARA and K. KAWADE[2]

Beta-decay half-lives of neutron-rich nuclei are important in astrophysical calculations for nucleosyntheses through the rapid neutron capture process. Previously, we determined β-decay half-lives of new neutron-rich isotopes ^{161}Sm, ^{165}Gd and ^{166}Tb [1,2], and found that the experimental half-lives were systematically shorter than those of theoretical calculations. Especially, the calculated half-lives for ^{166}Tb were 4-8 times longer than the experimental one. In the present work, a more neutron-rich nucleus ^{167}Tb has been identified for the first time. The experimental half-lives of ^{166}Tb and ^{167}Tb are compared with those of the recent calculations by the gross theory with new one-particle strength function (GT2-1996) [3].

The ^{167}Tb nuclei were produced through proton-induced fissions of ^{238}U. A stack of eight ^{238}U targets was bombarded with a 20 MeV proton beam of about 1 μA intensity. Each target was electrodeposited with a thickness of about 4 mg/cm^2 on an aluminum-foil backing. Fission products emitted from the targets were thermalized in Ar gas loaded with PbI$_2$ aerosols, then transported into an ion source of an isotope separator on-line through a capillary. The ^{167}Tb nuclei were ionized and mass-separated as monoxide ions. Details of the system are described in Ref. [4]. The mass-separated ions of interest were collected on an aluminum-coated Mylar tape in a tape transport system, and periodically transported to a measuring position. The measuring position was equipped with a sandwich-type plastic scintillator, a semi-planar n-type HPGe detector and a 35% coaxial n-type HPGe detector. Gamma-ray singles, β-γ and γ-γ coincidence measurements were performed.

Figure 1 shows a β-coincident γ-ray spectrum obtained at the mass 167+16 fraction. Dy KX rays originating from the β^- decay of ^{167}Tb were clearly observed. From the decay of Dy K$_\alpha$X and K$_{\beta_1}$X-ray counts, the half-life of the ^{167}Tb was determined to be 19.4(27) s.

In Table 1, the experimental half-lives of ^{166}Tb and ^{167}Tb are compared with theoretical ones by the new and old calculations of the gross theory (GT2-1996, GT2-1992 [5]) and by the proton-neutron quasiparticle random-phase approximation (pn-QRPA) [6] using three different input data of Q_β value and deformation. The calculated half-lives by the GT2-1992 and pn-QRPA for ^{167}Tb are 3-7 times longer than the experimental one, like the case for ^{166}Tb. On the other hand, the calculated half-lives by the GT2-1996 for both ^{166}Tb and ^{167}Tb were greatly improved, and showed good agreements with the experimental ones.

[1]Department of Chemistry, Tokyo Metropolitan University
[2]Department of Energy Engineering and Science, Nagoya University

Table 1. Comparison between measured and calculated half-lives of ^{166}Tb and ^{167}Tb.

	Half-life [s]		(Calc./Exp.)	
	^{166}Tb		^{167}Tb	
Experimental	21 ± 6		19.4 ± 2.7	
GT2-1996	33.6	(1.60)	18.2	(0.94)
GT2-1992	114	(5.43)	82.6	(4.26)
pn-QRPA	83.7	(3.99)	67.3	(3.47)
	166	(7.90)	130	(6.70)
	82.8	(3.94)	63.0	(3.25)
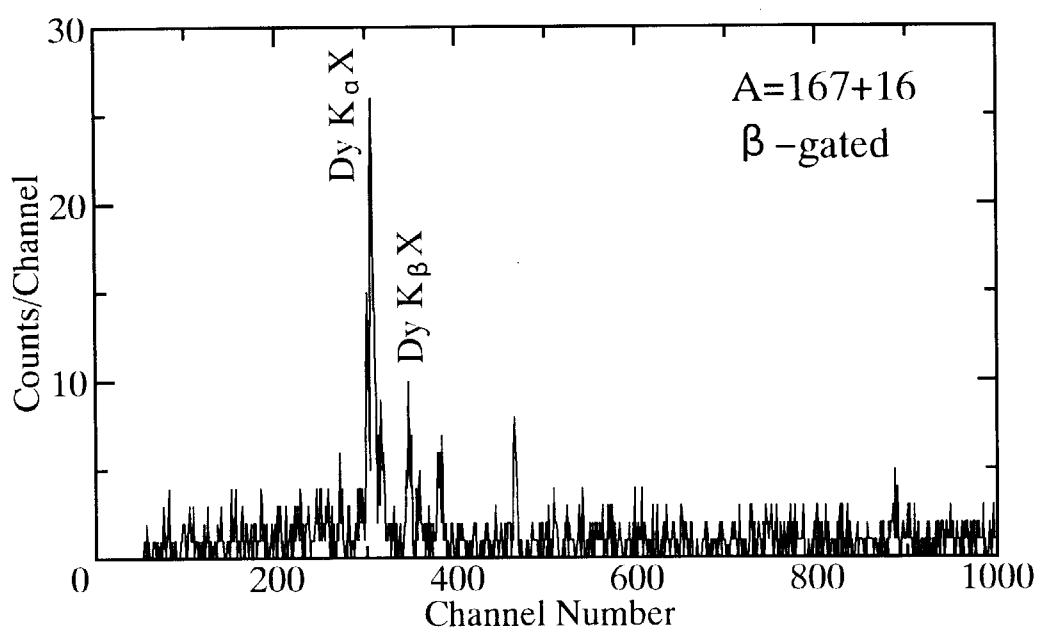
Fig. 1. Beta-coincident γ-ray spectrum obtained at the mass-183 fraction.

References

1) M. Asai, K. Tsukada, S. Ichikawa, A. Osa, Y. Kojima, M. Shibata, H. Yamamoto, K. Kawade, N. Shinohara, Y. Nagame, H. Iimura, Y. Hatsukawa and I. Nishinaka, J. Phys. Soc. Jpn. **65** (1996) 1135.

2) S. Ichikawa, K. Tsukada, M. Asai, A. Osa, Y. Kojima, T. Hirose, Y. Oura, M. Shibata, I. Nishinaka, Y. Hatsukawa, H. Iimura, K. Hata, Y. Nagame and K. Kawade, JAERI-Review 97-010 (1997) 44.

3) T. Tachibana and M. Yamada, ENAM 95 (Editions Frontières, Gif-sur-Yvette, 1995) p. 763.

4) S. Ichikawa, M. Asai, K. Tsukada, A. Osa, T. Ikuta, N. Shinohara, H. Iimura, Y. Nagame, Y. Hatsukawa, I. Nishinaka, K. Kawade, H. Yamamoto, M. Shibata and Y. Kojima, Nucl. Instrum. Methods A **374** (1996) 330.

5) T. Tachibana, M. Yamada and Y. Yoshida, Prog. Theor. Phys. **84** (1990) 641.

6) A. Staudt, E. Bender, K. Muto and H. V. Klapdor-Kleingrothaus, At. Data Nucl. Data Tables **44** (1990) 79.

2.2 NEW NEUTRON DEFICIENT ISOTOPE ^{206}Ac

J. LU[1], H. IKEZOE[1], T. IKUTA[1], S. MITSUOKA[1], T. KUZUMAKI[1],
Y. NAGAME[1], I. NISHINAKA[1], K. TSUKADA[1], T. OHTSUKI [2]

An effort to study the most neutron deficient ^{206}Ac isotope was carried out with the recoil mass separator (RMS) at Japan Atomic Energy Research Institute (JAERI)[1]. The effective energy of ^{35}Cl^{11+} beam at half-target-thickness was 186 MeV which coincided with the maximum cross section of $5n$ de- excitation channels according to HIVAP calculation [2]. The 307 $\mu g/cm^2$ thick hafnium target sputtered on a 1.5 μm aluminum foil had an isotopic composition of 64.6% ^{176}Hf, 21.7% ^{177}Hf, 6.8% ^{178}Hf, 2.2% ^{179}Hf and 4.7% ^{180}Hf. The typical beam intensity was about 600 enA and the irradiation time was 47 hours.

A detail analysis of the time and position correlated series of events was performed in the present study. Four quadruple events (evaporation residue ER-α1-α2-α3) were attributed to new activeties. Two of α2 and other two α3 escaped before it deposited its full energy in the PSSD. Another one triple event (ER-α1-α2) was also recorded as the same activity. An α spectrum obtained in this study was shown in fig. 1. The measured half life and α-particle energy with estimated error limits are $(0.8^{+0.7}_{-0.3})$ s and (7183 ± 50) keV for daughter decay and $(6.8^{+3.2}_{-2.3})$ s and (6742 ± 50) keV for granddaughter decay. The values of these pairs corresponded to the α decay of ^{202}Fr with (0.34 ± 0.04) s and (7237 ± 8) keV and ^{198}At nuclide with (4.2 ± 0.3) s and (6755 ± 4) keV [3], respectively. The daughter and granddaughter decays can be unambiguously assigned to ^{202}Fr and ^{198}At. Based on these facts, the parent activity is identified as the decay of ^{206}Ac with an α energy (7894 ± 50) keV and half life (11^{+9}_{-3}) ms. The α energy difference between the present data and that (7790 ± 30) keV (or 7750 ± 20 keV) of α decay from $J^\pi=3^+$ (or 10^-) isomeric level reported in [4] is obviously out of error limits. Therefore, the activity must come from a decay of new isomeric level of ^{206}Ac.
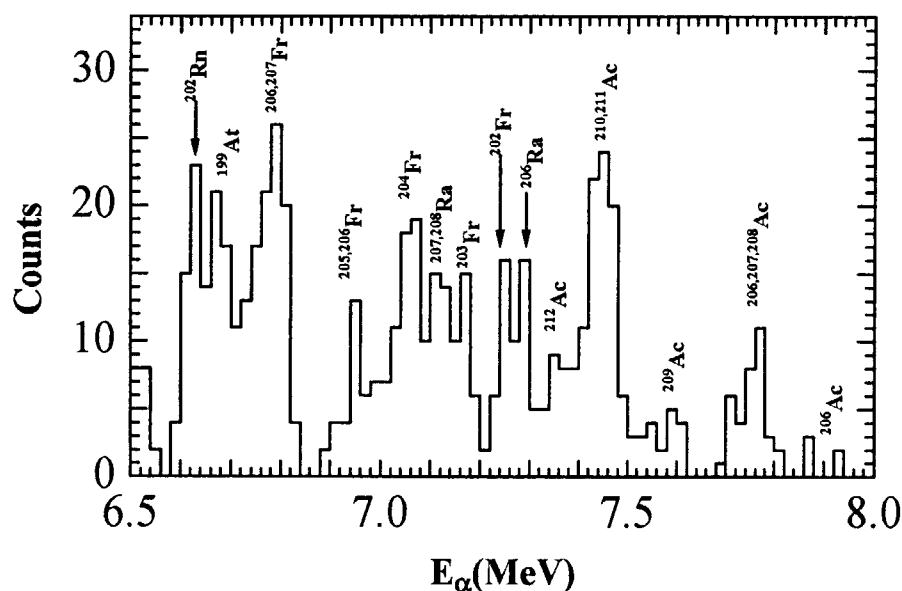

Fig. 1. α energy spectrum accumulated in the ^{35}Cl + ^{176,177}Hf reaction at 192MeV. Only the prominent α peaks were assigned to known activities.

[1] Japan Atomic Energy Research Institute, Tokai-mura, Naka-gun, Ibaraki-ken, 319-1195 Japan
[2] Laboratory of Nuclear Science, Tohoku University, Japan

Table 1. α energies and half lives of ^{206,207,208}Ac and corresponding reported values.

Nuclide	Reaction Channel	E_α (keV)	$T_{1/2}$ (ms)	E_α (keV)	$T_{1/2}$ (ms) Literature	J^π	Ref.
^{206}Ac	5n	7894±50	11^{+9}_{-3}				
		7772±50	46^{+62}_{-17}	7790±30	22^{+9}_{-5}	3^+	[4]
				7750±20	33^{+22}_{-9}	10^-	[4]
^{207}Ac	4, 5n	7734±50	65^{+32}_{-16}	7693±25	27^{+11}_{-6}		[4]
^{208}Ac	4, 5n	7747±40	82^{+47}_{-15}	7758±20	25^{+9}_{-5}	10^-	[5]
		7562±50	199^{+121}_{-55}	7572±15	95^{+24}_{-16}	3^+	[5]

Three triple events were observed. The parent nuclide decayed with an energy of (7772±50) keV and a half life of (46^{+62}_{-17}) ms. The last α-decay had an average energy of 6760 keV. The parent decay properties are in agreement with the decay behavior from 3^+ isomeric level reported in reference [4]. The last α energy is identical with the literature value (6755±4) keV of $J^\pi=3^+$ isomeric level decay in ^{198}At. These facts suggest that these triple events would be the 3^+ isomeric level decay of ^{206}Ac with the daughter α decay undetected.

Four position and time correlated chains of ER-α1-α2-α3 type were collected with one of the third α escaping. Other 17 events of ER-α1-α2 type were sorted into the same activities as the previous 4 events. The average α particle energies and half lives for the three members of the series are α1 (7747±40) keV and (82^{+47}_{-15}) ms; α2 (7051±30) keV and ($2.8^{+1.6}_{-0.5}$) s and α3 (6465±50) keV and (18^{+18}_{-6}) s. The reported values for ^{204}Fr $J^\pi=10^-$ isomeric decay are (7013±5) keV and $\simeq$1.0 s and for $J^\pi=7^+$ isomeric level in ^{200}At (6414±2) keV and (47±1) s [3]. The daughter and granddaughter decays can be unambiguously assigned to ^{204}Fr of J^π 10^- isomeric level and $J^\pi=7^+$ ^{200}At isomer. Based on the fact, the parent activity is assigned to ^{208}Ac. According to the evidence reported in [3], that $J^\pi=10^-$ isomer of ^{200}At mostly decays by E3 internal transition ($\sim$80% [6]) to $J^\pi=7^+$ isomer and then it decays by α emission to ^{196}Bi $J^\pi=7^+$ isomer, the α decay scheme for the quadruple chain is then determined as ^{208}Ac($J^\pi=10^-$)$\xrightarrow{\alpha1}{}^{204}$Fr($J^\pi=10^-$)$\xrightarrow{\alpha2}{}^{200}$At($J^\pi=10^-\xrightarrow{E3\gamma}7^+$)$\xrightarrow{\alpha3}{}^{196}$Bi($J^\pi=7^+$).

The experimental data for the newly found activities and other decays in ^{35}Cl + ^{176,177}Hf reaction are summarized in table 1 together with the available reported values. The overall producing cross section for ^{206}Ac is estimated to be $\sim$27 nb by assuming the calculated transmission efficiency of JAERI-RMS 7 %.

References
1) H. Ikezoe, Y. Nagame, T. Ikuta, S. Hamada, I. Nishinaka, and T. Ohtsuki, Nucl. Instr. and Meth. 376, 420 (1996).
2) W. Reisdorf, M. Schädel, Z. Phys. 343, 47 (1992).
3) M. Huyse, P. Decrock, P. Dendooven, G. Reusen, P. Van Duppen, and J. Wauters, Phys. Rev. C46, 1209 (1992), and references therein.
4) K. Eskola, P. Kuusiniemi, M. Leino, J. F. C. Cocks, T. Enqvistetal., Phys. Rev. C57, 417 (1998).
5) M. Leino, J. Uusitalo, T. Enqvist, K. Eskola, A. Jokinen, K. Loberg, W. H. Trzaska, J. Äystö, Z. Phys. A348, 151 (1994).
6) M. R. Schmorak, Nucl. Data Sheets 51, 689(1987).

2.3 OBSERVATION OF NEW ISOMERIC STATE IN ^{217}Pa

S. MITSUOKA, T. IKUTA, H. IKEZOE, Y. NAGAME, K. TSUKADA,
I. NISHINAKA, J. LU [1] and T. KUZUMAKI [2]

We have performed ^{28}Si+^{194}Pt reaction to investigate long-lived isomeric states in the N=126 isotones of actinide nuclei by α-decay spectroscopy [1]. A 25 pnA beam of ^{28}Si^{10+} from the JAERI-tandem accelerator was used to bombard 460~630 μg/cm^2 thick ^{194}Pt targets (95.54% enriched). The beam energies were chosen to be 163 MeV and 175 MeV in order to maximize the yield of the 5n and 6n evaporation channels, respectively. Evaporation residues of interest were separated from the primary beam by the JAERI recoil mass separator (JAERI-RMS) [2]. M/Q (mass/unit charge) dispersion of the JAERI-RMS was set to zero to provide large angular acceptance (20msr) and energy acceptance ($\pm$12%). The definite identification of the separated recoil was achieved by the correlation analysis of its decay events. Details of the detection system and analysis procedure were described in our previous papers [3, 4].

We observed several α-lines of ^{216}Pa and ^{217}Pa produced via the p5n and p4n evaporation channels, respectively. Since the subsequent decay properties of these nuclei are very similar until it reaches to the great-granddaughter nuclei of ^{204,205}At, the definite identification of these nuclei was achieved by the excitation functions [1]. Observed decay properties of ^{216}Pa and ^{217}Pa are summarized in Table 1. We observed the previously reported α-transition with E_α=10.155(15) MeV of ^{217}Pa [5, 6]. This transition has been estimated to be the decay from the 1.86 MeV (29/2$^+$) state of ^{217}Pa to the ground state of ^{213}Ac from systematic trends in neighboring nuclides. We also observed the α-transition of E_α=9.54(5) MeV with half-life of $1.5^{+0.9}_{-0.4}$ ms. This transition is similar to that of E_α=10.155(15) MeV. If the 1.86 MeV excited state decays with E_α=9.54(5) MeV, a 0.63 MeV excited state having a spin of 15/2 is expected in ^{213}Ac. The corresponding level scheme of ^{213}Ac is not known. It is then reasonable that our observed α-transition of E_α=9.54(5) MeV is assigned to the decay from another excited state in ^{217}Pa.

We place a new 1.23 MeV level in the level scheme of ^{217}Pa as shown in Fig.1 [1]. As is pointed in Ref. [5], the $(h_{9/2})^n$ configuration which brings about a long-lived isomeric state of 21/2$^-$ is not allowed in ^{217}Pa. It is then possible to assign the $[(h_{9/2})^{n-1}f_{7/2}]_{23/2-}$ configuration to a new 1.23 MeV isomeric state in ^{217}Pa. Calculated α-decay half-life with an angular momentum of l=7 for E_α=9.54(5) MeV completely supports the 23/2$^-$ → 9/2$^-$ transition. There exists a discrepancy of 1 $\hbar$ between the calculated l=9 and the momentum transfer of 29/2$^+$ → 9/2$^-$ transition for the α-decay of E_α=10.14(5) MeV. This difference gives rise to nearly an order of magnitude in half-life, but one must bear in mind that the calculation dose not take account of a parity change of the transition which brings a certain amount of additional hindrance.

---

[1]On leave from Institute of Modern Physics, Chinese Academy of Science, 730000 Lanzhou, China

[2]Department of Physics, Tohoku University, Sendai, 980 Japan

Table 1: Decay properties of ^{216}Pa and ^{217}Pa.

Nuclide	Present [1] E_α (MeV)	$T_{1/2}$ (ms)	Calculated [7] $T_{1/2}$(ms)	l	Other [6] E_α(MeV)	$T_{1/2}$(ms)
^{216}Pa	7.830(50)	150^{+70}_{-40}	500	0	7.838(20)	105(12)
	7.960(50)	140^{+50}_{-30}	200	0	7.948(10)	105(12)
^{217}Pa	8.330(50)	$2.3^{+0.5}_{-0.3}$	9.1	0	8.330(10)	3.4(2)
	9.540(50)	$1.5^{+0.9}_{-0.4}$	1.9	7	–	–
	10.140(50)	$1.7^{+0.7}_{-0.4}$	2.4	9	10.155(15)	1.5(2)
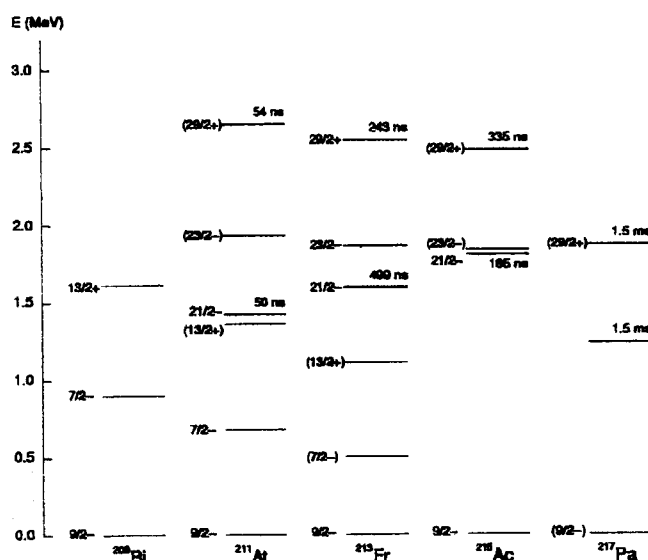
Fig.1 Proposed level of ^{217}Pa in comparison with partial level schemes of N=126 isotones.

References

1) T. Ikuta, H. Ikezoe, S. Mitsuoka, Y. Nagame, K. Tsukada, I. Nishinaka, and L. Jun, accepted by Phys. Rev. C.

2) H. Ikezoe, Y. Nagame, T. Ikuta, S. Hamada, I. Nishinaka, and T. Ohtsuki, Nucl. Instr. and Meth. **A376**, 420 (1996).

3) H. Ikezoe, T. Ikuta, S. Hamada, Y. Nagame, I. Nishinaka, K. Tsukada, Y. Oura, and T. Ohtsuki, Phys. Rev. C **54**, 2043 (1996).

4) S. Mitsuoka, H. Ikezoe, T. Ikuta, Y. Nagame, K. Tsukada, I. Nishinaka, Y. Oura, and Y. L. Zhao, Phys. Rev. C **55**, 1555 (1997).

5) K. -H. Schmidt, W. Faust, G. Münzenberg, H. -G. Clerc, W. Lang, K. Pielenz, D. Vermeulen, H. Wohlfarth, H. Ewald, and K. Güttner, Nucl. Phys. **A318**, 253 (1979).

6) A. N. Andreyev, A. G. Popeko, A. V. Eremin, S. Hofmann, F. P. Heßberger, H. Folger, V. Ninov, and S. Saro, Bull. Rus. Acad. Sci. Phys. **60**, 119 (1996).

7) B. Buck, A. C. Merchant, and S. M. Perez, Phys. Rev. C **45**, 2247 (1992).

2.4 The 773 keV $\pi g_{9/2}$ isomer in ^{79}As

I. HOSSAIN[1], T. ISHII, A. MAKISHIMA[2], M. ASAI, S. ICHIKAWA, M. ITOH[1], M. ISHII, P. KLEINHEINZ[1], and M. OGAWA[1]

We have measured the lifetime of 773 keV $\pi g_{9/2}$ isomer in ^{79}As using the isomer-scope [1] by taking coincidences between γ rays and projectile-like fragments (PLF) produced in deep-inelastic collisions. A ^{198}Pt target, 95.7% enriched and 4.3 mg/cm^2 thick, was bombarded with a beam of 635 MeV ^{76}Ge generated by the tandem booster facility . The coincidences between PLF and γ rays as well as between γ rays were taken by registering events on tape.

Figure 1 shows the decay curves of the 542 and 231 keV transitions. These curves give the half-life of the isomer as

$$T_{1/2}(9/2^+, 773 \text{ keV}) = 0.87(6) \text{ μs},$$

and the strength of the isomeric transition as

$$B(M2, 9/2^+ \to 5/2^-, 542 \text{ keV}) = 0.042(3) \text{ W.u.}.$$
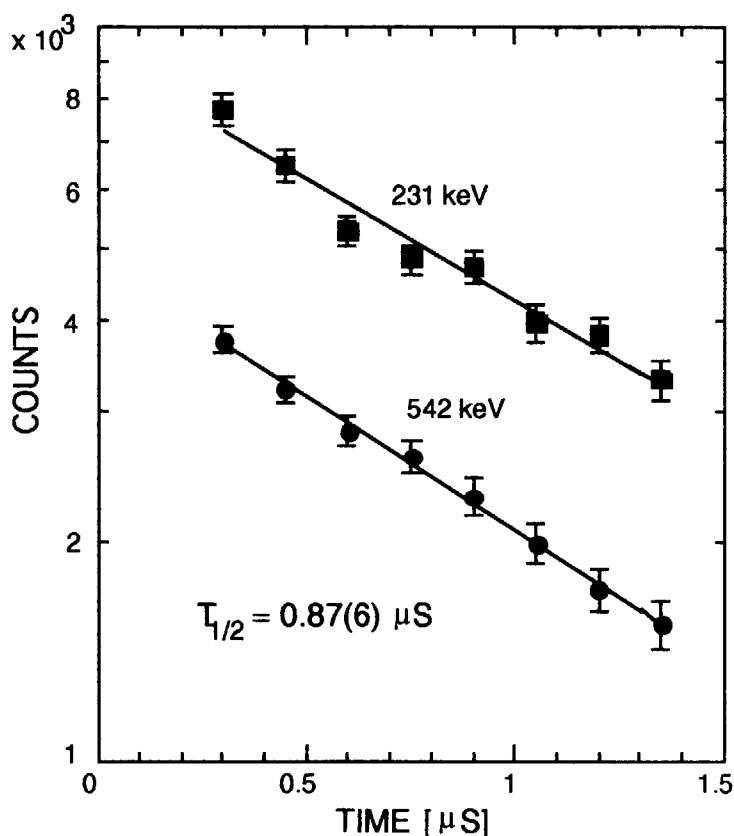
Fig.1. Decay curves of the 542 and 231 keV γ rays from the 773 keV isomer

1) Research Laboratory for Nuclear Reactors, Tokyo Institute of Technology

2) Department of Liberal Arts and Sciences, National Defense Medical College

The isomeric M2 transitions between the $9/2^+$ and $5/2^-$ states were observed earlier in the odd As isotopes with A=69 to 77 [2]. Their B(M2) values, and the present result for ^{79}As, are plotted against the mass number in Fig.2(a); the excitation energies of the $3/2^-$, $5/2^-$ and $9/2^+$ levels, which should largely be single proton character, are shown in Fig. 2(b). The energy of the $9/2^+$ state decreases towards higher masses up to A=75, and for the same range the B(M2) values show a similar tendency. For yet heavier masses, however, where the $9/2^+$ energy goes up again, the M2 strengths remain small and nearly constant.
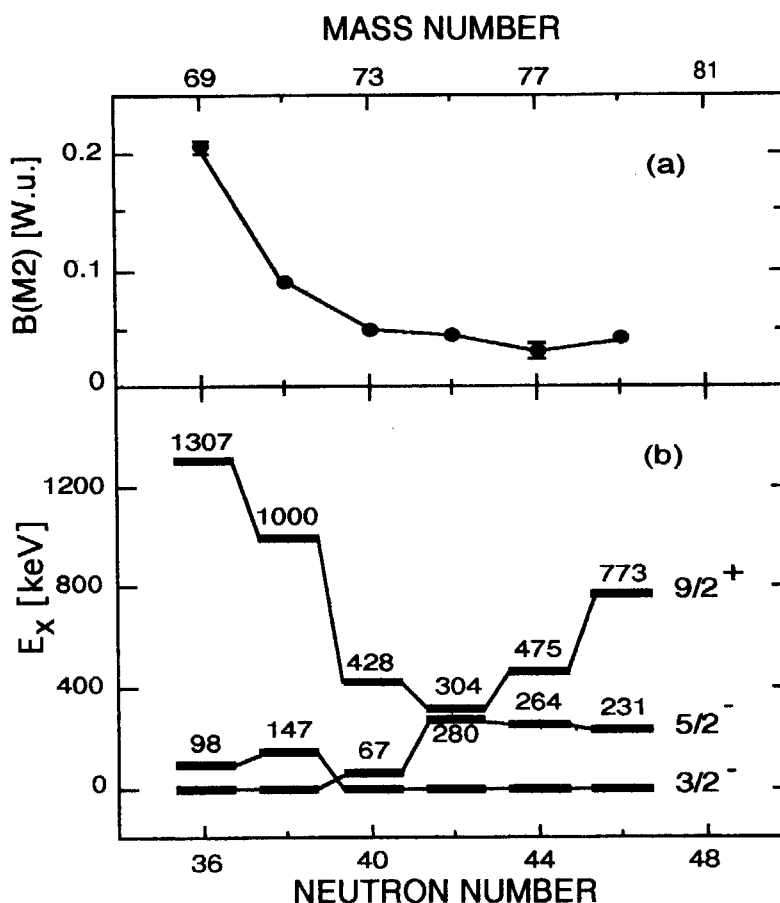
Fig.2. Systematic of (a) B(M2, $9/2^+ \rightarrow 5/2^-$) values and (b) excitation energies of the lowest $3/2^-$, $5/2^-$ and $9/2^+$ states in odd As isotopes.

The B(M2) values seem to relate to the configuration of the $5/2^-$ state as well as to the deformation of the nuclei. The $5/2^-$ state is the ground state in ^{69,71}As, but turns to be an excited state in $^{73-79}$As. This fact suggests that the $5/2^-$ states in $^{73-79}$As are mixtures of the configurations of $\pi f_{5/2}(\pi f_{5/2})^2_{I=0} (\pi p_{3/2})^2_{I=0}$ and $\pi f_{5/2} (\pi p_{3/2})^4_{I=0}$; in other words, the closure of the $\pi p_{3/2}$ orbital, $(\pi p_{3/2})^4_{I=0}$ is weak in $^{73-79}$As. Such a configuration mixing could reduce the B(M2) values in $^{73-79}$As.

References

1) T. Ishii, M.Itoh, A.Makishima, M.Ogawa, I.Hossain, T.Hayakawa, and
   T.Kohno, Nucl. Instrum. Methods, Phys.Res. A395 ,210(1997)
2) R.B. Firestone and V.S. Shirley, Table of Isotopes 8th ed. (John Willy &
   Sons, New York, 1996)

2.5 HIGH SPIN STATES OF ^{155}Gd

T.HAYAKAWA, M.OSHIMA, Y.HATSUKAWA, J.KATAKURA, H.IIMURA, M.MATSUDA,
S.MITARAI[1], R.SHIMIZU[1], T.SHIZUMA[2], M.SUGAWARA[3] and H.KUSAKARI[4]

High-spin states of ^{155}Gd nucleus have been investigated using the ^{150}Nd(^{12}C, α3n) reaction. The target was a self-supporting ^{150}Nd metallic foil enriched to 96.1 % with 2 mg/cm^2 thickness. Gamma-rays were deteced with an array of 11 HPGe detectors with BGO Compton suppressers. Two rotational bands of ^{155}Gd have been observed. The band 1 with 3/2[651] configration was observed up to 49/2$^+$, and the band 2 with 11/2[505] configuration was extended up to 33/2$^-$. Fig. 1 shows the partial level scheme.
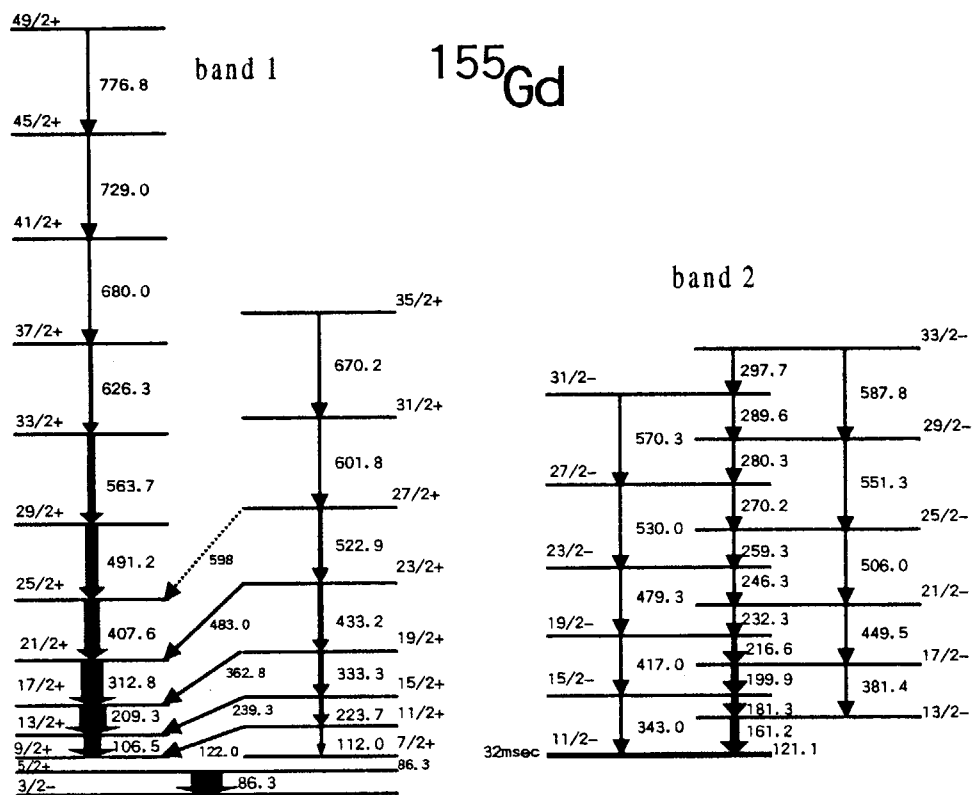
Fig. 1

[1]Kyushu University, Hakozaki, Hukuoka 812-8581, Japan
[2]University of Tsukuba, Tsukuba, Ibaraki 305-8577, Japan
[3]Chiba University, Inage, Chiba 263-8522, Japan
[4]Chiba Institute of Technology, Narashino, Chiba 275-8588, Japan

2.6 CONVERSION ELECTRON MEASUREMENTS IN ^{127}Ba

H. IIMURA, S. ICHIKAWA, T. SEKINE, M. OSHIMA and M. MIYAJI[1]

Neutron-deficient nuclei in the A=120-130 mass region exhibit a transition from triaxial to prolate shapes, providing a good chance of testing various nuclear models. It has also been suggested that a number of nuclei in the neighborhood of ^{128}Ba possess stable octupole deformations[1]. In ^{127}Ba, high-spin level structure was studied by in-beam γ-ray spectroscopic method, as summarized in ref. 2, and several rotational bands were proposed. However, multipolarities of transitions in this nuclei have not been established yet. In this work we measured conversion electrons in ^{127}Ba following the ß-decay of ^{127}La ($T_{1/2}$=5.1 m). The ß-decay of ^{127}La was studied by Gizon also[3].

The experiment was performed by using the on-line mass separator at tandem accelerator facility. The ^{127}La nucleus was produced by the reaction ^{nat}Mo(^{32}S,pxn)^{127}La with 160-MeV ^{32}S beam. Reaction products were ionized in a surface-ionization ion source, and mass-separated electromagnetically. Electrons and γ-rays were measured simultaneously with Si(Li) and HPGe detectors. From the measurements, 16 conversion coefficients were determined for ^{127}Ba.

The K conversion coefficients of the 79.4-, 114.3-, 134.3-, 220.4-, 253.2-, 269.4-, 285.6- and 318.9-keV transitions were consistent with M1 and/or E2 multipolarities. Our results confirm the multipolarities of 134.3-, 220.4- and 253.2-keV transitions reported by Cottle *et al.*[4], while others have been determined for the first time. From the multipolarities of transitions, the 195.4-, 415.7- and 669.0-keV levels have been determined to have the same parities as the 81.1-keV level. In the same way, the parities of the 269.5- and 375.1-keV levels have been assigned as positive, and those of 159.7-, 293.9- and 579.5-keV levels as negative. Those parities are shown in Fig. 1, in which the parities of the 0-, 56.2-, 80.3- and 81.1-keV levels and the spins of all levels are from ref. 2. Present results are consistent with the previous band assignments of 5/2[402], 1/2[411] and 7/2[523] Nilsson orbitals[2]. It has been confirmed that the low-spin states within each rotational band have the same parity. Thus, alternating parity structure, which is indicator of static octupole deformation, has not been observed. Further analysis is in progress.
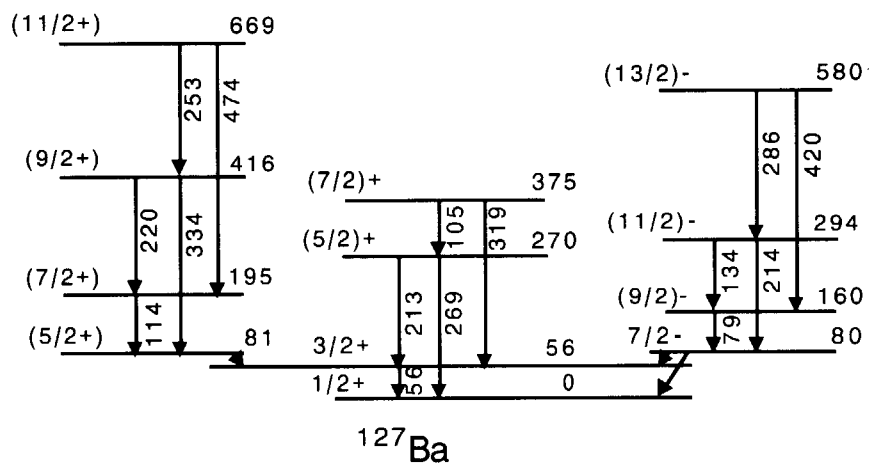
Fig. 1. Low-lying levels in ^{127}Ba

References
1) P.D. Cottle, Z. Phys. A338, 281(1991).
2) K. Kitao and M. Oshima, Nucl. Data Sheets 77, 1(1996).
3) A. Gizon, *Proc. of 25th Zakopane School on Physics*, World Scientific, 1990, Vol.2, p. 93.
4) P.D. Cottle *et al.*, Phys. Rev. C48, 136(1993).

[1]Toshiba Corporation, Kawasaki, Kanagawa 210

2.7 MEASUREMENT OF THE LIFETIME OF THE $\Delta I = 1$ BAND IN ^{134}Ce

K. FURUNO[1] , Y. SASAKI[1], T. SHIZUMA[1], T. KOMATSUBARA[1],
H. ISHIYAMA[1], T. JUMATSU[1]

M. OSHIMA, T. HAYAKAWA, Y. HATSUKAWA, and M. MATSUDA

Recently, many $\Delta I = 1$ bands are reported in even-even nuclei around the mass number $A \sim 190$ and $A \sim 130$[1,2]. The remarkable features of these $\Delta I = 1$ bands are that the intensities of $\Delta I = 1$ cascade transitions are stronger than those of $\Delta I = 2$ cross-over transitions; dynamic moments of inertia defined by $\mathcal{J} = dI/d\omega$ are about 1/3 of those in the ground-state band of typical deformed nuclei; the E2/M1 mixing ratios in the $\Delta I = 1$ transitions are negative. The measurement of lifetime which provides the transition probability between the band members is very useful to understand the structure of the $\Delta I = 1$ bands. In nuclei with mass numbers $A \sim 190$, lifetimes have been measured[3], but no lifetime measurement has been reported in $A \sim 130$ nuclei. The present work is aimed at the measurement of lifetimes of the band members of $\Delta I = 1$ band in the nucleus ^{134}Ce which was assigned in our previous works[4].

Since the lifetime of the $\Delta I = 1$ band is expected to be of the order of pico seconds, nuclear reactions using the inverse kinematics is advantageous to obtain high recoil velocities. The excited states of ^{134}Ce were, therefore, populated through the ^{11}B(^{127}I,$4n$)^{134}Ce reaction at a bombarding energy of 580 MeV. The ^{127}I beam was provided by the accelerator complex consisting of the 20UR tandem accelerator and the superconducting linear accelerator at the Japan Atomic Energy Research Institute(JAERI). Two experiments were performed in November 1997 and in February in 1998.

The first experiment was a test of a plunger system. The target was prepared by vacuum evaporation of natural boron onto a thin carbon foil. A thick lead plate was used for the stopper. This experiment, however, was not successful because of the locally large deformation of the target. This could be caused by local heating due to the large energy loss of ^{127} ions. Furthermore, a foil of boron with carbon backing was very fragile so that the fabrication of thin targets with tight and smooth surfaces was difficult.

The second experiment was performed with a thick target to observe the line shape of γ-ray spectra. A 890 μg/cm^2 thick natural-boron target was prepared by vacuum evaporation using electron bombardment. A foil of lead with the thickness of 40.7 mg/cm^2 was used as a backing. Gamma rays were observed by means of 11 Ge detectors with BGO anti-Compton shield. Two detectors were placed at every 4 angles of $\theta = 31.7°$, $\theta = 58.3°$, $\theta = \pi - 31.7°$ and $\theta = \pi - 58.2°$. Three detectors were mounted at $\theta = 90°$ with respect to the beam direction. Gamma-gamma coincidence events were accumulated event by event on magnetic tapes. The beam currents of ^{127}I were in the range from 0.2 to 0.7 nA in the charge state of 28$^+$. About 20 million two-fold coincidence events were recorded. The coincidence data were sorted off line to form 4k×4k matrices.

---

[1] Institute of Physics and Tandem Accelerator Center, University of Tsukuba,
Tsukuba, Ibaraki 305 JAPAN

Fig. 1 shows γ-γ coincidence spectra for γ rays emitted from the states of $\Delta I = 1$ band in ^{134}Ce. These spectra are very tentative because the counting statistics was very low due to low beam currents in the present experiment. The coincidence matrix assigned to 30° was obtained by summing up each coincidence matrix sorted for the γ-ray detector at 30° and all other detectors. Similar sortings of coincidence data were made for the angles of 60°, 90°, 120° and 150°. The uppermost spectra in Fig. 1, four gated spectra obtained by placing the gates on 196, 239, 275 and 332 keV γ rays in the $\Delta I = 1$ band in the coincidence matrix for 30° were summed up. The spectra for other angles were produced in a similar manner as 30°.
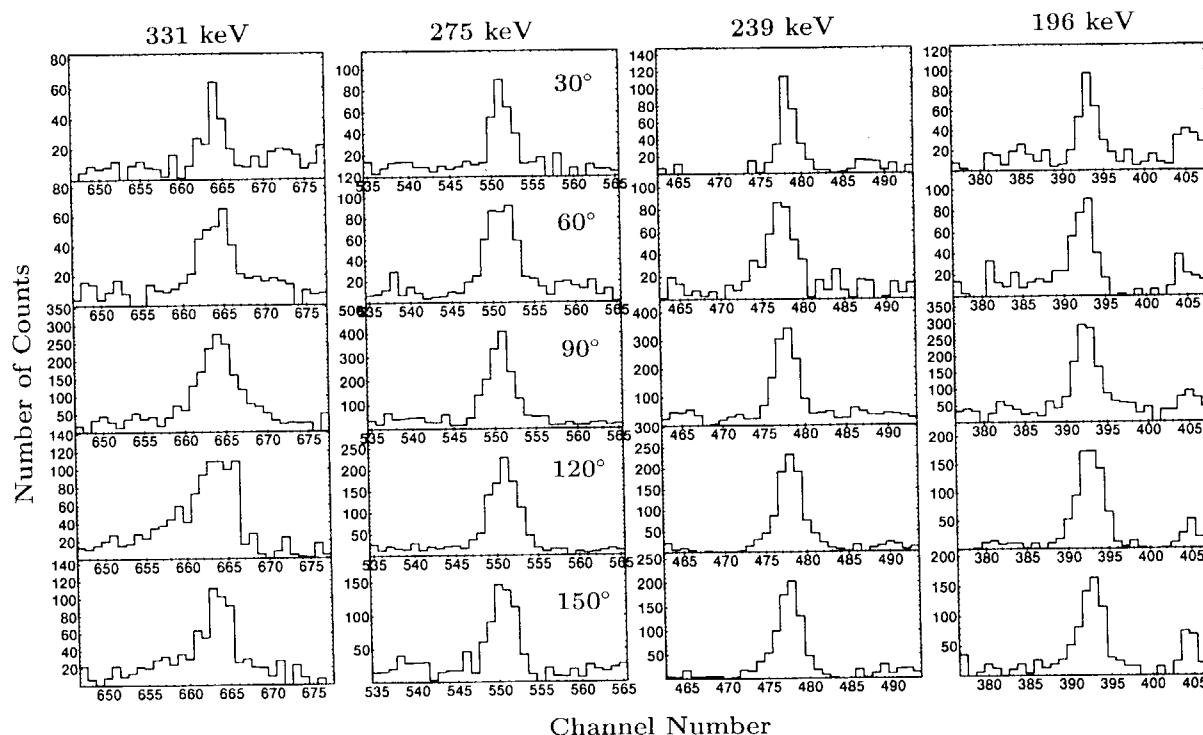
Fig. 1. Gamma-gamma coincidence spectra for γ rays emitted from the states of $\Delta I = 1$ band in ^{134}Ce.

The widths of all peaks in Fig. 1 are almost comparable to the energy resolution of $2 \sim 2.5$ keV of the γ-ray detectors. The value of $\beta = v/c$ in the present experiment is 7 % when recoil nuclei penetrate into the lead layer. According to the calculation of a line shape with this value of β and the stopping power dE/dx of ^{134}Ce ions in lead, the line shape for a γ ray from a state with a halflife of 1 ps consists of a large stopped peak and a small tail due to the Doppler broadening. The ratio of the heights for the stopped peak to the bump of the tail is approximately to be 1:0.2. The more careful analysis of the coincidence data is in progress. The present data, however, imply that the lifetimes in the band members of the $\Delta I = 1$ band in ^{134}Ce would be longer than 1 ps. An improved experiments with a plunger are necessary to determine the life time more precisely.

References
1)M.A. Deleplanque, Nucl. Phys. **A557**(1993)39c
2)D.B. Fossan, J.R. Hughes, Y. Liang, R.Ma, E.S. Paul and N. Xu, Nucl. Phys. **A520**(1990)259c
3)M. Neffgen, G. Baldsiefel, S. Frauendorf, et al.,Nucl. Phys. **A595**(1995)479
4)J. Lu, T. Komatsubara, T. Hayakawa, T. Saito, N. Hashimoto and K. Furuno, UTTAC Annual Report 1996, UTTAC-63, 36

2.8 THREE-NUCLEONS CLUSTER STRUCTURE IN LIGHT NUCLEI

A.YAMAZAKI[1] , T.NAKAGAWA[1], Y.FUJII[1], M.MATSUNAGA[1],
K.KUMAGAI[1], M.HIRAI[1], T.SUEHIRO[2] , S.KATO[3] ,
H.ISHIYAMA[4] Y.SUGIYAMA and S.HAMADA

There are various nuclear models to explain experiments about nuclear structure. Cluster model is one of them. The most famous one is the alpha cluster model, that a nucleus consists of an inert core and alpha cluster. A great amount of experiments and calculations have been accomplished, and as a result it has been found that there exists the alpha cluster structure not only in light nuclei but also in fp-shell nuclei [1), 2)].

For an analogy of the alpha cluster model, it could be thought a three-nucleons cluster model consisting of an inert core plus three-nucleons cluster. There are some theoretical and experimental studies about three-nucleons cluster structure, but the explanation for the existence of this structure has not been achieved as such success like the alpha cluster model until now. One of the reason of this is a lack of the information about highly excited states of nuclei which is interested in from the viewpoint of three-nucleons cluster structure. From the threshold rule, the information about states in excitation energy region which is in the vicinity of cluster separation energy or those above thresholds would be very important for the study of three-nucleons cluster structure.

On the other hand, it is well known that some states are very selectively excited through multi-nucleons transfer reactions . From this property many studies of alpha cluster structure is done through the alpha transfer reaction. Therefore, we selected the three-nucleons transfer reactions, $(^6Li,t)$ and $(^6Li,^3He)$ on ^{12}C to explore the three-nucleons cluster structure in residual nuclei, ^{15}O and ^{15}N respectively.

The experiment was carried out using a 60 MeV $^6Li^{3+}$ beam from the JAERI Tandem Van de Graff accelerator. A natural carbon self-supporting foil was used as the ^{12}C target. The thickness was 120 μm/cm^2. The emitted t and ^3He particles were momentum-analyzed with the JAERI magnetic spectrograph ENMA, and were detected by a single wire proportional counter and thin plastic scintillator placed behind the counter. Some modifications for the detection system were accomplished for a light-ion detection [3)]. because the ENMA had been designed for a heavy-ion reaction study [4)]. Particle identification was made using a ΔE-E method.

---

[1] Department of Physics. Tohoku University.
[2] Tohoku Institute of Technology.
[3] Department of Physics. Yamagata University.
[4] National Laboratory for High Energy Physics. Tanashi branch
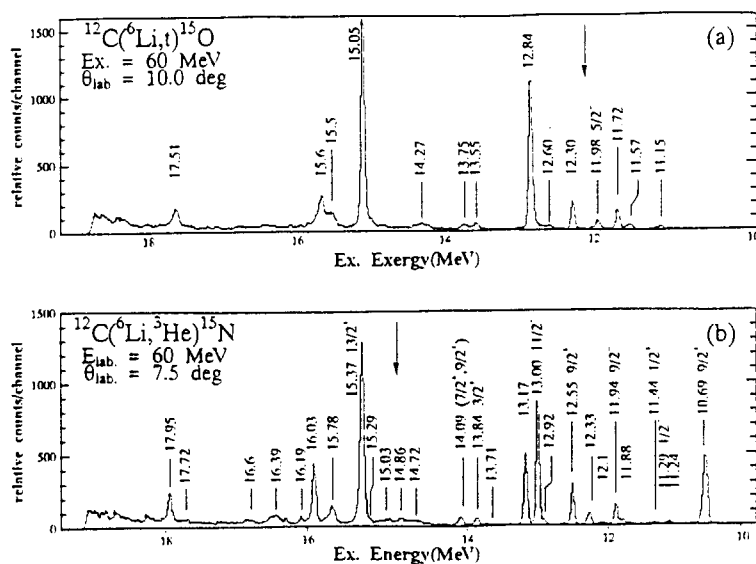
Fig. 1: The typical energy spectra of t from (^{6}Li,t) reaction (a) and of ^{3}He from (^{6}Li,^{3}He) reaction (b).

Fig. 2: The angular distributions of the cross section for several strongly excited analog states.

Figure 1(a) and 1(b) show typical energy spectra of t from the (^{6}Li,t) reaction and of ^{3}He from the (^{6}Li,^{3}He) reaction, respectively. The observed overall energy resolution for the emitted particles was about 80 keV. Downarrows in Figure 1(a) and 1(b) indicate the threshold energies for the separation of t and ^{3}He clusters from the ^{12}C core, respectively. The residual nuclei from these two reactions are mirror nuclei, and analog states should be populated strongly.

Figure 2 shows angular distributions of the cross section for several strongly excited analog states. It is found that they are analogous each other not only in magnitude but also in shape. One of the residual nucleus ^{15}O is unstable, so spin-parity assignment in highly excited energy region is not sufficient in the present. However, this analyses, spin-parity of these states could be assigned and a possibility for the t and ^{3}He cluster structure will be discussed.

References

1) T.Yamaya, S.Oh-ami, M.Fujiwara, T.Itahashi, K.Katori, M.Tosaki, S.Kato, S.Hatori and S.Ohkubo, Phys. Rev. **C42**(1990)1935.

2) T.Yamaya, M.Saitoh, M.Fujiwara, T.Itahashi, K.Katori, T.Suehiro, S.Kato, S.Hatori and S.Ohkubo, Nucl. Phys. **A573**(1994)154.

3) A.Yamazaki, T.Yamaya, H.Ishiyama, M.Kato, J.Tojima, T.Kuzumaki, H.Yahata, T.Suehiro, S.Kato, Y.Sugiyama and S.Hamada, JAERI TANDEM & V.D.G. Annual Report 1996 pp.35-36.

4) Y.Sugiyama, H.Shikazono, H.Ikezoe and H.Ikegami, Nucl. Instrum. Methods **187**(1981)25.

2.9 DIPOLE AND QUADRUPOLE CASCADES
IN THE YRAST REGION OF ^{143}Gd

M. SUGAWARA[1], H. KUSAKARI[2], Y. IGARI[2], K. MYOJIN[2], D. NISHIMIYA[2],
S. MITARAI[3], M. OSHIMA, T. HAYAKAWA, M. KIDERA, K. FURUTAKA
and Y. HATSUKAWA

Europium and gadolinium nuclei just below the semi-magic ^{146}Gd core are rather spherical at low excitation energy. However, as the excitation energy and spin get higher, many different nuclear structures are showing up along the yrast line. One of the most interesting characters is the coexistence of dipole and quadrupole cascades in the yrast region. In fact such cascades were found in ^{142,143,144}Eu and ^{144}Gd recently[1,2]. The main purpose of this study is to search for such cascades coexisting along the yrast line in ^{143}Gd.

We made an in-beam spectroscopic study on high spin states of ^{143}Gd by the reaction of ^{111}Cd(^{35}Cl,1p2n)^{143}Gd. A 7-mg/cm^2 thick Cd foil, enriched in ^{111}Cd to 96.30% was bombarded with a 170-MeV ^{35}Cl beam. Gamma-rays from excited states populated after the reaction were measured by the GEMINI array[3] consisting of 11 BGO anti-Compton spectrometers in coincidence with charged particles detected by a Si ball[4] made up of 21 detector segments. Approximately 3.1×10^8 two- or higher fold $\gamma\gamma$ events were collected and sorted into an individual E_γ-E_γ matrix tagged with the number of protons and α particles detected in the Si ball.

A relatively clean matrix for the 1pxn-channel was obtained by subtracting 2p and 1p1α contributions from the 1p matrix. We constructed the level scheme of ^{143}Gd as shown in Fig.1 using this matrix. The spins and parities were deduced from the DCO ratios evaluated using the spectra gated by the appropriate stretched E2 transitions at lower excitation energy.

Before this experiment, two ΔI=1 and one ΔI=2 sequences (denoted by "(A)", "(B)" and "(C)" in Fig.1 respectively) were known up to 31/2$^{+,}$ 35/2, 31/2$^-$ states respectively[5]. We could extend these sequences to higher spin states as shown in Fig.1. We could identify a new γ-ray of 70 keV at the bottom of the sequence "(B)" which was overlooked in ref.5. The existence of this transition was finally confirmed by the observation of a new dipole cascade (denoted by "(D)" in Fig.1) decaying to both "(A)" and "(B)". Also we could observe the unfavored I_{max}-1 members of the coupling $(\nu h_{11/2}^{-1}) \otimes (2^+, 4^+$ in ^{144}Gd) slightly above the favored I_{max} members. Corresponding states have been already observed in the N=79 isotone ^{141}Sm[5] at similar excitation energies.

Moreover three new quadrupole cascades denoted by "(E)", "(F)" and "(G)" have been found.

---

[1]Chiba Institute of Technology
[2]Faculty of Education, Chiba University
[3]Faculty of Science, Kyushu University

Among them the sequence "(G)" is of a peculiar character that it has only weak connections to the other dipole and quadrupole cascades and decays mostly through an irregular sequence of E2 transitions between 500 and 800 keV. This feature resembles those of similar sequences recently observed in neighboring nuclei[1,2]. Unfortunately we could observe too few transitions decaying out from the sequence "(G)" to account for its population intensity.

B(M1)/B(E2) ratios have been deduced to be 7.9(5), 44(6) and 51(17) $(\mu_N/\mathrm{eb})^2$ for the decays from the 31/2$^+$ state in "(A)", the (31/2)$^-$ and (41/2) states in "(B)" respectively. This means that more high spin proton particles or neutron holes are involved in the sequence "(B)" than in "(A)". In the cascade "(D)" which is of the highest excitation energy among the dipole cascades identified here, there were no crossover E2 transitions observed.
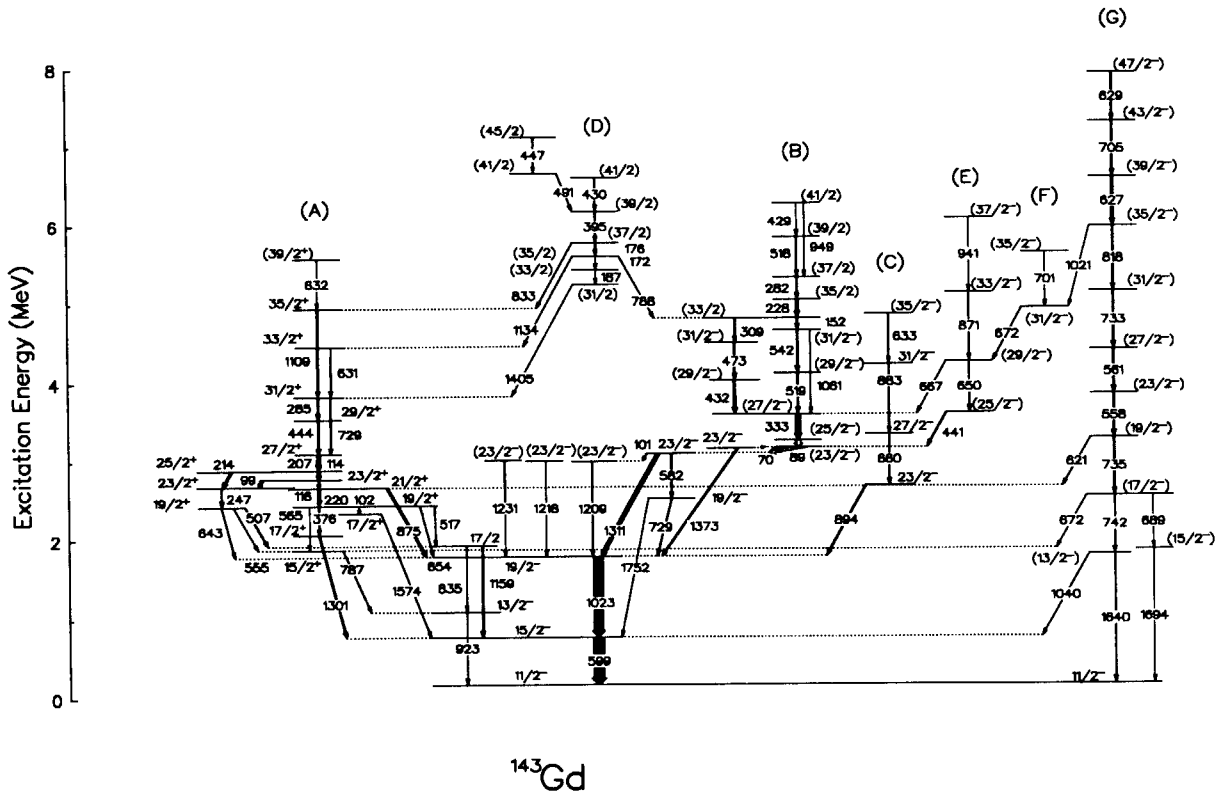

Fig.1 The level scheme of ^{143}Gd

References
1) M. Piiparinen et al., Nucl. Phys. A605(1996)191
2) T. Rzaca-Urban et al., Nucl. Phys. A579(1994)319
3) K. Furuno et al., Nucl. Instrum. and Methods(1998) to be published.
4) T. Kuroyanagi et al., Nucl. Instrum. and Methods A316(1992)289.
5) M. Lach et al., Z. Phys. A345(1993)427

2.10 ENHANCED SIDE-BAND POPULATION IN COULOMB EXCITATION OF
155Gd

M. OSHIMA, T. HAYAKAWA, Y. HATSUKAWA, K. FURUTAKA,[1] J. KATAKURA,
M. MATSUDA, H. IIMURA, H. KUSAKARI,[2] K. TERUI,[2] K. MYOJIN,[2] D. NISHIMIYA,[2]
M. SUGAWARA[3] and T. SHIZUMA[4]

In Coulomb-excitation (COULEX) experiments with heavy ions, it is well known that the E2 excitation is the dominant excitation process and the ground-state rotational band (ground band), the members of which are connected with enhanced E2 transitions, is the most strongly excited. So far there is no exception for this rule. In our previous paper[1], however, we reported a new phenomenon of exceptionally strong population of the side band of 155Gd in a Coulomb excitation experiment by a heavy 90Zr projectile.

The low-lying level structure of 155Gd has been studied through the previous investigations[2,3]. The ground-state is known to have a configuration of a negative-parity ν3/2[521] orbit and a one-quasiparticle positive-parity side band based on a ν3/2[651] orbit has been identified with the band head at 86 keV. Since the parities of the two bands are different, the side-band members are considered to be excited via E1 and/or E3 transitions from the ground-band members in multiple COULEX process. Eλ matrix elements of intraband and interband transitions are used in evaluating the COULEX cross section. Even when such matrix elements have not been measured, we know at least their upper limits, i.e., the recommended upper limits (RUL) derived from the compilations of the experimental data in the whole mass region[4]. The COULEX cross section is calculated using the computer code, COULEX [5]. In the previous analysis[1] which took account of the RUL for E1 and E3 strength it was difficult to explain the enhanced populations of the side band members; in order to reproduce the measured cross section enhanced E3 strength as large as 600 Weisskopf (single particle) unit are required, which exceeds well the RUL. In the present experiment, we investigated the excitation process which is much dependent on the Coulomb field produced in the heavy-ion collisions by using lighter 32S and 58Ni beams. From the dependence of the Coulomb-excitation cross section on the kind of projectiles and the scattering angle, the enhancement relative to the calculation for the RUL is roughly proportional to the electric field accomplished in the Coulomb-scattering process as shown in Fig. 1.

This phenomenon is analyzed in several ways. One is based on the inelastic scattering due to the nuclear force. And secondly, strong K-mixing among many low-lying one-quasiparticle rotational bands may provide many excitation pass ways to the side band. The third possibility is that a transition between members of the ground and side bands might be enhanced in the strong photon field accomplished in the COULEX process. These possibilities will be pursued in further experiments.

1) present address: Power Reactor and Nuclear Fuel Development Corporation, Tokai-mura, Ibaraki-ken.
2) Faculty of Education, Chiba University.
3) Chiba Institute of Technology.
4) Tandem Accelerator Center, Tsukuba University.
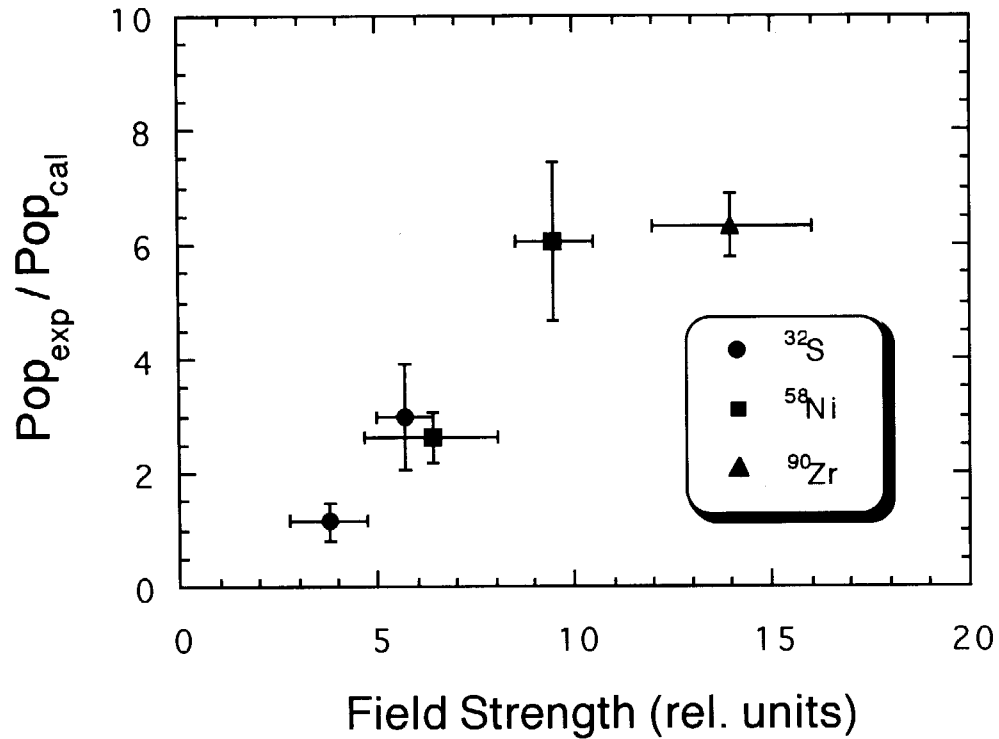
Fig. 1. Experimental enhancement of the side-band population relative to COULEX calculation for RUL as a function
of the electric field accomplished in the Coulomb-scattering process.

References

1) M. Kidera et al., J. of the Phys. Soc. of Japan **66**, 285 (1997) .

2) G. Lovhoiden et al., Nucl. Phys. **A148**, 657 (1970).

3) M.A. Riley et al., Z. Phys. **A345**, 121 (1993).

4) W. Andrejtscheff et al., Atom. D. Nucl. D. Tbls **16**, 515 (1975); P.M. Endt, ibid **26**, 47 (1981).

5) A. Winther and J. de Boer, in *Coulomb Excitation* (Academic, New York, 1966) p.303.

2.11 THE $(\pi p_{3/2}\nu g^2_{9/2})_{19/2^-}$ ISOMER DECAY IN ^{71}Cu

T. ISHII, M. ASAI, I. HOSSAIN[1], P. KLEINHEINZ[1], M. OGAWA[1] A. MAKISHIMA[2], S. ICHIKAWA, M. ITOH[2], M. ISHII and J. BLOMQVIST[3]

We have found an isomer in ^{71}Cu by deep-inelastic collisions of 8 MeV/nucleon ^{76}Ge projectiles with ^{198}Pt, using a new instrument isomer-scope [1]. The isomer decays with $T_{1/2} = 0.25(3)$ μs through a γ-ray cascade of 133–495–939–1189 keV to the ground state. A $\gamma\gamma$-coincidence sum spectrum for the four intense transitions is displayed in Fig. 1 and the decay scheme of this isomer is shown in Fig. 2. The spin sequence in ^{71}Cu radically differs from the isomer in other three-particle nuclei with the $j^2 j'$ configuration; e.g., the $(\pi g^2_{9/2}\nu d_{5/2})_{21/2^+}$ isomer in ^{93}Mo has 6.8h halflife and decays through $E4 - E2 - E2$ to the $\nu d_{5/2}$ ground state. The isomerism of these aligned three-particle states is well known to be caused by the strongly attractive $\pi\nu$ two-body residual interaction for the maximum-spin coupling, whereas the couplings with spins one or two units less have significantly smaller attraction. To elucidate the unusual isomer cascade of ^{71}Cu, its energy spectrum was calculated from the shell model in the minimum model space $\nu g^2_{9/2}\pi p_{3/2}$. The two-nucleon residual interactions are taken from the experimental energy levels in ^{70}Ni and ^{70}Cu shown in Fig. 3(a). These nine level energies fully specify the model space for our calculation. The energy levels calculated for ^{71}Cu are illustrated and compared to experiment
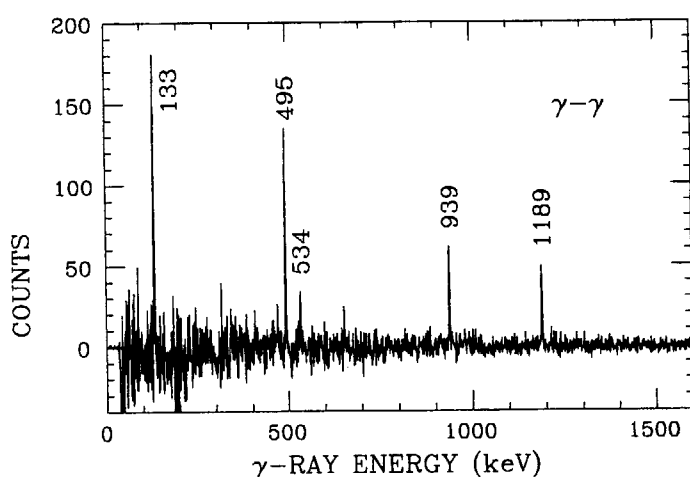
Fig. 1. A γ-γ coincidence spectrum representing the sum of coincidence gates on the 133, 495, 939 and 1189 keV transitions.
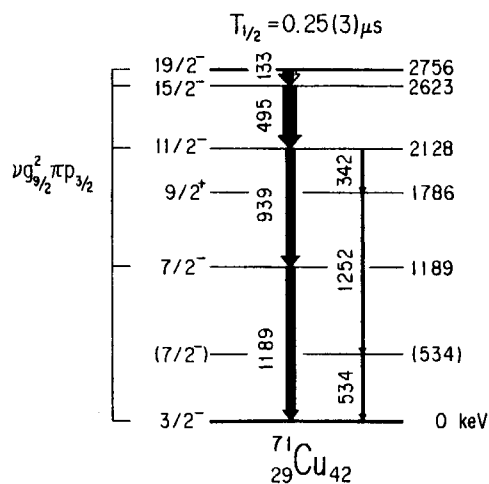
Fig. 2. The decay scheme of the isomer in ^{71}Cu.

[1]Department of Energy Sciences, Tokyo Institute of Technology
[2]Department of Liberal Arts and Sciences,National Defense Medical College
[3]Physics Department, Royal Institute of Technology, Stockholm, Sweden

in Fig. 3(b). The agreement of calculation and experiment is excellent. Most significantly, theory correctly predicts the regular increase of spin with excitation similar as in the ^{70}Ni neighbour. This agreement clearly indicates that the configurations of the five ^{71}Cu yrast states must be quite pure in terms of the $\nu g_{9/2}^2 \pi p_{3/2}$ model space. The unusual monotonic spin sequence of ^{71}Cu is not in a simple manner related to a specific cause. However, it is clear that two input-quantities are of significance, namely the spacing of the two highest levels in the j^2 spectrum, and the attraction in the $jj'_{I_{max}-2}$ coupling, which is much larger in ^{70}Cu than in heavier nuclei and contributes to push the $(j^2 j')I_{max}$ and $-I_{max-2}$ states apart.
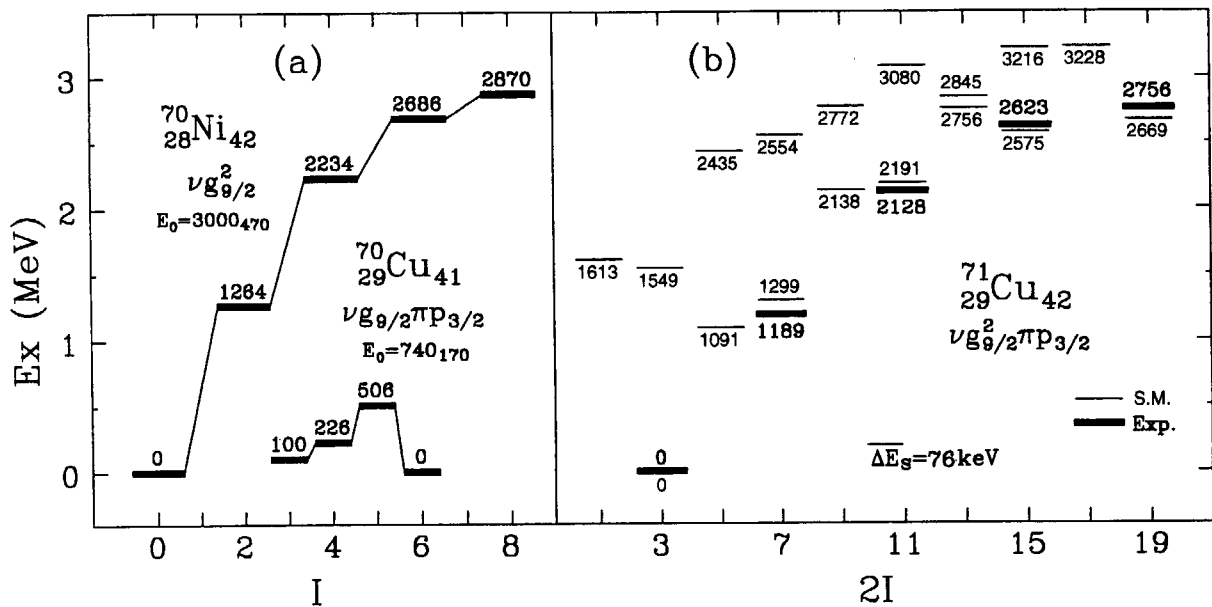
Fig. 3. (a) Interaction energies used in the shell model calculation for ^{71}Cu. (b) Experimental levels of ^{71}Cu compared to calculated values normalized at the ground state. The calculated ground state energy is $-133(480)$ keV. Mean deviation for the four level spacings is 76 keV.

References
1) T. Ishii et al., Nucl. Instrum. Methods Phys. Res. A395, 210.

2.12 A NEW POSITION-SENSITIVE SCINTILLATION DETECTOR FOR COULOMB EXCITATION EXPERIMENT

M. OSHIMA, T. HAYAKAWA, Y. HATSUKAWA, K. FURUTAKA,[1] J. KATAKURA,
M. MATSUDA, H. IIMURA, H. KUSAKARI,[2] K. TERUI,[2] K. MYOJIN,[2] D. NISHIMIYA,[2]
M. SUGAWARA[3] and T. SHIZUMA[4]

Coulomb excitation is a powerful method for the investigation of nuclear collective motion. By using heavy-ion beams, multiple excitation process becomes important and high-spin states can be excited. Heavy-ion beams like ^{208}Pb can easily excite states higher than 20^+. For these cases the γ-ray energies need to be corrected for Doppler shift, because they are emitted from a recoiled nucleus with high velocity. The particle-γ angular correlation information for wide particle angular ranges is often valuable to extract electromagnetic properties of excited states. A position-sensitive particle detector for this purpose should afford high counting rate at forward angles and good angular resolution. Another important requirement is that it should sustain high dose of particle injection; widely-used position-sensitive Si detectors is not suited in this respect, because radiation damage due to heavy ions, say 390-MeV ^{90}Zr beam particle, causes the lifetime of Si detectors as short as 12-24 hours in a condition of 10^4/sec counting rate. Thus we developed a new device utilizing a plastic scintillator and position-sensitive photomultiplier.

We used a BC418(PILOT-U)[1] plastic scintillator with a thickness of 2mm coupled with the Hamamatsu R5900 photomultiplier [2] with a sensitive area of 20mm x 20mm. The latter consists of an array of photomultipliers and four electrodes in each x and y directions behind it. The information of four outputs in x and y direction is converted to linear positions. To detect both projectile and recoil nucleus four detectors are arranged at forward and backward angles.
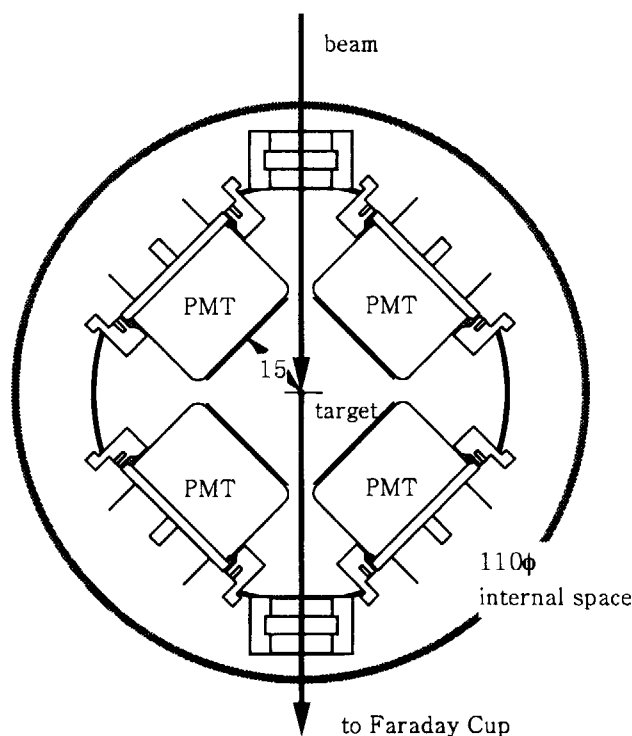
Fig. 1. A setup of Coulomb-excitation experiment.

---

1) present address: Power Reactor and Nuclear Fuel Development Corporation, Tokai-mura, Ibaraki-ken.
2) Faculty of Education, Chiba University.
3) Chiba Institute of Technology.
4) Tandem Accelerator Center, Tsukuba University.
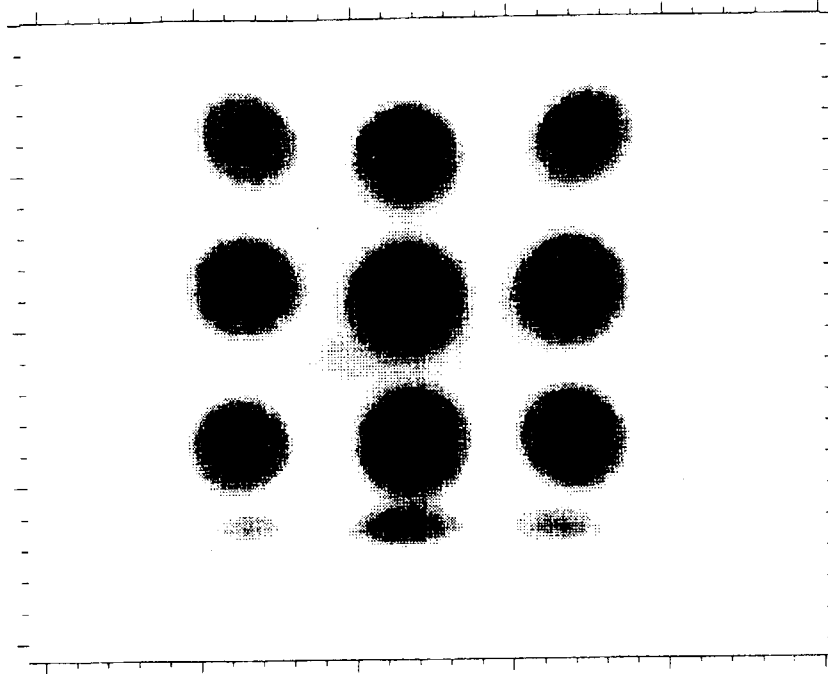
Fig. 2 A positional spectrum measured with ^{252}Cf fission source.

Figure 1 shows the whole setup. Since the target chamber needs to be fitted in the internal space of the γ-ray detector array[3], *GEMINI*, the diameter needs to be smaller than 110mmφ. To obtain positional resolution of the detector system we put a mask with 2mmφ holes in 5mm intervals in front of the scintillator, and measured particles emitted from a ^{252}Cf fission source. The supply voltage was 900 V. The obtained two-dimensional position spectrum is shown in Fig. 2. The positional resolution is derived to be 1.8mm FWHM: a sufficiently good positional resolution for Coulomb excitation experiments has been achieved. The largest advantage of the present detector is that the plastic scintillator can sustain the radiation damage much better than usual solid state Si detectors do.

References

1) Products from Nippon BICRON Co., Room No. 805 1-8, 1-Chome Shinyokohama, Kohoku-Ku,Yokohama 222, Japan.
2) Products from Hamamatsu Photonics K. K., 5000 Hirakuchi, Hamakita-city 434, Japan.
3) K. Furuno et al, Nucl. Instrum. Meth. (1998) in press.

2.13 IMPROVEMENT OF OVERALL EFFICIENCY OF THE GAS-JET COUPLED JAERI-ISOL SYSTEM AND SEARCH FOR NEW NEUTRON DEFICIENT AMERICIUM ISOTOPES

M. SAKAMA[1], K. TSUKADA, M. ASAI, S. ICHIKAWA, Y. OURA[1], Y. NAGAME, I. NISHINAKA, H. NAKAHARA[1], Y. KOJIMA[2], A. OSA, M. SHIBATA[2] and K. KAWADE[2]

To investigate nuclear properties of unknown neutron deficient actinide isotopes produced by heavy ion fusion reactions, we have developed the Gas-jet coupled JAERI-ISOL system [1]. The overall efficiencies for the separation of ^{143m}Sm produced in the ^{141}Pr(^{6}Li, 4n) reaction and ^{237}Am in ^{235}U(^{6}Li, 4n) were determined to be 0.14% and <0.1%, respectively. The half-life of new americium isotope ^{236}Am produced via the ^{235}U(^{6}Li, 5n) reaction with the cross section of about 70 μ b was determined with this system [2].

Since production cross sections of further neutron deficient and unknown actinide isotopes are expected to be less than 10 μ b, it is needed to improve the transport efficiency which depends considerably on the gas-jet apparatus coupled with the ion-source of ISOL. In order to examine the transport efficiency in the He gas-jet apparatus, the following aerosol cluster materials which catch reaction products are used : KCl, PbCl$_2$ and PbI$_2$ [3].

Fig. 1 shows the transport efficiencies of the gas-jet apparatus for the separation of ^{143m}Sm produced via the ^{141}Pr(^{6}Li, 4n) reaction as functions of the sublimation temperature of the aerosol clusters, PbI$_2$ and KCl, and the flow rate of the He gas. The overall efficiencies including the ionization of Sm$^+$ are shown in Fig. 2. Although the transport efficiency was about 1.5 times increased by using the PbI$_2$ aerosol cluster, it should be noted that the overall efficiency with the PbI$_2$ cluster becomes about 30 times larger than that for the case with KCl. For the explanation of the above results, it is convenient to use a ratio of the overall efficiency $\varepsilon_{overall}$ to the transport efficiency $\varepsilon_{transport}$, R= $\varepsilon_{overall}$/ $\varepsilon_{transport}$. The ratio is 1/6 for the PbI$_2$ aerosol cluster, while 1/100 for KCl. This indicates that the large positive-potassium-ion density would have suppressed the ionization of an atom of interest in the thermal ion-source, because the ionization efficiency of potassium is about 10^5 times higher than that of lead, in accordance with the Langmuir equation.

The overall efficiency for the separation of ^{237}Am produced in the ^{235}U(^{6}Li, 4n) reaction was found to be 0.21-0.26% when PbCl$_2$ and PbI$_2$ are used as cluster materials, as summarized in Table 1 ; the efficiency is improved about 8 times larger than that for the previous system with KCl.

Using the PbCl$_2$ aerosol cluster, we have carried out the experiments for the direct

---

[1] Department of Chemistry, Tokyo Metropolitan University
[2] Department of Energy Engineering and Science, Nagoya University

identification of the isotope ^{235}Am produced by the ^{235}U(^{6}Li, 6n) reaction. Pu $K_{\alpha 1}$ x-ray associated with the EC decay of ^{235}Am were observed in the mass-235 fraction. As preliminary results, the half-life was determined to be 7.2 ± 2.6 min, and the production cross section with 50-57 MeV was evaluated to be about 6.6μ b.
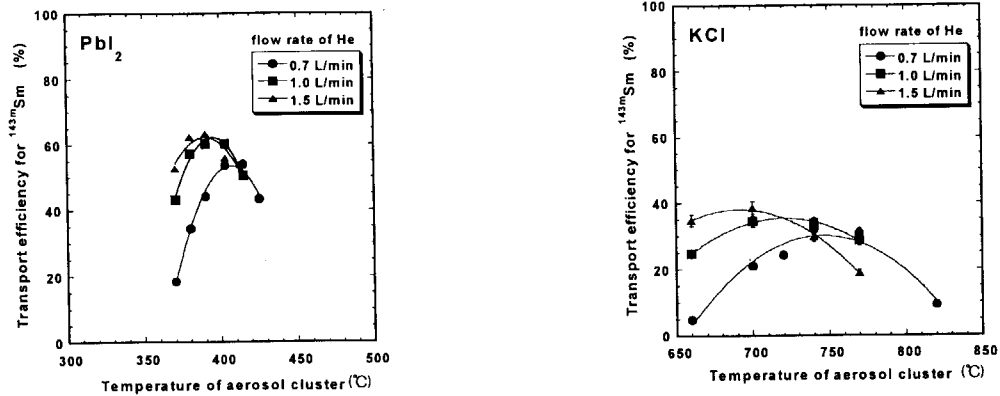
Fig. 1. Transport efficiencies of the gas-jet apparatus for the separation of ^{143m}Sm produced via the ^{141}Pr(^{6}Li,4n) reaction as functions of the sublimation temperature of the aerosol clusters, PbI_2 and KCl, and the flow rate of the He gas.
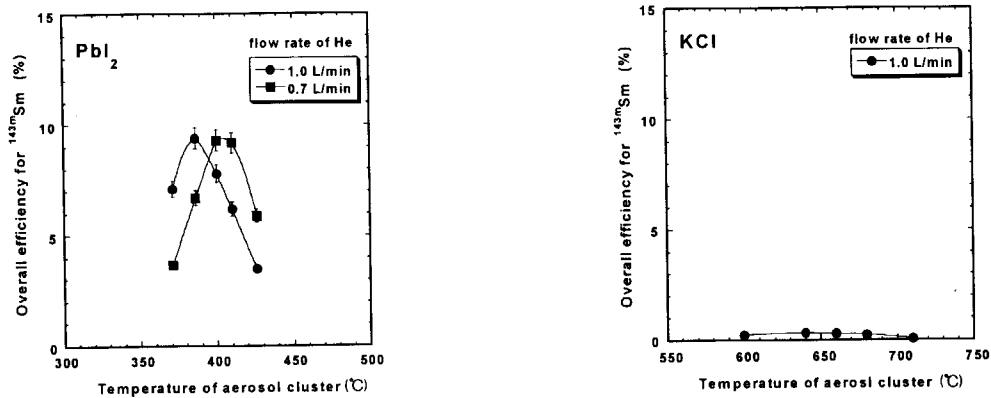
Fig. 2. Overall efficiencies including the ionization of Sm^+ of the gas-jet coupled ISOL as functions of the sublimation temperature of the aerosol clusters, PbI_2 and KCl, and the flow rate of the He gas.

Table 1. Overall efficiencies for the separation of ^{237}Am.

Aerosol cluster	Overall efficiency (%)	Temperature (℃)	He gas (L/min)
PbI_2	0.26 ± 0.04	390	1.0
$PbCl_2$	0.21 ± 0.03	470	0.9
KCl	0.03	650	0.8

References

1) S.Ichikawa *et al.*, Nucl. Instrum. Methods Phys. Res. A **374** (1996) 330.

2) K.Tsukada *et al.*, Phys. Rev. C **57** (1998) 2057.

3) M.Brugger *et al.*, Nucl. Instrum. Methods Phys. Res. A **234** (1985) 218.

3. Nuclear Reactions

This is a blank page.

3.1 STUDY OF PROTON-INDUCED BREAKUP REACTIONS ON ^{12}C FOR ENERGIES UP TO 30 MeV

M. HARADA[1], Y. WATANABE[1], S. YOSHIOKA[1], K. SATO[1], N. KOORI[2],
S. CHIBA, T. FUKAHORI, O. IWAMOTO, and S. MEIGO

Neutron and proton nuclear data for ^{12}C are required in various applications, such as advanced cancer therapy using high-energy proton and neutron beams. Recently, some of the authors have evaluated the neutron nuclear data of ^{12}C [1]. In the work, the calculation showed that α particle emission occurs mainly via sequential and simultaneous breakup processes of intermediate excited nuclei, such as ^{12}C* and ^{9}Be*, around 20 MeV of the incident neutron energy. However, there is no available experimental data of energy spectra of emitted nucleons and α particles not only in neutron-induced reactions but also in proton-induced reactions in the energy region of interest, which will be necessary for detailed analyses of the breakup processes. In the present work, we have measured the double-differential cross sections of protons and α particles emitted in the p+^{12}C reaction at an incident energy of 26 MeV [2], in order to investigate nucleon-induced breakup reactions on ^{12}C for energies up to 30 MeV.

The experiment was carried out using a 26-MeV proton beam from the JAERI Tandem accelerator. The experimental procedure was same as described in Refs. [2,3]. The target used was a natural carbon foils of 100 μ g/cm^2 thickness. A stacked ΔE-E silicon counter telescope with an active collimator made of an NE102A plastic scintillator was employed. Energy spectra of protons and α -particles were measured at angles from 20° to 150° in step of 10°.

The experimental results are shown together with the calculated spectra in Fig. 1. The observed continuous components of protons and α -particles were analyzed by assuming sequential decay of intermediate reaction products and simultaneous 3-body breakup (3BSB) process as shown in Table I. A Monte Carlo code [1,2] was used to calculate the energy spectra of protons and α - particles emitted via these many-body breakup processes. The result indicates that the 3BSB process becomes predominant with increasing emission energy, while the sequential decay process mainly contributes to the lower emission energy region. Some discrepancies between the measured and calculated spectra are due to no inclusion of the (p,np) reaction for proton emission and the (p, α)^{9}B*$_{7MeV}$ reaction for α -particle emission in the calculation. More detailed analyses are now in progress together with our other experimental data for 14 and 18 MeV [2].

References
[1] M. Harada et al., J. Nucl. Sci. and Technol., 34, 116 (1997).
[2] M. Harada et al., JAERI-Conf 98-003 (1998), p.273.
[3] Y. Watanabe et al., Proc. of Int. Conf. on Nuclear Data for Science and Technology, Trieste, Italy, May 19-24, 1997 (SIF, Bologna, 1997), p.580.

[1] Department of Advanced Energy Engineering Science, Kyushu University
[2] Faculty of Integrated Arts and Sciences, The University of Tokushima

Table I : Reaction processes considered in the present analysis

1, p + ^{12}C $\rightarrow$ p' + ^{12}C* (0$^+$, ex.=7.65MeV)	5, p + ^{12}C $\rightarrow$ p' + ^{12}C* (1$^-$, ex.=10.8MeV)
2, p + ^{12}C $\rightarrow$ p' + ^{12}C* (3$^-$, ex.=9.64MeV)	6, p + ^{12}C $\rightarrow$ p' + ^{12}C* (2$^-$, ex.=11.8MeV)
$\rightarrow$ α + ^{8}Be$_{g.s.}$	7, p + ^{12}C $\rightarrow$ p' + ^{12}C* (1$^+$, ex.=12.7MeV)
$\rightarrow$ α + α	8, p + ^{12}C $\rightarrow$ p' + ^{12}C* (4$^+$, ex.=14.1MeV)
3, p + ^{12}C $\rightarrow$ α + ^{9}B$_{g.s.}$	9, p + ^{12}C $\rightarrow$ p' + ^{12}C* (1$^+$, ex.=15.1MeV)
$\rightarrow$ p + ^{8}Be$_{g.s.}$	10, p + ^{12}C $\rightarrow$ p' + ^{12}C* (2$^+$, ex.=16.1MeV)
$\rightarrow$ α + α	$\rightarrow$ α + ^{8}Be* (2$^+$, ex.=2.94MeV)
4, p + ^{12}C $\rightarrow$ α + ^{9}B*(5/2$^-$, ex.=2.36MeV)	$\rightarrow$ α + α
$\rightarrow$ α + ^{5}Li	11, p + ^{12}C $\rightarrow$ p + α + ^{8}Be* (2$^+$, ex.=2.94MeV)
$\rightarrow$ p + α	$\rightarrow$ α + α [3BSB]

Figure 1: Comparisons of the measured and calculated energy spectra of (a) protons and (b) α particles emitted to an angle of 30° from the p+^{12}C reaction at 26 MeV.

3.2 PAIR-NEUTRON TRANSFER REACTIONS IN THE NICKEL REGION AROUND THE COULOMB BARRIER

Y.SUGIYAMA, S.HAMADA, T.IKUTA and A.YAMAZAKI[1]

It was pointed out that the nuclear Josephson effect could be observed in pair-transfer reactions between superfluid nuclei near the Coulomb barrier, since the probability of pair-transfer could be enhanced by the coherent nature of the nuclear states in both nuclei [1] . Recently elastic two-neutron transfer reactions were measured for the $^{58}Ni+^{60}Ni$ and $^{62}Ni+^{64}Ni$ systems at energies above the Coulomb barrier [2] . The pair-transfer cross section was observed to increase as the number of valence neutron. The $^{62}Ni+^{64}Ni$ system had the large pair-transfer cross section comparable to the one predicted for the the g.s. BCS wave function. We suggested a possible existence of the nuclear Josephson effect in the $^{62}Ni+^{64}Ni$ system.

In order to get more insight into the nuclear Josephson effect, we measured pair-neutron transfer cross sections leading to the ground state for the $^{58}Ni+^{58}Ni$ and $^{64}Ni+^{64}Ni$ sytems at $E_{cm}=110MeV$ and the $^{58}Ni+^{64}Ni$ system at $E_{cm}=118.8MeV$ by using the JAERI tandem accelerator and the heavy-ion magnetic spectrograph "ENMA" [3] . Angular distributions of ^{64}Ni $(^{64}N,^{64}Ni_{g.s.})$ $^{64}Ni_{g.s.}$ and ^{64}Ni $(^{64}N,^{62}Ni_{g.s.})$ $^{66}Ni_{g.s.}$ at $E_{cm}=110MeV$ are shown in Fig.1. Elastic scattering was analyzed by the coupled-channels calculation including the first 2^+ and 3^- states of target and projectile nuclei. We obtained the optical potential parameter by fitting the data. The solid line in the figure is the result.

The two-neutron transfer amplitude was calculated by using the macroscopic pair-transfer form factor of $F(r) = (\beta_p R/3A)(dU/dr)$, where β_p was the pair-deformation parameter which measured the collective strength of the pair modes [4] . R,A and U are the nuclear radius, mass number and the optical potential, respectively. For the case of superfluid systems, a large pair-transfer cross section is predicted by the BCS approximation in which the pair-deformation parameter β_p is expressed as $\beta_p=2\Delta / G$, where Δ and G are the gap parameter and the pairing strength,respectively [5] . For the Ni+Ni system, the pair-deformation parameter is estimated as $\beta_p \sim 9.5$ with the approximated values of $\Delta=12/A^{1/2}$ (MeV) and $G=20/A$ (MeV) . The calculated results are shown by solid lines in Fig.1. The values are averaged over the solid angle. The data of the $^{64}Ni+^{64}Ni$ system are reproduced well with a pair-deformation parameter of $\beta_p=9.2$ which is a little larger than the one of $^{62}Ni+^{64}Ni$. Therefore the $^{64}Ni+^{64}Ni$ system is seen to have the large pair-neutron transfer cross section comparable to the one predicted for the the g.s. BCS wave function.This result can suggest a possible existence of the nuclear Josephson effect not only in the $^{62}Ni+^{64}Ni$ but also in the $^{64}Ni+^{64}Ni$ systems .
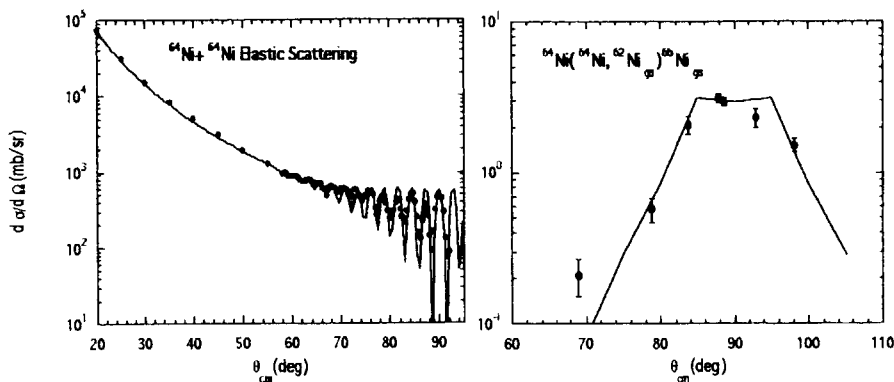
Fig.1 Elastic scattering (left) and the pair-neutron transfer reaction (right) of the $^{64}Ni+ ^{64}Ni$ system at $E_{c.m.}=110MeV$. Solid lines are the results of the theoretical calculations.

[1]Physics Department, Tohoku University

References
1) V.I.Gol'danskii and A.I.Lapkin, Th. Eksp.Theor. Fiz.53 (1967) 1032.
2) Y.Sugiyama et al.,Phys. Rev. C55 (1997) R5.
3) Y.Sugiyama et al.,Nucl. Instrum. Methods Phys. Res.A281 (1989) 512.
4) C.H.Dasso and G.Pollarolo, Phys. Lett. 155B (1985) 223.
5) D.R.Bes, P.Lotti, E.Maglione and A.Vitturi, Phys. Lett. 169B (1986) 5.

3.3 SINGLE PARTICLE EXCITATION ON A HALO INTRUDING IN S-HOLE DOORWAY BASED ON α CLUSTER DIMER BAND OF ^{11}B

S. Hamada, Y. Sugiyama, T. Ikuta and †A. Yamasaki

Recent interests on Borromean [1] nuclei are based on the two significant nature of light p-sd shell nuclei. One is the loosely bound neutron orbits characterized as halo like matter density, and the second is a large component of two center cluster configuration known as molecular structure. W. von Oertzen has pointed out the existence of α-cluster dimer chains appearing systematically on the molecular bands mostly above the alpha particle thresholds of neutron rich nuclei ranging from ^{9}Be via ^{10}Be/^{10}B and ^{11}Be/^{11}B upto ^{12}Be, ^{13}B and ^{16}C [2]. Y. Kanada-En'yo and H. Horiuchi are succeeding to exhibit the clustering aspects of two center molecular dynamics combined to the outskirts of neutron halo skins in the systematic of N $\gg$ Z toward neutron rich isotopes [3]. Among these scenario, by which the theoretical predictions are succesfully derived, but the experimental evidences for dimer structures are not so clear, except the trivial case of ^{8}Be and ^{9}Be [4]. In order to investigate the possibility of the dimer-chain structure in light nuclei, we have done revival experiments of $(^{6,7}$Li, $\alpha)$ transfer reaction of Ogloblin [5].

We have investigated these significances of clustering aspects of ^{11,12}B nuclei, by way of deuteron and triton transfer reaction with ^{6,7}Li incident beam of E_{lab}=60 MeV on ^{9}Be nucleus. The reaction ejectile was momentum analysed by QDD type spectrograph ENMA with resolution as well as 50 keV for discrete bound states. For ^{9}Be(^{6}Li, $\alpha)^{11}$B reaction, more than 20 eigen states appear in excitation reagion g.s.$\leq E_{ex} \leq$ 20 MeV. For $(^7$Li, $\alpha)$, 30 eigen states were also obtained in g.s. $\leq E_{ex} \leq$ 16 MeV. We show here a typical spectrum of $(^6$Li, $\alpha)$ reaction of continium reagion $14 \leq E_{ex} \leq 18$ MeV, in which two significant peaks of upper band $(T_>)$, E_{ex} = 16.44 and 17.43 MeV are clearly populated. In contrast, the eigen states in the lower band $(T_<)$ does not show a prominent peak, E_{ex} = 11.61 and 13.16 MeV, unlike as expected in this excitation selectivity. Although an important relevance of excited states E_{ex}=16.44 and 17.43 MeV are attributed to the theoretical implications of cluster configuration symmetry $SU(3)[443]$ and $SU(3)[4421]$ [6], present data shows a preference of much more single particle configuration caused by the s-wave halo analog of 3.96 MeV of ^{11}Be based on n + ^{10}Be*(3.37), intruding to inner shell which invokes sequencial spin flip transition seen in ^{9}Be(^{3}He, p)^{11}B reaction [7].
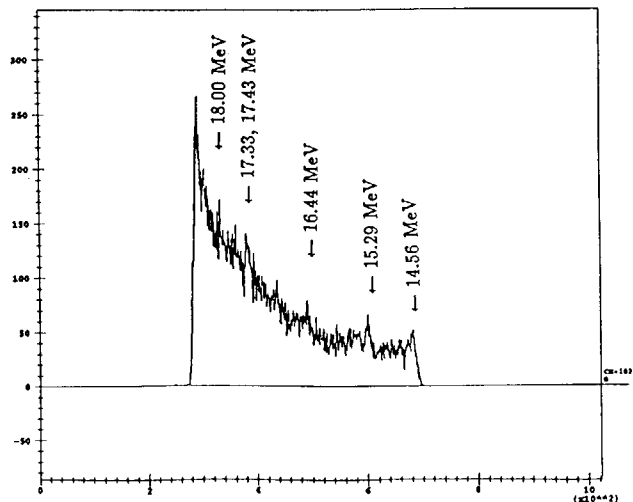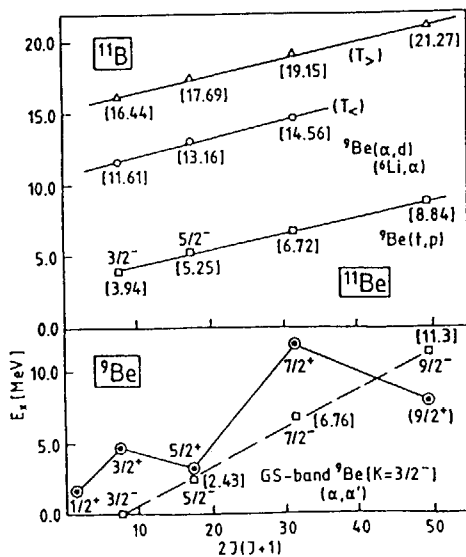
Fig.1. (Left) Predicative indication of large moment-of-inertia band common for ^{9}Be, ^{10}Be/^{10}B and ^{11}B [2]. Fig.2. (Right) A typical spectrum of ^{9}Be(^{6}Li, α)^{11}B reaction in higher excited continium region.

References
[1] M.V. Zhukov et al. Phys. Rep. 231, No.4 (1993) 151-199
[2] W. von Oertzen, Z. Phys. A354 (1996) 37-43, ibid, A357 (1997) 355-365
[3] Y. Kanada-En'yo et al. Phys. Rev. C52 (1995) 626, ibid 647, ibid C55 (1997) 2860
[4] H. Furutani et al. Supp. Prog. Theo. Phys. No. 68 (1980) 193
[5] A.A. Ogloblin. Nuclear Reactions induced by heavy ions, North-holland, 1970, 231
[6] T. Yamada et al. Phys. Rev. C53 (1996) 752
[7] B. Zwieglinski, Nucl. Phys. A389 (1982) 301

3.4 OBSERVATION OF A NEW SPONTANEOUS FISSION DECAY IN THE REACTION ^{30}Si + ^{238}U

H. IKEZOE, T. IKUTA, S. MITSUOKA, Y. NAGAME, I. NISHINAKA, Y. TSUKADA,
T. OHTSUKI[1], T. KUZUMAKI[1] and J. LU[2]

The spontaneous fission half-lives of heavy even-even nuclei decrease with increasing the atomic number Z up to 104. Recently, the heavy seaborgium isotopes ^{265,266}Sg have been synthesized in the heavy-ion fusion reactions at Dubna [1] and GSI [2]. These isotopes mainly decay by emitting α-particles. This fact indicates that the nuclear stability against fission caused by nuclear shell structure increases significantly near the neutron number 162. In order to study the decay property of the elements heavier than Z = 104, an effort was made to synthesize a new seaborgium isotope ^{264}Sg in the reaction ^{30}Si + ^{238}U.

Beams of ^{30}Si were used to bombard a $^{nat.}$UF$_4$ target whose thickness was 580μg/cm^2. The target was mounted on a wheel which was rotated with 2 cycles per second. The reaction products recoiling from the target foil were separated in-flight from the primary beam and by-products of various background reactions by the recoil mass separator (JEARI-RMS) [3]. The bombarding energy of 157.6 MeV which was about 1 MeV lower than the Bass fusion barrier was chosen to correspond to the maximum of 4n deexcitation channel. The beam intensity was about 100 pnA and the total dose was 2.64 x 10^{17} particles.

The details of the detection method are shown elsewhere [4]. The α-decays from the heavy fusion residues were not observed in the present experiment, while six spontaneous fission decays correlated with implanted heavy reaction products were observed within the correlation time of 400 s. Among these spontaneous fission events, two events were attributed to the fission of the ^{264}Sg-like recoils, because the observed recoil energy and mass number were consistent with those of the ^{264}Sg-like recoils. The half-life and the production cross section of the two spontaneous fission events were 54 (+98, -21) s and 180 (+240, -120) pb, respectively.

The nuclei ^{263}Sg may be considered as a parent nucleus of the observed spontaneous fission decays in addition to the nucleus ^{264}Sg, because these nuclei can be produced with the same order of magnitude of the cross section. The nucleus ^{263}Sg whose half-life is 0.8 s decays into ^{259}Rf by α-decay with the branching ratio of 30 % and also decays by spontaneous fission with

[1]Laboratory of Nuclear Science, Tohoku University, Mikamine, Taihaku-ku, Sendai 982
[2]Institute of Modern Physics, Chinese Academy of Sciences, 730000 Lanzhou, China

the branching ratio of 70 % [5]. In addition, the β-decay of ^{263}Sg is theoretically predicted with the half-life of 17.5 s [6]. The daughter nucleus ^{263}Db whose half-life is 27 s decays by α-particle emission (43 %) and spontaneous fission (57 %) [5].

The obtained half-life is close to the fission half-life of ^{266}Sg [2] and the one order of magnitude larger than the calculated spontaneous fission half-life 2.3 s [7] for ^{264}Sg.

References
1) Yu. A. Lazarev et al., Phys. Rev. Lett. 73, (1994) 624.

2) M. Schadel et al., Nature 388 (1997) 55.

3) H. Ikezoe et al., Nucl. Instr. and Meth. A376 (1996) 420.

4) H. Ikezoe et al., Phys. Rev. C54 (1996) 2043.

5) Table of Isotopes edited by V. S. Shirley et al., A Wiley-Interscience Publication (1996).

6) P. Moller et al., Atomic Data and Nuclear Data Tables 66 (1997) 131.

7) R. Smolanczuk et al., Phys. Rev. C52 (1995) 1871.

3.5 MASS YIELD DISTRIBUTIONS IN PROTON-INDUCED FISSION OF ^{248}Cm

Y. NAGAME, Z. QIN[1], K. TSUKADA, N. SHINOHARA, Y.L. ZHAO[2],
Y. HATSUKAWA, I. NISHINAKA, S. ICHIKAWA and K. HATA

Gross features of mass yield distributions in the proton-induced fission were systematically studied on the light and medium actinides (Th, U, Np, Pu and Am). The effects of atomic number Z, neutron number N and excitation energy of a fissioning nucleus on the mass yield distributions were discussed in terms of mean mass numbers of the light and heavy asymmetric mass yield peaks, a width of the heavier asymmetric peak and a peak-to-valley ratio [1]. To extend the systematic trend of mass yield distribution in low energy fission of actinides as functions of Z and N of a fissioning nucleus, we have measured mass yield distributions in the proton-induced fission of ^{248}Cm with the inicident proton energy range of 10.5 - 20.0 MeV by a radiochemical technique.

The ^{248}Cm target was prepared with electrodeposition onto a 5.4 mg/cm^2 thick aluminum foil. The target thickness estimated by α-ray spectrometry was about 50 μg/cm^2. Proton bombardments were carried out at the tandem accelerator. Formation cross sections of each nuclide were determined by γ-ray spectrometry and mass yield distributions were constructed from the observed cross sections.

Figure 1 shows the typical mass yield distribution for the proton energy of 20.0 MeV. The solid circles indicate the observed chain yields, while the open ones show the so-called "mirror points". The distribution is typically asymmetric and no clear fission products are observed in the symmetry region at the fragment mass number A~122. The weighted mean mass numbers of the light and heavy asymmetric peaks, $\overline{A_L}$ and $\overline{A_H}$, respectively, are depicted in Fig. 2(a) and the width (FWHM: full width at half maximum) of the heavier asymmetric peak is plotted in Fig. 2(b) as a function of excitation energy of the system. The data at $E_X=0$ taken from the spontaneous fission of ^{248}Cm [2] are almost the same as those in the
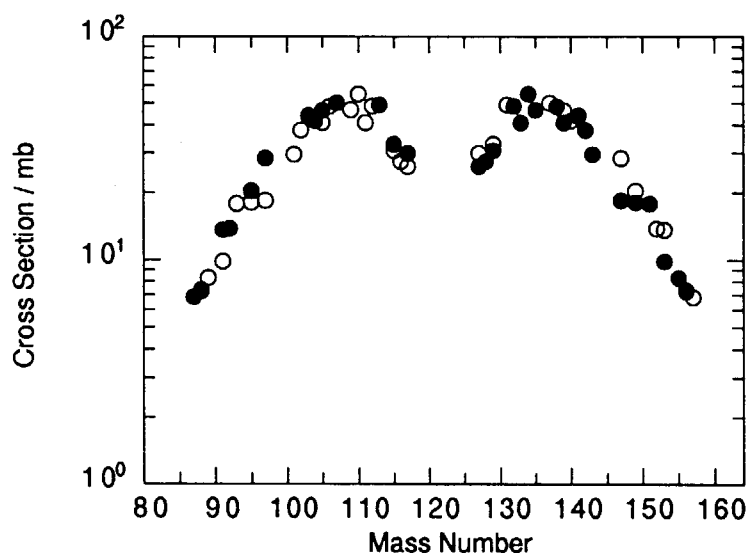
Fig. 1. Typical mass yield distribution for the proton-induced fission of ^{248}Cm in the incident proton energy of 20.0 MeV. Solid circles indicate the observed chain yields and open circles are their reflected points.

[1]On leave from Institute of Modern Physics, Chinese Academy of Science, Lanzhou 730000, People's Republic of China

[2]Department of Chemistry, Tokyo Metropolitan University

present work. As shown in Fig. 2, these values are independent of the excitation energy studied: $\overline{A_L}$=105±2, $\overline{A_H}$= 139±2 and FWHM=16.4±1.2. It was also found that the present $\overline{A_L}$ and $\overline{A_H}$ values are located in the extended lines of the systematic trends in Ref. [1]; $\overline{A_H}$ stays around the fragment mass number A=137, while $\overline{A_L}$ increases monotonously with the fissioning mass number A_C. The width of the asymmetric peak had a maximum at around A_C=236 and a small minimun at A_C ∼240 [3].
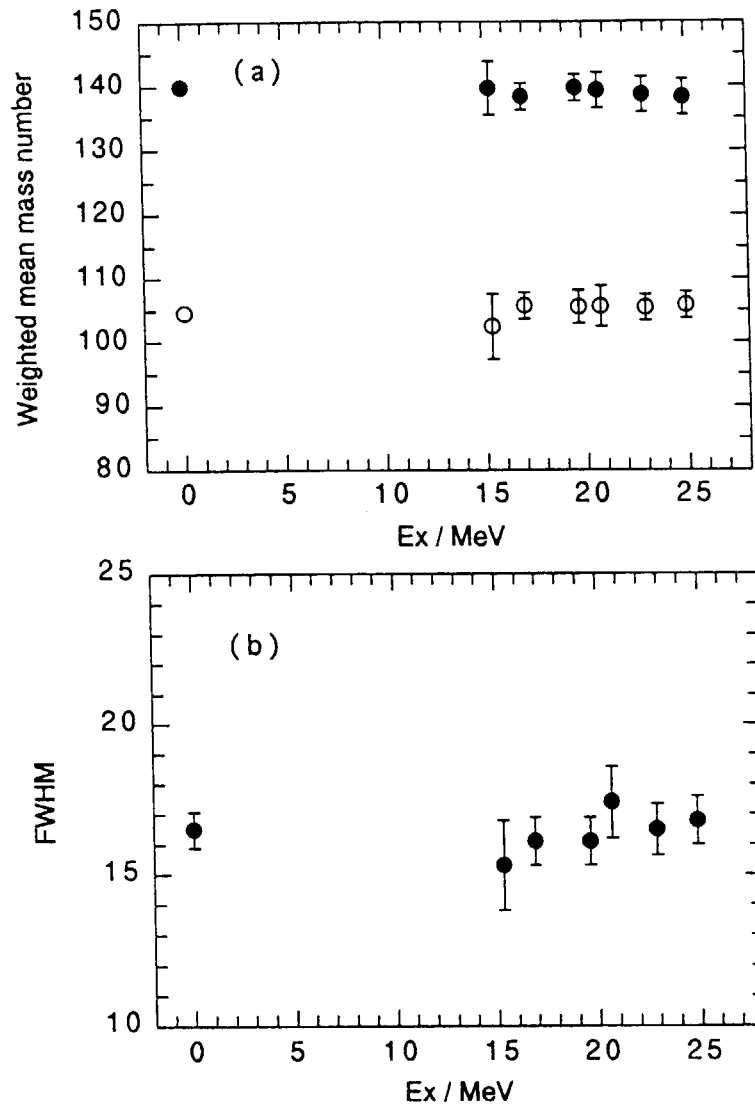
Fig. 2. (a) Weighted mean mass numbers of the light (open circles) and heavy (solid circles) asymmetric peaks and (b) FWHM of the heavy asymmetric mass yield as a function of the excitation energy. The data at E_X=0 are taken from [2].

References
1) T. Ohtsuki, H. Nakahara and Y. Nagame, Phys. Rev. C **44** (1991) 1405.
2) K.F. Flynn, J.E. Gindler and L.E. Glendenin, J. Inorg. Nucl. Chem. **39** (1977) 759.
3) Z. Qin et al., to be submitted.

3.6 INCIDENT ENERGY DEPENDENCE OF THE RELATIVE INTENSITIES OF TWO DIFFERENT SCISSION CONFIGURATIONS IN ACTINIDES FISSION

Y.L. ZHAO[1], I. NISHINAKA, Y. NAGAME, K. TSUKADA, S.ICHIKAWA, S. MITSUOKA, H. IKEZOE, Y. OURA[1], K. SUEKI[1], H. NAKAHARA[1], M. TANIKAWA[2], T. OHTSUKI[3], S. GOTO[4], H. KUDO[4], and K. TAKAMIYA[5]

The fact that the yield at the symmetry of a mass yield curve increases more rapidly than those at the asymmetric peak as increasing the excitation energy of the fissioning nuclide has been studied in detail by many investigators[1], and, at the early stage of fission studies, it led to the so-called "two-mode" hypothesis[2]. Only recently, however, it is found that two distinctly different kinetic-energy distributions exist even for the same mass division observed not only in spontaneous fission of heavy actinides and transactinides but also in low-energy fission of light actinides[3]. The latter observation indicates the presence of two type of scission configurations, compact and elongated ones, for some region of fragment mass division. However, there still exists no report on the existence of any correlation between them. In this work, efforts have been concentrated on the accurate measurements of the mass-yield and TKE-yield distributions for each mass split in low energy proton-induced fission of actinides in order to clarify the correlation between the saddle and scission states.

The proton beams were supplied from the JAERI tandem accelerator. The proton energies were from 11 to 16 MeV, and the targets were ^{232}Th and ^{238}U. The measurements were performed with a double velocity TOF spectrometer in the TOSCA (Time Of flight Scattering Chamber for Actinide fission) apparatus. The experimental method is similar to the one described in ref. [3]. The radiochemical works were completed in previous experiments by Kudo et al. (see ref. [1]).

From the measured velocity of each fragment, the mass and the total kinetic energy (TKE) of the fragment were determined. In the fragment mass region from A=124 to 134, the binary structures of the TKE-distribution for a certain fragment mass were observed. It was then decomposed into two components, high-TKE distribution and low-TKE distribution, via a two-Gaussian function analysis as described in ref. [3]. From each distribution, the intensity for each TKE-component was obtained.

As well kown, the TKE values are mostly determined at the last stage of fission process, i.e., the scission configurations[4]. Therefore, the quantity of TKE directly reflects the property at the scission state of the fissioning nucleus. On the other hand, the fission probabilities (namely the fission yields) are determined in the first stage of the fission process, i.e., the evolution from the ground-state (in the induced case from the excited-state) of the fissioning nucleus to the saddle state[5]. In other words, as the nucleus deforms upto the saddle state the fission probability is already determined even though some kinds of fluctuation forces which emerge in the further descent from saddle to scission will affect finer details of mass and TKE distributions. However, from our previous work, it has been demonstrated that the shapes of the asymmetric and symmetric mass yield curves are essentially not varied by the incident energy. Accordingly, the fragment mass yield directly reflects the properties of saddle configurations. In figs. 1, the intensity ratios of the yield of the high-TKE component to that of the low-TKE component (open circles) are plotted as a function of

[1] Department of Chemistry, Tokyo Metropolitan University
[2] Department of Chemistry, University of Tokyo
[3] Laboratory of Nuclear Science, Tohoku University
[4] Department of Chemistry, Niigata University
[5] Department of Chemistry, Osaka University

incident proton energy. The ratios of peak to valley of the fragment mass yield curves (open triangles for the data obtained by radiochemical method and the solid triangles for those by TOF telescope) are together plotted. Fig. 1(a) is for $p+^{232}$Th and Fig. 1(b) is for $p+^{238}$U fission. The results indicate that the high-TKE to low-TKE intensity ratio has the similar energy dependence with the peak-to-valley ratio of the fragment mass yield curve. Namely, high-TKE fission events experience a lower fission threshold at saddle and are correlated with asymmetric mass division whereas the low-TKE fission experience a higher threshold energy and correlated with the symmetric mass division. From this definite correlation, a conclusion can be drawn now that there are at least two independent deformation paths between saddle and scission states in fission process of light actinides at low energy.
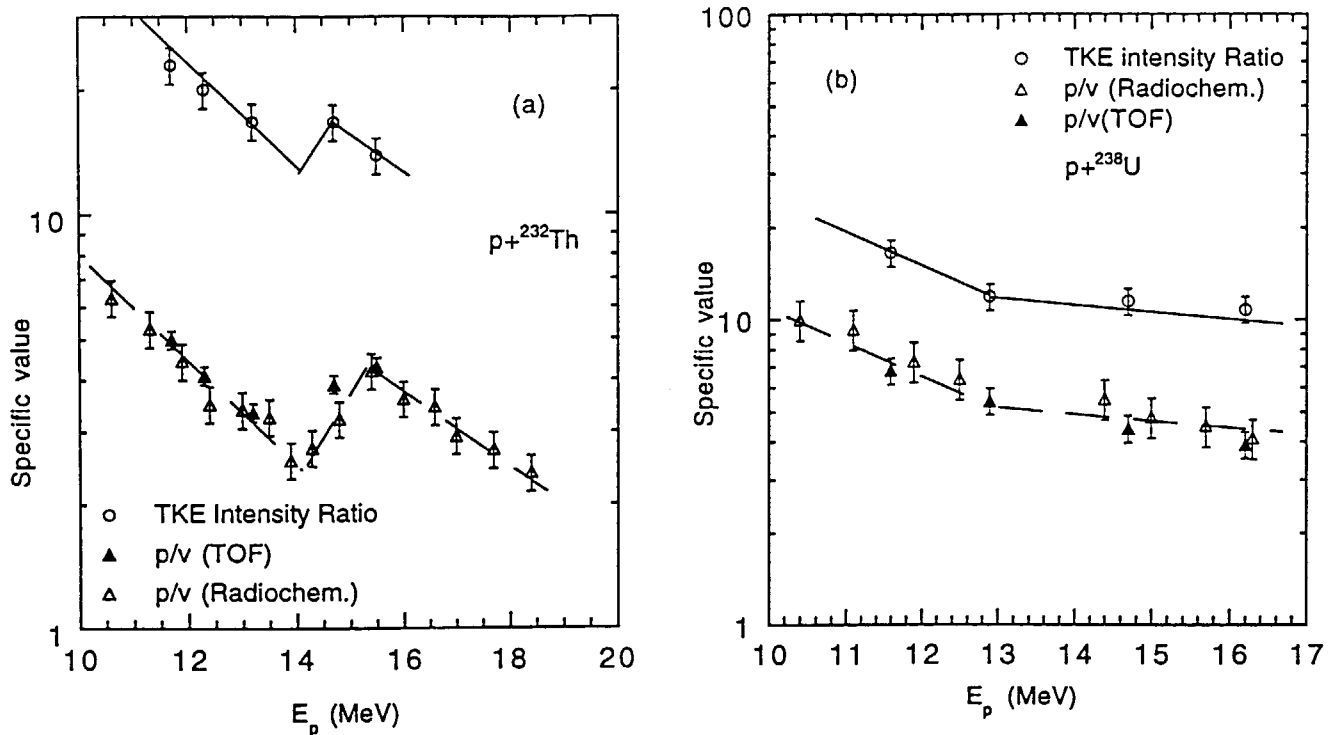
Fig. 1. The energy dependence of the intensity ratios for the TKE$_{high}$-/TKE$_{low}$-components, and the peak/valley ratios for the fragment mass yield distributions. The p/v ratios of the open triangles obtained by radiochemical method and the solid triangles by the TOF telescope, respectively. Figs. 1(a) is for $p+^{232}$Th and (b) for $p+^{238}$U fission.

References

1) H. Nakahara,et. al, J. Radioanal. Nucl. Chem., Articles, 142, 231 (1990);　E. Konecny, and H.W. Schmitt, Phys. Rev. 172, 1226 (1968);　H. Kudo, et. al, Phys. Rev. C 25, 3011 (1982);　M. G. Itkis, et. al, Nucl. Phys., A502, 243c (1989).

2) A. Turkevich et. al, Phys. Rev., 84, 52 (1951).

3) Y. Nagame, et. al, Phys. Lett. B387, (1996) 26;　E. K. Hulet, et. al, Phys. Rev. Lett. 56, 313 (1986);　T. Ohtsuki, et. al, Phys. Rev. Lett. 66, 17 (1991).

4) V.E. Viola, et. al, Phys. Rev. C 31, 1550 (1985);　B.D. Wilkins, et. al, Phys. Rev. C 15, 1832 (1976).

5) R. Vandenbosch, and G. T. Seaborg, Phys. Rev., 110. 507 (1958).

3.7 CORRELATION BETWEEN MASS DIVISION MODES AND NEUTRON MULTIPLICITY IN 12 MeV PROTON INDUCED FISSION OF ^{232}Th

I. NISHINAKA, Y.L. ZHAO [1], Y. NAGAME, K. TSUKADA, S. ICHIKAWA,
H. IKEZOE, Y. OURA [1], K. SUEKI [1], H. NAKAHARA [1], M. TANIKAWA [2],
K. TAKAMIYA [3], and K. NAKANISHI [3]

The average number of neutrons $\bar{\nu}$ emitted from fission fragments is closely related to the average excitation energies of fragments scince excitation energies are released by the neutron and γ–ray emission. $\bar{\nu}(A)$ has been investigated by indirect or direct measurement to know how the total excitation energy is shared by the two fragments in the mass division process. The sawtooth behavior of $\bar{\nu}(A)$ in low-energy fission of actinides is expected to be related to the fragment shell effects at A $\simeq$ 130 (Z = 50, N = 82).

The aim of this work is to investigate how the fragment shell effects at A $\simeq$ 130 relate to the mass division modes in the 12 MeV proton induced fission of ^{232}Th, by measuring $\bar{\nu}(m^*)$ coincident with fragment mass and E_k. The parts of experimental data of kinetic energy E_k and primary fragment mass have been published in the previous reports [1, 2], in which the correlations between the threshold energy, the total kinetic energy and the mass division mode was confirmed experimentally. In order to decompose the fission process into two modes from mass and kinetic energy distributions, we accurately obtained the velocities of the complementary fission fragment and kinetic energy of one fragment by time-of-flight and energy measurements. The number of prompt neutrons of fragment was determined indirectly from the difference of the primary and secondary fragment masses.

The mass division modes were decomposed into high-E_k asymmetric $Y_a(m^*, E_k)$ and low-E_k symmetric ones $Y_s(m^*, E_k)$ by fitting E_k distributions $Y_T(m^*, E_k)$ to two gaussians in the mass region of A= 98–107 and 127–135 as shown in fig. 1. The dotted- and dashed-lines correspond to asymmetric and symmetric modes, respectively. The neutron multiplicities were also decomposed clearly into the asymmetric and symmetric modes by fitting the $\bar{\nu}(m^*, E_k)$ curves as a function of E_k to two linear functions corresponding to two modes as follows:

$$\bar{\nu}(m^*, E_k) = \bar{\nu}_a(m^*, E_k)\frac{Y_a(m^*, E_k)}{Y_T(m^*, E_k)} + \bar{\nu}_s(m^*, E_k)\frac{Y_s(m^*, E_k)}{Y_T(m^*, E_k)},$$

$$\bar{\nu}_i(m^*, E_k) = \frac{\delta\bar{\nu}}{\delta E_{ki}}(m^*)E_k + \bar{\nu}_{i0}(m^*) \quad (i = a, s),$$

where the subscripts a and s refer to the asymmetric and symmetric modes, respectively. $\frac{\delta\bar{\nu}}{\delta E_{ki}}(m^*)$ and $\bar{\nu}_{i0}(m^*)$ are parameters of the fitting by two linear functions. The parameter of $\frac{\delta\bar{\nu}}{\delta E_{k\,s}}$ was fixed as 2.02×10^{-2} for $m^* = 116 - 117$. The calculated and experimental $\bar{\nu}(m^*, E_k)$ values are shown by thick solid lines and solid circles, respectively, in fig.1.

---

[1]Faculty of Science, Tokyo Metropolitan University
[2]School of Science, The University of Tokyo
[3]Faculty of Science, Osaka University

Thick dotted- and dashed-lines indicate decomposition of $\bar{\nu}(m^*, E_k)$ into the asymmetric and symmetric modes.

Figure 2 shows the mass yield curves and the average neutron multiplicities $\bar{\nu}$s as a function of the primary fragment mass. The dotted- and dashed-lines indicate the mass yield curves of the asymmetric and symmetric modes, respectively. $\bar{\nu}_a(m^*)$ for the asymmetric mode (solid circles) shows an increase from lighter to heavier masses in both the light- and heavy-fragment groups. The small values of $\bar{\nu}_a(m^*)$ in the region of A=128-134 (Z $\simeq$ 50 and N $\simeq$ 82) are seemed to be similar to those of the low-excitation fission of actinides. While, $\bar{\nu}_s(m^*)$ for the symmetric mode (open circles) increases monotonically with mass and no dip appears around mass number A $\simeq$ 130. The excitation energy of the fragments around A $\simeq$ 130 in the asymmetric mode is expected to be 20 MeV smaller than that in the symmetric mode, estimated from the defference between $\bar{\nu}_a(m^*)$ and $\bar{\nu}_s(m^*)$.

A dip of the non-decomposed $\bar{\nu}(m^*)$ (thick solid line) at A $\simeq$ 130 can be interpreted as a result of the contribution of the symmetric mode. The shell effects still remains strongly in the asymmetric mode in the fission even at medium excitation energy.

References

1) Y. Nagame et al., Phys. Lett. **B387**, (1996) 26.
2) Y. Nagame et al., Radiochim. Acta **78**, (1997) 3.
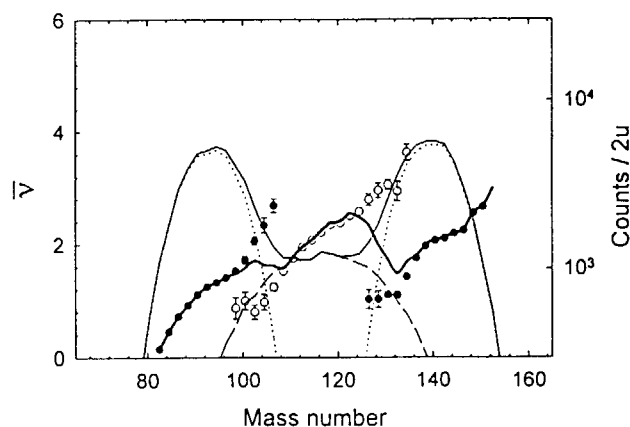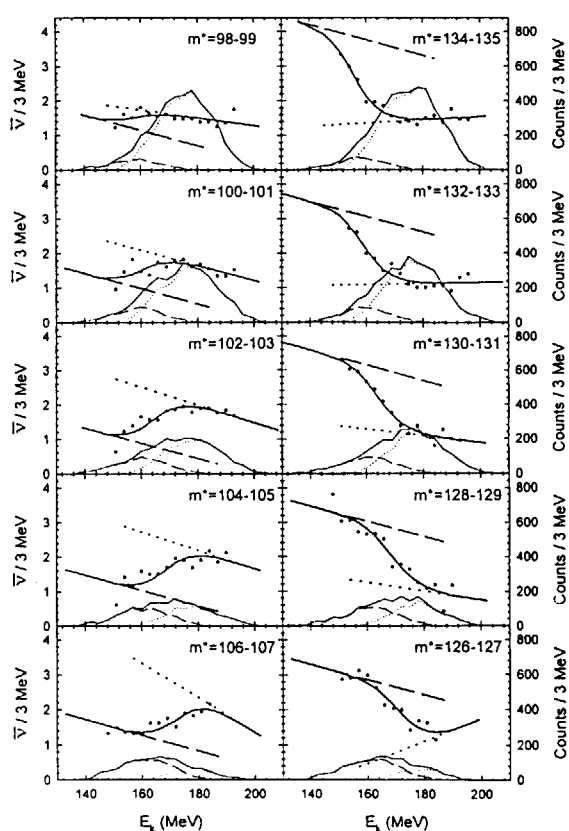
Figure 2. Mass yield curves and $\bar{\nu}$s as a function of the primary fragment mass.

Figure 1. $\bar{\nu}(E_k)$ (solid circles) as a function of E_k and E_k distributions (thin solid lines) for A = 98 – 107 and 127 – 135. The thick solid line shows the calculated $\bar{\nu}(E_k)$. The dotted- and dashed-lines correspond to the asymmetric and symmetric modes, respectively.

3.8 THE FRAGMENT EXCITAION ENERGY IN THE PROTON-INDUCED FISSION OF ^{238}U

K. NAKANISHI[1], K. TAKAMIYA[1], T. SAITO[2], A. YOKOYAMA[1], H. BABA[1],
I. NISHINAKA, Y. NAGAME, Y.L. ZHAO[3] and M. TANIKAWA[4]

The proton-induced fission reactions of ^{238}U with various excitation energies were observed. The excitation energy of fission fragment was estimated in order to elucidate the energy balance in the fission process.

The experiments were carried out at the tandem accelerator in Japan Atomic Energy Research Institute. In order to measure the time-of-flight of fission fragments, an MCP detector was used as the start detector and a PPAC was used as the stop detector. In addition, an SSBD was also used for a precise measurement of kinetic energy of the fission fragment coincident with a TOF event. The excitation energies of the compound nuclei were 16.9, 18.0, 19.8 and 21.3 MeV. In the present experiment, masses and kinetic energies of the fission fragments and multiplicities of the prompt neutrons were determined. The mass and kinetic energy distributions were divided to two components correlated with symmetric and asymmetric modes.

The excitation energies of fragments, EX_i, were calculated from the first moment of the number of emitted prompt neutrons[1] in the region where either of the components is predominant to the extent of 80% to the total yield of the relevant mass. The ratio of the excitation energy of fragments to the total excitation energy, TXE, was calculated as shown in Fig. 1 as a function of the fragment mass. Here TXE was obtained as the sum of EX_i of the complementary fragments. In Fig. 1, solid line indicates the calculated value with an assumption that the total excitation was distributed to the both fragments in proportion to mass number. The obtained values are close to the calculated line except for the mass regions 99<A<111 and 127<A<139. The excitation energies of the light fragments appear to be enhanced in the near symmetric region. In particular, the ratio at the mass number near 130 was small, and it suggests that the double spherical shell gives a large influence to the heavy fragment while the light fragment is subject to a strong deformation. Similarly, the ratio in the mass number around 90 is the least in the light fragment region.

Allowing for these results, we derived the scission configurations illustrated in Fig. 2 as

[1] Graduate School of Science, Osaka University
[2] Radioisotope Research Center, Osaka University
[3] Department of Chemistry, Faculty of Science, Tokyo Metropolitan University
[4] Department of Chemistry, School of Science, The University of Tokyo

possible postulates. The left-side picture indicates the configuration of symmetric fission. Fragments equally deformed are connected with a neck. The scission points, A, B and C give the linear excitation energy distribution. The right-side picture indicates the configuration of asymmetric fission. A spherical heavy fragment (A=130) and a slightly deformed light fragment (A=89) are connected with a neck (A=20). The scission point A gives a low-excited light fragment (A=89) and a highly excited (deformed) heavy fragment (A=150), and similarly, the scission point C gives a highly excited light fragment (A=119) and a low-excited heavy fragment(A=130). The case of the scission point B, that is, the center of the neck corresponds to the most probable division and the excitation energies of complementary fragments are comparable to each other, even for the configuration on the right side.

Reference

1) C. Wagemans, "The Nuclear Fission Process", CRC Press, Boca Raton, 1991, p.520.
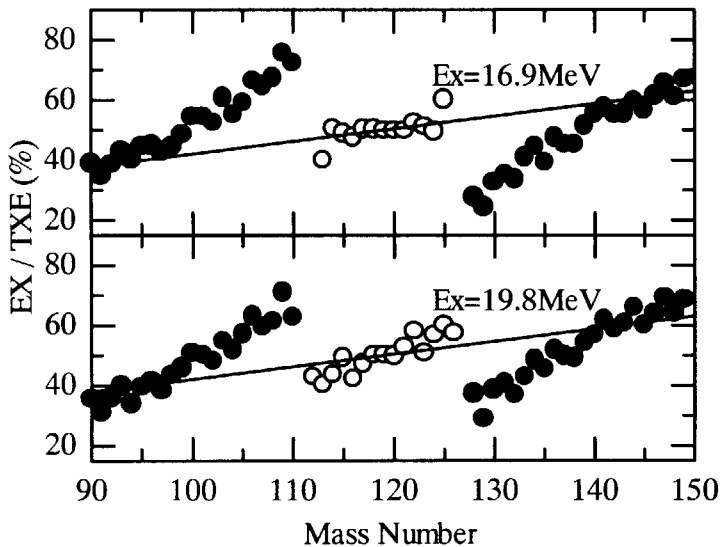
Fig. 1. Ratio of the fragment excitation energy EX to the total excitation energy TXE as a function of mass number. Upper and lower panels indicate the results of Ex = 16.9MeV and 19.8 MeV, respectively. Open and closed circles indicate the ratio of EX for symmetric and asymmetric components.
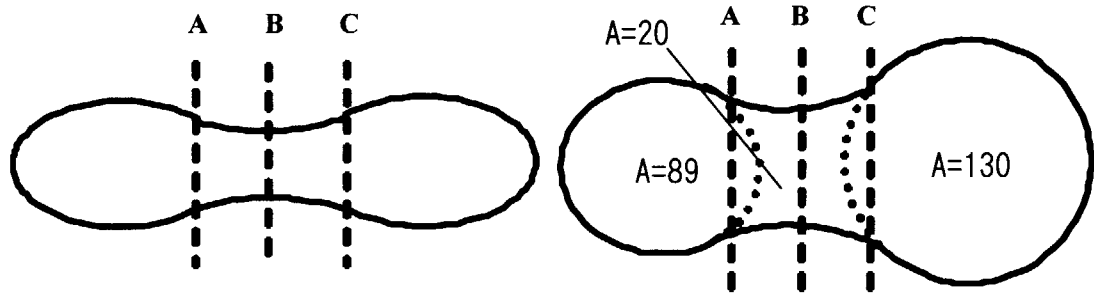
Fig. 2 The derived scission point configurations. Left- and right-side illustrations represent those for symmetric and asymmetric fission, respectively.

4. Nuclear Theory

This is a blank page.

4.1 New Scissors-type Excitation of Octupole-Quadrupole Deformed Nuclei

M. SUGITA

We discuss a new scissors-type excitation mode of the octupole-quadrupole deformed nuclei in terms of a geometrical model and the SDF and/or SPDF interacting boson models. This mode occurs due to a small angle oscillation of the relative orientation of the quadrupole- versus octupole-deformation [Fig. 1]. This mode is an isoscalar excitation, and it completely differs from the usual scissors mode between proton and neutron deformations [Fig. 2] describing the isovector magnetic dipole excitation.

In Refs. [1,2], we presented a unified description of the octupole and quadrupole deformed nuclei in terms of the SPDF boson model, taking the actinides as examples. In Ref.[2], by means of the projected Tamm-Dancoff method, we investigated the excited bands in ^{228}Th and suggested the existence of two low-lying beta bands; we referred to the lowest $K = 0^+$ band as the "super" beta band and the other one as the "usual" beta band. In addition to these beta bands, the SPDF boson model also predicts the existence of the $K = 1+$ band in a relatively low excitation energy Ex~ 1.2 MeV. We will present a close relationship between this low-lying $K = 1+$ band and the new scissors-type excitation, and also discuss the strong connections of this $K = 1+$ band to the "super" beta band. The isoscalar nature of the new scissors mode explains the relatively low excitation energy of the $K = 1$ band.

The new scissors mode can also be characterized by its decay scheme. We can expect possible M1 transitions from $J = 1^+$ to 0_1^+, relatively large E1 transitions from $K = 1+$ to $K = 1-$, and $\Delta K=1$ E2 transitions from $K = 1+$ to the ground band.

Weber et al [3-5] have recently done experiments on ^{228}Th and suggest the existence of the $K=1$ band at Ex~1.4 MeV. The new experimental data will be compared with our SDF/SPDF results. We will also discuss the relationship between the new scissors mode with the proton-neutron scissors mode.
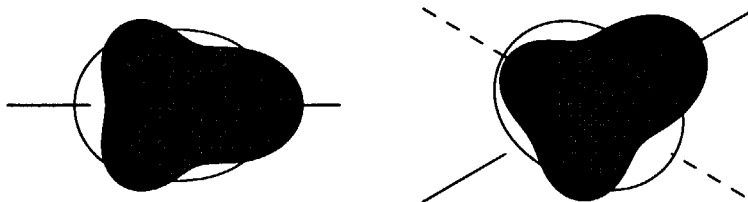
Figure 1: Quadrupole-octupole scissors mode
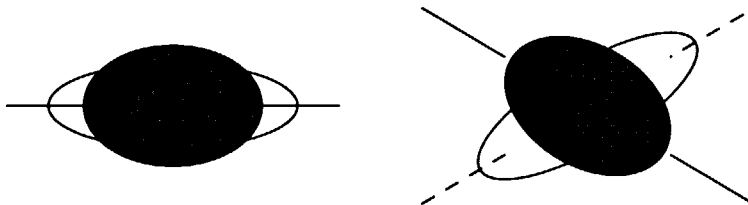
Figure 2: Proton-neutron scissors mode

References

1. T. Otsuka and M. Sugita, Phys.Lett.B209(1988)140
2. T. Otsuka and M. Sugita, J. Phys. Soc. Jpn. 58(1989)Suppl.530-537
3. T. Weber, J. de Boer, K. Freitag, J. Groeger, C. Guenther, J. Manns and U. Mueller
   Z.Phys.A 358 (1997) 281,
4. T. Weber, J. Groeger, C. Guenther and J. de Boer,
   Eur. Phys. J. A 1 (1998) 39
5. T. Weber, J. de Boer, K. Freitag, J. Groeger, C. Guenther, V.G. Soloviev,
   A.V. Suchkov, N.Lu. Shirikova, to be submitted to Eur. Phys. J. A

4.2 EFFECT OF NUCLEON EXCHANGE IN HEAVY-ION FUSION REACTIONS

A. IWAMOTO, V. KONDRATYEV[1] and A. BONASERA[2]

Multi-dimensional tunneling is most typically discussed for the subbarrier fusion of heavy-ions. The coupled-channel model and its classical analogues have been used extensively and the general understanding of the mechanism of the enhancement of the subbarrier fusion cross section was obtained.[1] However, when the projectile and the target both are heavy, the number of the intrinsic states to be coupled becomes so large and the realistic calculations exceed the capacity of the computer. We present here our model based on the Vlasov and imaginary-time methods[2, 3, 4]which can be applied in such heavy systems.

Starting point is the Vlasov equation written as

$$\frac{\partial f(\mathbf{r}, \mathbf{p}, t)}{\partial t} + \{h(\mathbf{r}, \mathbf{p}, t), f(\mathbf{r}, \mathbf{p}, t)\} = 0, \tag{1}$$

where $f(\mathbf{r}, \mathbf{p}, t)$ is one-body distribution function, the symbol $\{...\}$ represents the Poisson bracket and $h(\mathbf{r}, \mathbf{p}, t) = T + U(\rho, \mathbf{r})$ is the hamiltonian. This Vlasov equation is solved by test-particle method where the one-body distribution function is expanded by the superposition of delta function,

$$f(\mathbf{r}, \mathbf{p}, t) = \frac{1}{N} \sum_{i=1}^{N \times A} \delta(\mathbf{r} - \mathbf{r}_i(t))\delta(\mathbf{p} - \mathbf{p}_i(t)), \tag{2}$$

where N is the number of TP per nucleon and A is the total mass number. Inserting eq.(2) into eq.(1), we get the equation of motion for test particles.

$$\begin{cases} \mathbf{p}_i = m\dot{\mathbf{r}}_i, \\ \dot{\mathbf{p}}_i = -\nabla U(\mathbf{r}_i). \end{cases} \tag{3}$$

For simplicity and transparency, let's assume a fusion of mass-symmetric system with small overlap. We first define the collective coordinate of the fission process R and its conjugate momentum P as

$$\mathbf{R}(\mathbf{P}) = \int_B d\mathbf{r}d\mathbf{p} \; \mathbf{r}(\mathbf{p})f(\mathbf{r}, \mathbf{p}, t) - \int_A d\mathbf{r}d\mathbf{p} \; \mathbf{r}(\mathbf{p})f(\mathbf{r}, \mathbf{p}, t), \tag{4}$$

where A and B represent regions $z < 0$ and $z > 0$ respectively.

In the semiclassical theory of tunneling, the motion in classically forbidden region is effectively achieved by changing the time from real to pure imaginary. What happens is that the force coming from conservative potential changes sign. We follow this procedure for our

coordinate **R**. It is to be noted that there happens a nonlocal force acting on this collective coordinate in addition to the normal potential force. Since this nonlocal force has different time-reversal characteristics from a normal potential force, it plays a special role when we go to the classical forbidden region. By using the test-particles, the form of forces acting on collective coordinate are written as

$$F_{coll} = F^{local} + F^{nonlocal}, \tag{5}$$

$$F^{local} = \frac{1}{N} \sum \left\{ -s(z_i) \nabla_z U(\mathbf{r}_i) + \frac{2}{m} \delta(z_i) p_{zi}'^2 \right\}, \tag{6}$$

$$F^{nonlocal} = \frac{P^2}{2mN} \sum \delta(z_i), \tag{7}$$

where $s(z)$ represents the step function which takes minus and plus one for negative and positive values of z respectively, and $\mathbf{p}_i'$ represents the Fermi motion part of the momentum of a test particle. From this expression, we define the effective barrier as

$$V_{effective} = \int F_{coll} \, dR \tag{8}$$

and the potential barrier as

$$V_{pot} = \int F^{local} \, dR \tag{9}$$

It is to be noted that the delta-function parts of eq.(6) and (7) are coming from the particle exchange across the dividing plane. The former one comes from the normal Fermi motion and is thought to a pressure effect across the plane. On the other hand, the latter one is related to the collective motion, which represents the effect of dynamical particle exchange.

Finally, we find that in the tunneling region, we should change the equation of motion of test particles from eq.(3) to

$$\begin{cases} \mathbf{p}_i = m\dot{\mathbf{r}}_i, \\ \dot{\mathbf{p}}_i = -\nabla U(\mathbf{r}_i) - 2\frac{F^{local}}{A} s(z_i) \mathbf{e}_z. \end{cases} \tag{10}$$

In the numerical calculations [4], Skyrme force with compressibility 200MeV was used as a basic interactions. In addition, we used symmetry energy and surface term of Yukawa form adjusted to reproduce the $^{16}O+^{16}O$ barrier height for above-barrier reactions. The number of test particles are chosen as $N = 10^5$ and time-step of $\delta t = 0.2$fm/c ~ 0.05fm/c was used.

In Fig.1a, we show the potential barriers calculated according to our model for the head-on collision of $^{16}O + ^{16}O$. The case of incident energies below and above the barrier are shown to yield very similar interaction barriers, which rather well agree with the one extracted from experimental data. For an example of the medium-mass nuclei, we show in Fig.1b the case of $^{56}Ni + ^{56}Ni$. For heavy nuclei, the effects of deformation, neck formation and nonlocality become more important and affect the effective barrier height. What important is that at subbarrier energy, the effect of nonlocality tends to lower the barrier further, on the contrary, at above-barrier energies, the effect of nonlocality is to push the barrier height higher. At near barrier energies, the effect of nonlocality is very small. This nonlocal force has just the same properties as the coordinate dependent mass tensors[6].
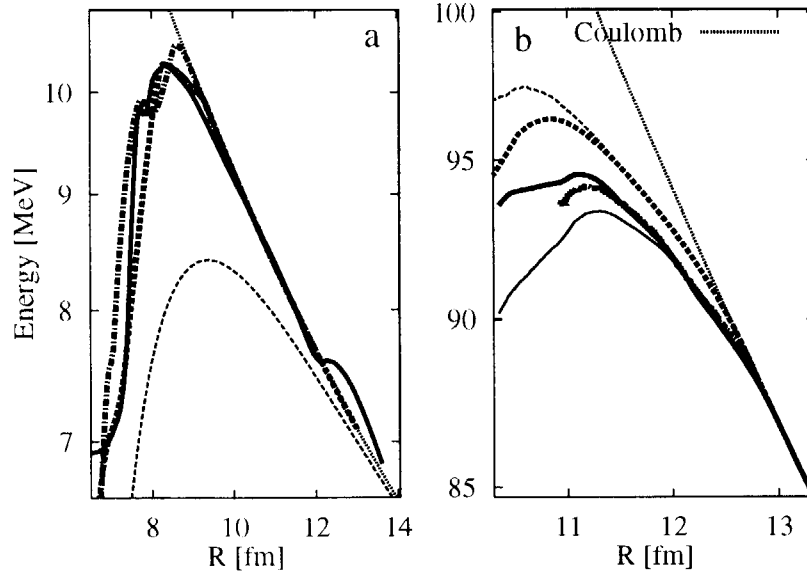
Figure 1: The potential for the fusion reaction. Left a-panel represents ^{16}O + ^{16}O system: the full line shows the empirical potential, the dashed and dashed-dotted lines are the results of the Vlasov simulation at energies 8 and 16MeV, respectively, the thin dashed line denotes the Bass parametrization[5]. Right b-panel shows the potential barriers(bold lines) and effective barriers (thin lines) obtained by the Vlasov simulation for ^{58}Ni + ^{58}Ni reaction at the energies 90MeV (solid lines), 93MeV (dashed-dotted lines, which start from 11fm and bold and thin lines almost coincide) and 145MeV (dashed lines). The thin dotted line gives the values of Coulomb interaction between the point-like object.

The effect of nonlocality is caused by the dynamical particle exchange across the dividing plane. Therefore, the particle exchange causes the barrier lowering for subbarrier energies and causes the barrier higher for above barrier energies. We expect that the former is responsible to the deep-subbarrier enhancement of the cross section which is very hard to reproduce by the coupled-channel model. On the other hand, the latter might be related to the extra-push phenomena. We expect that an entangled phenomena of subbarrier enhancement and above-barrier reduction of the cross section for heavy systems is related to this particle-exchange mechanism.

References

[1] see for example, Proc. Int. Workshop on "Heavy Ion Collisions at Near Barrier Energies", J. Phys.G23 no.10 (1997).

[2] A. Bonasera and A. Iwamoto, Phys. Rev. Lett. 78 (1997) 187.

[3] A. Bonasera, V.N. Kondratyev and A. Iwamoto, J.Phys. G23 (1997) 1297.

[4] V.N. Kondratyev and A. Iwamoto, Phys. Lett. B423 (1998) 1.

[5] R. Bass, Nucl.Phys. A231 (1974) 45.

[6] A. Iwamoto. Z. Phys. A 349 (1994) 265.

This is a blank page.

5. Atomic Physics, Solid State Physics and Radiation Effects in Materials

This is a blank page.

5.1 HIGH-RESOLUTION ZERO-DEGREE ELECTRON SPECTROSCOPY (IV)

M. IMAI[1], M. SATAKA, S. KITAZAWA, K. KOMAKI[2], Y. YAMAZAKI[2],
T. AZUMA[2], K. KAWATSURA[3], H. SHIBATA[4], Y. KANAI[5] and H. TAWARA[6]

Dynamic properties of the collision processes inside a solid have been one of the major interests in ion-solid interactions[1]. Zero-degree electron spectroscopy is an excellent tool to study these phenomena by measuring the secondary electrons emitted from the projectile and/or electrons captured or lost to the continuum[2]. Concerning the measurements of Coster-Kronig(C-K) electrons from Rydberg states, it has been shown that an intense series of electrons are observed as for gas target measurements[3-5] although they can not survive inside the solid, which indicates that the Rydberg states are formed upon or near the exiting surface of the solid. The three-step model for producing such Rydberg or convoy electrons and subsequent enhancement of high angular momenta are of great interest[6,7]. Another advantage in precise measurement of C-K electron is that the configurations inside the solid can be proved by specifying the core configurations of the observed Rydberg states.

In the present work, the authors have measured C-K electron from 2MeV/u silicon projectiles passing a carbon foil of 9.6 $\mu g/cm^2$ in thickness, and studied the charge state and its configurations inside the foil.

The experiment was performed at HIR2-2 beam line of the Tandem Accelerator of JAERI. The experimental apparatus have already been presented previously[4,5,7,8] only the major parameters are given here. Measured are the electrons emitted from silicon projectile passing through C-foil of $9.6\mu/cm^2$. Ions of 2MeV/u Si^{5+} were provided by the accelerator and injected directly into the target. Electrons emitted from the projectile were energy analyzed by a tandem electrostatic analyzer at zero degrees. The laboratory frame spectrum, which have a famous cusp-shaped peak around 1keV and C-K electron peaks on both wings of the cusp, is obtained by scanning the retarding potential between the first and the second analyzers. The projectile rest frame spectrum, obtained by converting the laboratory frame spectrum into the projectile rest frame, results in the energy resolution of 0.02~0.2eV.

In figure 1 we show the high energy wing electron spectrum from 2MeV/u Si^{5+} through C-foil of $9.6\mu g/cm^2$ in thickness. The most significant peaks, which are marked by (a) or (a') indicator, come from C-K transitions of Si^{10+} $1s^22p(^2P_{1/2}°)nl - 1s^22s(^2S_{1/2})\varepsilon l'$ or $1s^22p(^2P_{3/2}°)nl - 1s^22s(^2S_{1/2})\varepsilon l'$, respectively. For both indicators, the principal quantum number n is 9 for the 1st peak, and counts up as the peak energy grows. The marked energies are obtained as

$$\Delta E - Q^2 Ry/2n^2,$$

where ΔE is the energy difference between the initial and the final orbits of the core configuration, Q is the effective charge of the core configuration (assumed to be +11 for the cases above), and $Ry/2$ is the Rydberg energy 13.606eV. For ΔE, transition energy values compiled by Kelly[9] were used. Precisely speaking, the observed peak energies are a bit (~0.05eV at n=9) smaller than the calculated values, and the difference gets smaller; i.e., observed energies come to agree well, as n grows. These shifts must be from the quantum defect for angular momentum l of the Rydberg electron, and the n of the equation has to be

---

[1]Department of Nuclear Engineering, Kyoto University.

[2]Graduate School of Arts and Sciences, University of Tokyo.

[3]Department of Chemistry, Faculty of Engineering and Design, Kyoto Institute of Technology.

[4]Research Center for Nuclear Science and Technology, University of Tokyo.

[5]The Institute of Physical and Chemical Research (RIKEN).

[6]National Institute for Fusion Sciences.

replaced with $(n-\mu_l)$, where μ_l is a small value representing the quantum defect of the angular momentum.

Using the same formula (without μ_l consideration), we investigated all the configurations for Si X, XI, XII, XIII, XIV transitions in the reference[9], to obtain the possible C-K electron energies in this energy region for Rydberg states of $Si^{8,9,10,11,12+}$, respectively, and carefully checked the appearance of these peaks. Transitions of Si^{9+} $1s^22p^2(^1D_2)nl - 1s^22s2p(^1P_1°)\varepsilon l'$ for $n \geq 9$, Si^{11+} $1s2p(^1P_1°)nl - 1s2s(^1S_0)\varepsilon l'$ for $n \geq 14$ and Si^{11+} $1s2p(^3P_2°)nl - 1s2s(^3S_1)\varepsilon l'$ for $n \geq 12$ are found to be weighty candidates for other peaks, which are shown by (b), (c) and (c') indicators, respectively, in the figure. No other transition is found to consistently reproduce the series of peaks in the figure.

Taking the three step model into account, this indicates that Si^{11+} $1s^22p(^2P)$ state, Si^{10+} $1s^22p^2(^1D)$ state, Si^{12+} $1s2p(^1P)$ and $1s2p(^3P)$ states are formed inside the foil from the Si^{5+} projectile, while little fraction of other charge states can be formed inside the foil. The equilibrium mean charge for silicon of this energy through solid-carbon is known to be around 11.5[10]. Though ground state configurations can not be proved by this method, this spectrum must be a direct proof that Si^{10+}, Si^{11+} and Si^{12+} ions surely exist inside solid and lower charge state components are less when Si^{5+} projectile changes its charge in penetrating C-foil.
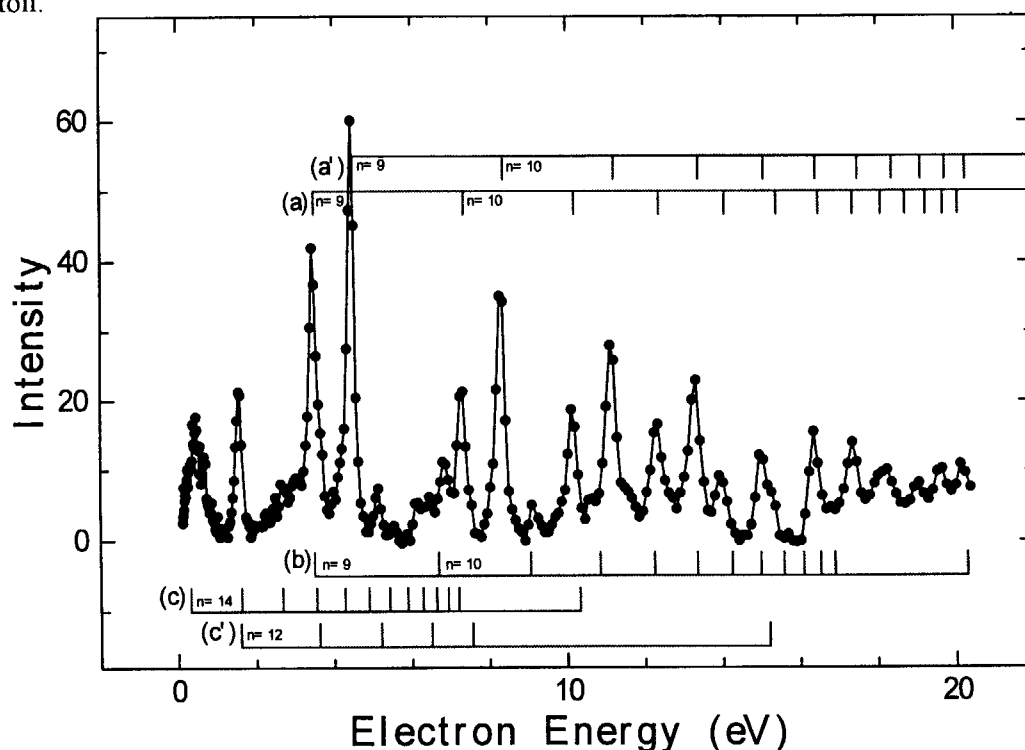
Fig.1. Spectrum of electrons ejected at 0 degree in 2MeV/u Si^{5+} + C(9.6μg/cm^2) collisions. The energy refers to the projectile rest frame.

References

1) Y.Yamazaki, Nucl. Instr. Meth. B96 (1995) 517.
2) N.Stolterfoht, Phys. Rep. 146 (1987) 315.
3) Y.Yamazaki et al., Phys. Rev. Lett. 61 (1988) 2913.
4) K.Kawatsura et al., Nucl. Instr. Meth. B48 (1990) 103.
5) K.Kawatsura et al., Nucl. Instr. Meth. B53 (1991) 421.
6) J.Burgdörfer and C.Bottcher, Phys. Rev. Lett. 61 (1988) 2917.
7) M.Imai et al., Nucl. Instr. Meth. B67 (1992) 142.
8) M.Sataka et al., Phys. Rev. A44 (1991) 7290.
9) R.L.Kelly, J. Phys. Chem. Ref. Data 16 Suppl. no. 1 (1987).
10) T.Ishihara et al., Nucl. Instr. Meth. 204 (1982) 235.

5.2 PARAMAGNETIC DEFECTS IN 6H SiC

Y. KAZUMATA[1], H. NARAMOTO AND M. SATAKA

The development of electronic devices resistant to radioactive radiation is required for space science and atomic power technologies. One of the most promising candidates in such semiconducting devices is silicon carbide (SiC). A considerable amount of work has been done on point defects in SiC, induced by irradiation such as electrons, neutrons and various kinds of ions. A brief review on paramagnetic radiation defects has been reported by Pavlov et al.[1]. Silicon carbide crystallizes in many structures called polytypes. In this report we focused on the 6H polytype which has the hexagonal structure.

In this experiment, single crystals of SiC in the size of 3x8x2 mm^3 were used. Three lines were observed in the esr spectrum prior to irradiation as shown in Fig.1. The lines were nearly isotropic for the rotation of angles between the c-axis of the crystal and applied magnetic field. The spectrum was described by the spin Hamiltonian,

$$H = \beta S \cdot g \cdot H + S \cdot A \cdot I \qquad (1),$$

where the first term describes the Zeeman term, and the second term gives the interaction between the electron spin and the nuclear spin I. The values of g and A obtained from the spectrum were 2.0039 and about 12 gauss, respectively, which values were in good agreement with those for nitrogen donors in SiC observed by Woodbury and Ludwig [2].
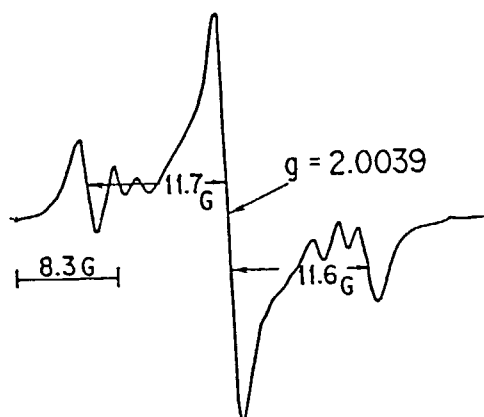
Fig.1. Esr spectrum of a 6H SiC single crystal prior to irradiation. Three lines separated by about 12 gauss are due to nitrogen donors.

The crystals containing nitrogen donors described just above were irradiated by 80 MeV N^{5+} ions to a dose of $\sim 10^{14}$ ions/cm^2 at a liquid nitrogen temperature (NT). After irradiation the crystals were once warmed up to room temperature and then were cooled down again to NT for measurements. The esr spectrum measured at NT consisted of six pairs of two lines, which were well described by the spin Hamiltonian,

$$H = \beta S \cdot g \cdot H + S \cdot D \cdot S \qquad (2).$$

The second term of this Hamiltonian gives the fine structure due to spin-spin

1. Nihon Advanced Technology Co.

interaction. The angular dependence of the spectrum with the rotation of the applied magnetic field to the c-axis of the crystal is shown in Fig.2 as open circles. The calculated values with $S = 1$, $g_{//}=2.0018$, $g_\perp=2.0092$ and D=592.5 gauss well describe the experimental spectrum as shown in Fig.2. This result suggests the model of the neutral carbon vacancy(V_c^0), as depicted in Fig.3, proposed by Balona and Loubser [3]. Standing on this model, D is calculated to be $-3g^2\beta^2/2R^3=-594.1$ gauss with R=3.61Å(the geometrical distance between atoms 1 and 2 in Fig.3), which is in fairly good agreement with the value obtained by the experiment mentioned just above.
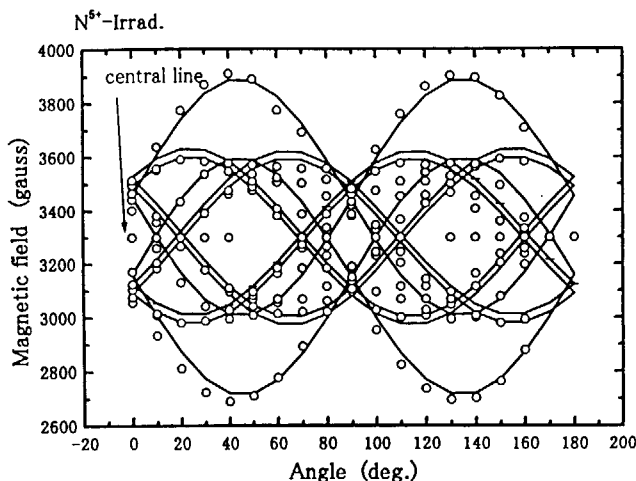
Fig.2. Angular dependence of the spectrum of 6H SiC irradiated by 80 MeV N^{5+} ions. Angles between the c axis and applied magnetic field are shown in the x-axis, and the positions of the lines in the applied field are in the y-axis. Open circles denote the experimental line positions, and solid lines are derived from the calculation by eq.(2).

(A) Normal lattice   (B) The model of V_c^0
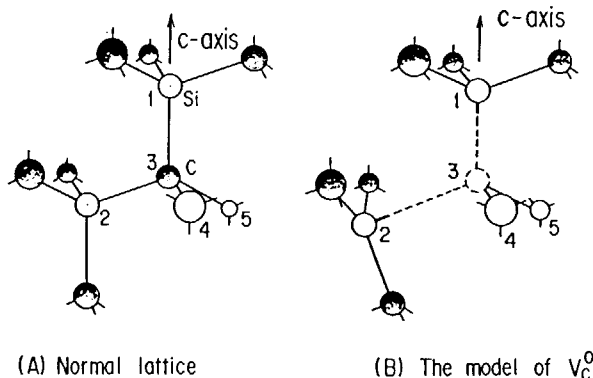
Fig.3. The model of neutral carbon vacancy (V_c^0) in 6H SiC proposed by Balona and Loubser from the citation of ref.[3].

Irradiation by 1 MeV p^+ and d^+, 120 MeV F^{7+} and 140 MeV Cl^{8+} promoted the growth of a single line at g=2.0035. This result indicates the formation of acceptors in consultation with the reference by Woodbury and Ludwig[2].

References
[1] N.M. Pavlov, M.I. Iglitsyn, M.G. Kosaganova, V.N. Solomatin, and
     Yu.V. Barinov, Sov. Phys.Solid State 13(1972)2363.
[2] H.H. Woodbury and G.W. Ludwig, Phys. Rev. 124(1961)1083.
[3] L.A.de S. Balona and J.H. Loubser, J. Phys. C:Solid St. Phys. 3(1970)2344.

5.3 EMISSION OF SECONDARY IONS FROM CONDUCTIVE MATERIALS BOMBARDED WITH HEAVY IONS

T. SEKIOKA[1], M. TERASAWA[1], M. SATAKA and S. KITAZAWA

Recently, the electronic sputtering in conductive materials has been attracting great interest. Several experiments have been performed to investigate the incident charge state dependence of the secondary ion yield from conductive materials irradiated with low energy highly charged ions (HCI) [1-3], and the incident charge state dependence of the energy loss of low energy HCI through thin carbon foils [4]. The results of the experiments suggest the importance of the electronic excitation effect in the interaction between low energy HCI and the conductive solid targets.

We have studied the secondary ions mass spectra from thin conductive solid targets irradiated with heavy ion beams from the JAERI tandem accelerator at the energy regions where the electronic stopping power is dominant. It is interesting to study the electronic sputtering in the conductive materials in a different way from the experiment using low energy HCI. Very fast neutralization occurs when a low energy HCI collides with a conductive material, so that the electronic excitation energy is deposited in a small region of the solid surface. On the contrary, when a high energy heavy ion penetrates a solid target, the electronic excitation energy is deposited along the ion track. It is also important to study the fundamental process of the extended defects production in a solid irradiated with high energy heavy ions.

The C-foil of $30\mu g/cm^2$ thickness, Ni, Cu and Au foil targets of approximately 1000Å thickness evaporated on C-foils were irradiated with high energy heavy ions beam from the tandem accelerator. The secondary ions ejected from the front surface of the target were collected by a time of flight (TOF) mass spectrometer by applying an acceleration voltage of $-500V$ and detected by an electron multiplier. Secondary electrons from the back side of the target were detected by another electron multiplier and this signal was used as a start signal of the TOF. The projectiles were 80 and 100 MeV I ions, 120, 200 and 300 MeV Au ions and 100 MeV Ni ions. We also measured the secondary ion yield from C and Au foils bombarded with 0.5, 0.8 and 1.0 MeV C^+ ions from the Van de Graaff accelerator.

Figure 1 shows the yield of the secondary ions of C^+, Ni^+, Cu^+ and Au^+ from C, Ni, Cu and Au target respectively, normalized by the counts of secondary electron signal as a function of the electronic stopping power. The values of the electronic stopping power are obtained from ref.[5]. As can be seen in the figure, the secondary ion yield increases remarkably above an electronic stopping power of 2keV/Å, and can be approximately fitted by $(dE/dx)^2$. The solid line in the figure represents the slope of $(dE/dx)^2$. On the contrary, in the region of electronic stopping power of 100eV/Å, the dependence of the secondary ions yield on the electronic stopping power is weak or declined.

The strong dependence of the secondary ion yield from conductive materials on the electronic stopping power suggests that even in the conductive materials, the electronic excitation effects play an important role in the secondary ion sputtering. To confirm this experimental results, it is important to study secondary ions mass spectroscopy in a wide range of electronic stopping power with various combinations of projectiles and conductive targets. In order to improve the resolution of the mass spectroscopy, we are planning to develop a magnetic spectrometer, which is also useful to measure the secondary ions from bulk solid targets.

---

[1] Faculty of Engineering, Himeji Institute of Technology

References
1) M.Terasawa, T.Sekioka, T.Mitamura, S.Winecki, M.P.Stöckli and C.L.Cocke, Physica Scripta, T73, 326 (1997)
2) Robert W.Schmieder and Robert J.Bastasz, Nucl. Instrum. Methods B43, 318 (1989)
3) T.Schenkel, M.A.Briece, A.V.Barnes, A.V.Hamza, H.Schmidt-Böcking, K.Bethge and D.H.Schneider, Phys. Rev. Lett., 78, 2481 (1997)
4) T.Schenkel, M.A.Briece, K.Bethge, H.Schmidt-Böcking and D.H.Schneider, Phys. Rev. Lett., 79, 2030 (1997)
5) J.F.Ziegler, Handbook of 'Stopping Cross-Sections for Energetic Ions in all Elements' (The Stopping and Ranges of Ions in Matter 5) (Pergamon, 1980)
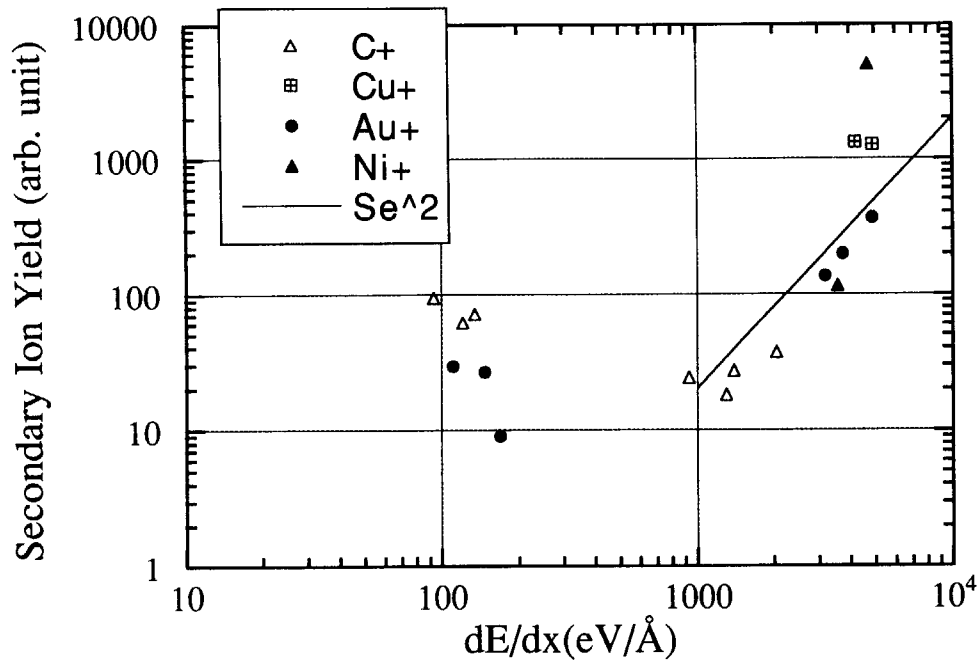
Fig. 1. The yield of the secondary ions of C^+, Ni^+, Cu^+ and Au^+ normalized by the counts of secondary electrons signal as a function of the electronic stopping power. The values of the electronic stopping power are obtained from ref.[5]. The solid line represents the slope of $(dE/dx)^2$.

5.4 ELECTRONIC EXCITATION EFFECTS
ON DEFECT PRODUCTION AND ANNIHILATION IN Fe
IRRADIATED WITH ENERGETIC IONS

Y. CHIMI, A. IWASE and N. ISHIKAWA

In the last decade, atomic displacements due to the high density electronic excitation have been found in several FCC metals irradiated with high energy (~100MeV) heavy ions [1]. Also, in the case of Fe which is one of the typical BCC metals, it has been observed that damage recombination and damage production are induced by the electronic excitation due to GeV-ion irradiations [2]. In the present work, we performed ~100MeV heavy ion irradiations in Fe at low temperature (~80K) and measured the electrical resistivity change as a function of ion fluence. By comparing the results with those for low energy (~1MeV) ion- and electron-irradiations, the effects of electronic excitation on defect production and annihilation in Fe could be observed clearly. The present results qualitatively agree with those for GeV-ion irradiations [2].

The specimens were polycrystalline Fe thin films about 190~370nm thick deposited on α-Al_2O_3 single crystal substrates by rf magnetron sputtering with an Fe target (99.99%) using Ar gas. These films were irradiated with the following particles; 0.5MeV ^{1}H, 1.0MeV ^{4}He, 1.0MeV ^{12}C, 1.0MeV ^{20}Ne, 2.0MeV ^{40}Ar, 120MeV ^{35}Cl, 150MeV ^{58}Ni, 125MeV ^{79}Br, 185MeV ^{127}I, 200MeV ^{127}I and 200MeV ^{197}Au ions and 2.0MeV electrons. As the projected ranges of these particles in Fe are much larger than the film thickness, most of the incident particles can pass through the specimen without remaining as impurities and the irradiation-produced defects are distributed uniformly in the specimen. In order to suppress the thermal motion of irradiation-produced defects in Fe, the irradiations were performed at liquid-N_2 temperature (~80K), because most of interstitials in Fe cannot move up to ~80K. During irradiation, the electrical resistivity of the specimen was measured at appropriate particle fluence intervals.

The defect production cross-section, σ_d, and the defect annihilation cross-section were evaluated from the experimental results. By analyzing the resistivity change rate, it seems that defects which have two sorts of stability against the radiation annealing were produced by high energy ion-irradiation. The defect production cross-section means the concentration of defects produced by the unit fluence of incident particles. The damage efficiency, ξ, is defined as $\xi = \sigma_d^{exp} / \sigma_d^{cal}$, where σ_d^{exp} is the experimental value of σ_d, and σ_d^{cal} is the value calculated by assuming that the defect production occurs only by the elastic interaction between incident particles and target atoms. The values of σ_d^{cal} for all ion-irradiations were calculated by using TRIM-92 [3]. For electron-irradiation, where the velocity was relativistic, the differential scattering cross-section analytically evaluated by McKinley and Feshbach [4] was used for the calculation of σ_d^{cal}.

In Fig. 1, the normalized damage efficiency, ξ/ξ_e, for each irradiation is plotted as a function of the PKA median energy, $T_{1/2}$, where ξ_e is the damage efficiency for electron-irradiation and $T_{1/2}$ is characteristic of the PKA energy spectrum [5,6]. The value of ξ_e should be close to 1, because the incident electrons produce mainly simple Frenkel pairs and not cascade damage. The normalized damage efficiencies, ξ/ξ_es, for low energy ion-irradiations show the same tendency as previous works in several FCC metals [1,5,6]. It indicates that the elastic interactions are dominant for the

defect production during low energy ion-irradiations. In the case of 125MeV ^{79}Br, 185MeV ^{127}I, 200MeV ^{127}I and 200MeV ^{197}Au ion-irradiations, the value of ξ/ξ_e is much larger than that for low energy ion-irradiation at the same $T_{1/2}$. It implies that the electronic excitation by these irradiations, which have comparatively large S_e above ~30MeV/(mg/cm^2), contributes a great deal to the defect production. A similar behavior was observed in GeV-ion irradiated Fe [2], where the damage efficiency increases abruptly above S_e~50MeV/(mg/cm^2).

References

1) A.Iwase and T.Iwata, Nucl. Instrum. Methods **B90**(1994)322; and references therein.
2) A.Dunlop, D.Lesueur, P.Legrand, H.Dammak and J.Dural, Nucl. Instrum. Methods **B90**(1994)330.
3) J.P.Biersack and L.G.Haggmark, Nucl. Instrum. Methods **174**(1980)257.
4) F.Seitz and J.S.Koehler, in: Solid State Physics, eds., F.Seitz and D.Turnbull, **Vol.2** (Academic Press, New York, 1956), p. 305.
5) R.S.Averback, R.Benedek and K.L.Merkle, Phys. Rev. **B18**(1978)4156.
6) R.S.Averback, R.Benedek, K.L.Merkle, J.Sprinkle and L.J.Thompson, J. Nucl. Mater. **113**(1983)211.
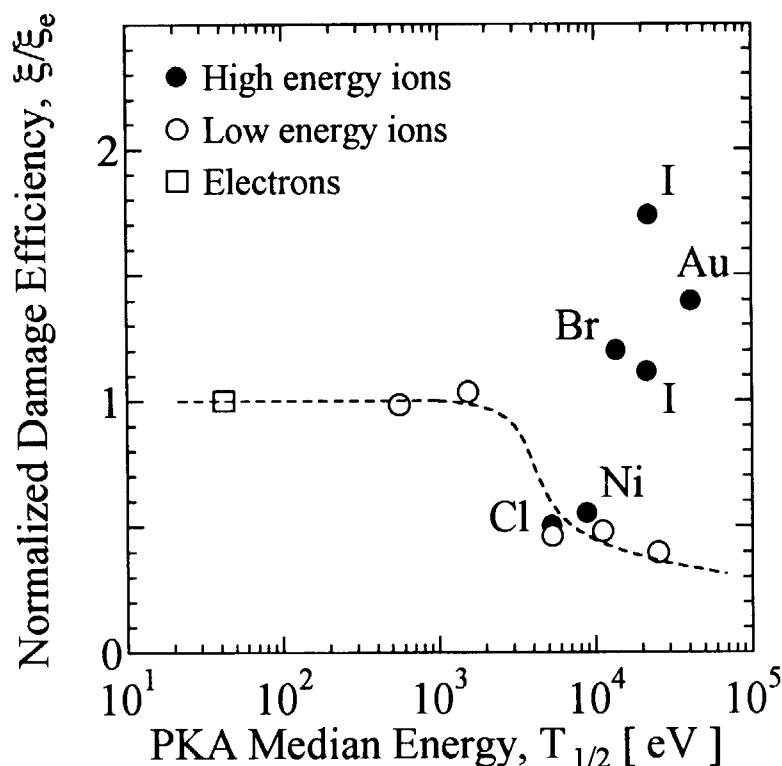
Fig. 1. Normalized damage efficiency, ξ/ξ_e, plotted against the PKA median energy, $T_{1/2}$, for each irradiation.

5.5 DAMAGE EFFICIENCY IN 180-MeV Fe-IRRADIATED Bi-2212 CRYSTALS:AN ION-VELOCITY-FREE PHENOMENON

D.X. HUANG, Y. SASAKI, S.OKAYASU, T. ARUGA and K. HOJOU

Ion irradiation is one of the most effective methods to artificially create crystal defects in superconductors. This kind of defects can act as flux-pinning sites and prominently increase the critical current density (Jc). Since the efficiency of irradiation-induced defects in flux pinning strongly depends on their microstructures and distributions, the morphologic study of such defects is simply very important step in clarifying the origin of flux pinning in ion-irradiated superconductors. In this study, we report on the continuous cross-sectional observation of irradiation damage morphology in 180-MeV Fe-irradiated Bi-2212 crystals. Combining with the experimental data reported previously, we emphatically discussed the influence of ion velocity on the damage efficiency and the influencing factors for the stopping power (dE/dx) threshold to produce columnar defects in Bi-2212 crystals.

The Bi-2212 single crystals used for ion irradiation were prepared using the floating-zone melting method. The crystals were cleaved into thin sheets of about 25 μm thick along a-b plane and cut to about 1-mm wide and 2-mm long. Perpendicular to the surface of the thin sheets, 180-MeV Fe-ion irradiation was performed with a dose about 3.3×10^{11} ions/cm^2 at room temperature using a Tandem accelerator at Japan Atomic Energy Research Institute. The usual method was used for the cross-sectional sample preparation of the irradiated Bi-2212 crystals. The TEM analyses for the damage morphology were performed using a Topcon EM-002B high-resolution TEM operated at 200 keV.

The change of the irradiation-damage morphology along Fe ion traces is shown in Fig. 1. As the reported results in 230 MeV Au-irradiated Bi-2212 crystals [1], the irradiation-damage morphology changed gradually from parallel columnar defects to deflected columnar defects, cascade-dotted columnar defects, ordered cascade defects and finally disordered cascade defects. Usually, the produced columnar defect size will also be decreased as the incident ion penetrates the target crystal and loses its energy gradually. In the case of Fe-irradiated Bi-2212 crystals,
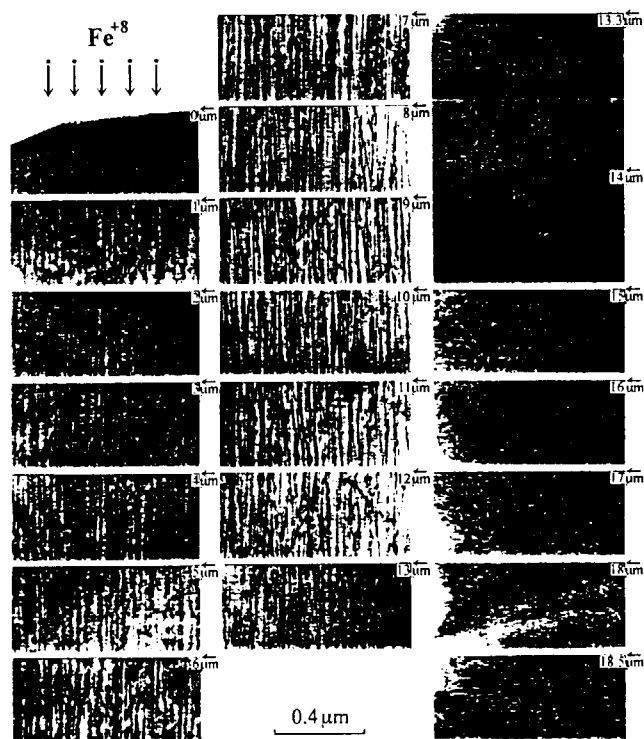
Fig. 1 A series of right-field images taken along the Fe-ion penetration path.

[1]Japan Fine Ceramics Center, 2-4-1 Mutsuno, Atsuta-ku, Nagoya 456, Japan

however, the columnar defect size was found to be almost a constant of ~ 3 nm in diameter in a large penetration depth region from the bombarded surface to the depth of about 13.5 μm in the target crystal.

Fig. 2 shows the change process of damage efficiency ε (ε = A/dE/dx, A is the damage cross section) with ion velocity in 180 MeV Fe-irradiated Bi-2212 crystals. As a comparison, the data of 230 MeV Au-irradiated Bi-2212 and 129MeV Xe-irradiated YIG (ferrimagnetic yttrium garnet) are also shown in the same figure. In this figure, we can clearly see that the damage efficiency usually strongly depends on the ion velocity and it appears a maximum value when the ion velocity is about 0.06 c (c, light velocity). However, in the case of Fe-irradiated Bi-2212, there is not such a peak-value of ε around the value of ion velocity of 0.06 c. The change of damage efficiency seems not sensitive to the change of ion velocity. The threshold of dE/dx to produce columnar defects in Fe-irradiated Bi-2212 crystals was estimated to be about 9 keV/nm by comparison of the TEM analyses and a calculation result of the stopping power using EDEP-1 code, which is much lower than the threshold (16 keV/nm) estimated in Au-irradiated Bi-2212 crystals.
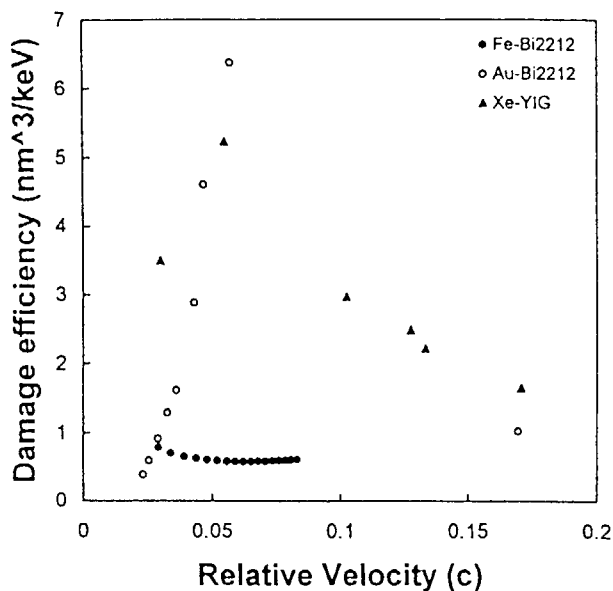
Fig. 2 Change of damage efficiency with the ion velocity in Fe-, and Au-irradiated Bi-2212 crystals and in Xe-irradiated YIG.

Reference
[1] D. X. Huang, Y. Sasaki, S. Okayasu, T. Aruga, K. Hojou and Y. Ikuhara, Phys. Rev. B 57, 1-8 (1998).

5.6 COLUMNAR DEFECTS IN HIGH-T$_c$ SUPERCONDUCTOR IRRADIATED WITH ENERGETIC IONS

N. ISHIKAWA, Y. CHIMI, A. IWASE, K. TSURU[1], O. MICHIKAMI[2]

When high-T$_c$ superconductors are irradiated with high energy heavy ions, and the energy deposited to the electrons of a target is high enough, columnar defects are formed along the ion paths[1].   The diameter and the resistivity of the damaged region have been determined from the resistivity-fluence curves. The results are discussed in terms of electronic stopping power, S$_e$.

The *in-situ* measurements of fluence dependence of electrical resistivity at 100K were performed for EuBa$_2$Cu$_3$O$_y$ (EBCO) irradiated at 100K with various energetic ions (Cl, Ni, Br, and I) at energy of 90-200MeV from the tandem accelerator at JAERI-Tokai.   All ion-irradiations were performed keeping the temperature at 100K.   The values of $\Delta\rho/\rho_0$ were measured *in-situ* as a function of fluence, Φ, at 100K by the standard four probe method, where $\Delta\rho$ is the change in resistivity, and ρ_0 the resistivity before irradiation.   Fig.1 shows $\Delta\rho/\rho_0$ plotted as a function of Φ in EBCO irradiated at 100K.
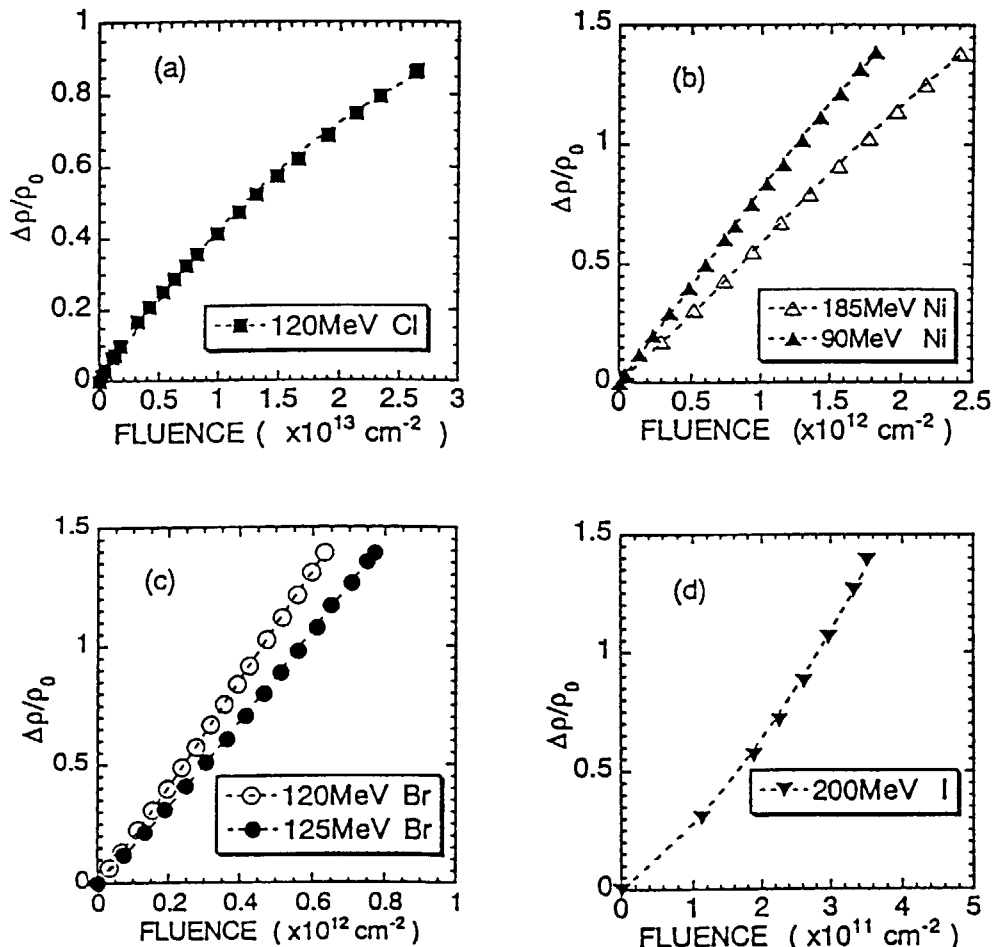
Fig.1

The fluence dependence of $\Delta\rho$ normalized by ρ_0 in EBCO irradiated with (a)120MeV Cl, (b) 90MeV and 185MeV Ni, (c)120MeV and 125MeV Br, (d)200MeV I. The dotted lines are the result of fitting the data with the equation (1).

---

1 Information Hardware Systems Laboratory, NTT Integrated Information & Energy Systems Laboratories.
2 Faculty of Engineering, Iwate University.
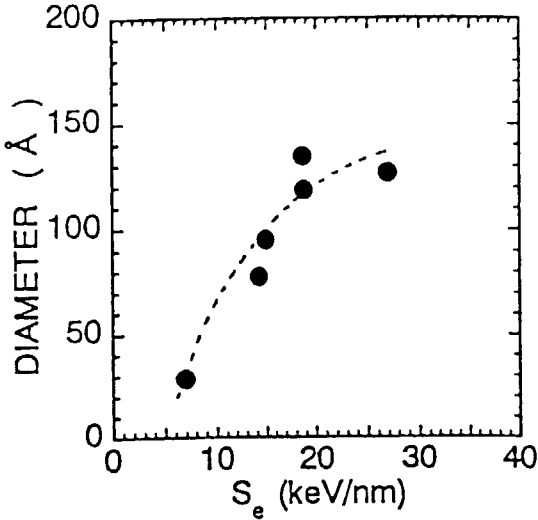
Fig.2

Diameter of the damaged region plotted as a function of electronic stopping power, S_e.
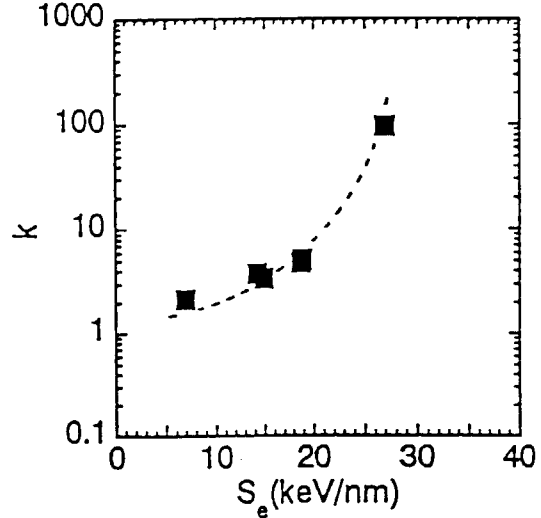
Fig.3

The value of k ($=\rho'/\rho_0$) plotted as a function of electronic stopping power, S_e.

The increase in normal-state resistivity due to irradiation is observed. The slope of the curves decreases with increasing fluence when EBCO is irradiated with 120MeV Cl, 90MeV Ni, and 185MeV Ni. On the other hand, the slope of the curve increases with increasing fluence when EBCO is irradiated with 120MeV Br, 125MeV Br, and 200MeV I. It is assumed that the damaged region has a cylindrical shape along ion path and a higher resistivity than the undamaged matrix region. When the cylindrically damaged region is introduced, the resistivity as a function of fluence is expressed by the following equation[2-4].

$$(\rho(\Phi)-\rho') (\rho_0/\rho(\Phi))^{0.5} = (1-\delta) (\rho_0-\rho'). \qquad (1)$$

In this equation, $\rho(\Phi)$ is the resistivity of irradiated sample measured perpendicular to the irradiation direction. The resistivity inside the damaged region is defined as $\rho'=k\rho_0$, where k(>1) is a constant which depends on the irradiating ions and energies, δ is the volume fraction of the damaged region and is assumed to follow $\delta=1-e^{-A\Phi}$, where A is a cross section of the damaged region. The value of ρ_0 is the resistivity of the undamaged region. By varying the values of k and A, we find that the observed $\Delta\rho/\rho_0-\Phi$ curves are reproduced. The dotted lines in Fig.1 are the lines fitted according to the equation (1) by taking A and k as fitting parameters. The diameter of the damaged region, $D=(4A/\pi)^{1/2}$, and $k=\rho'/\rho_0$ are plotted as a function of electronic stopping power, S_e in Fig.2 and Fig.3, respectively. We find that both the diameter and k increase with increasing S_e.

References
1) V. Hardy, D. Groult, M. Hervieu, J. Provost, and B. Raveau, Nucl. Instr. Meth. in Phys. Res. B54, 472 (1991).
2) J.W.Rayleigh, Phil. Mag. 34 (1892) 481.
3) D. A. G. Bruggeman, Annalen der Physik [5] 24, 636 (1935).
4) S.Klaumunzer, Rad. Eff. Defects Solids, 126, 141 (1993).

5.7 EFFECT OF HIGH-ENERGY HEAVY-ION IRRADIATION ON THE SUPERCONDUCTING PROPERTIES OF Bi-2212 SINGLE CRYSTALS

K.OGIKUBO[1], T.KOBAYASHI[2], T.TERAI[2], S.OKAYASU and K.HOJO

Particle-beam irradiation is one of the most promising methods to introduce strong pinning centers into High-T_c superconductors. We have been studying magnetic property change of $Bi_2Sr_2CaCu_2O_{8+y}$ (Bi-2212) single crystal due to irradiation with several kinds of particles such as light and heavy ions, neutrons and electrons. In order to realize a particle-beam irradiation technique as a method for J_c enhancement, many different conditions such as the kind, the energy and the fluence of particles should be examined. In particular, high-energy heavy-ions are expected to produce columnar defects, which gives a very large pinning force for the vortices parallel to the defects. In this study, we show experimental results on the superconducting properties such as the critical current density J_c and the pinning force density F_p of Bi-2212 single crystals irradiated with several kinds of high-energy heavy-ion beam.

The Bi-2212 single crystal specimens used were prepared by the floating-zone method. Their size was $2mm \times 2mm \times 0.1mm$. The specimens were irradiated with heavy-ion beam ($200MeV\ Au^{13+}$, $180MeV\ Cu^{11+}$ or $100MeV\ Cu^{9+}$) parallel to the c-axis with a tandem accelerator at JAERI. The fluences were from 1×10^{10} to $5 \times 10^{11}\ cm^{-2}$. Magnetization curves of the specimens were measured with a vibrating sample magnetometer at 20, 40 and 60K as a function of applied magnetic field parallel to the c-axis. The critical current density in a-b plane was calculated from the magnetization hysteresis curve using the modified Bean's model[1].

The critical current density J_c calculated from the magnetization curve increased due to irradiation all over the range of fluence and magnetic field regardless of ion species. The fluence dependence of J_c at typical conditions of magnetic field and temperature is shown in Fig.1. J_c took a maximum value around the fluence of $5 \times 10^{10} cm^{-2}$ and decreased at higher fluence for Au irradiation. On the other hand, J_c increased monotonously with the fluence up to $5 \times 10^{11}\ cm^{-2}$ for Cu irradiation.

In Fig.2, the macroscopic pinning force density F_p ($= J_c \times B$) curves for Au and Cu irradiation are compared. At the fluence of $5 \times 10^{10} cm^{-2}$, the value of F_p for Cu irradiation is approximately 10% of F_p for Au irradiation. F_p for Cu irradiation at the fluence of $5 \times 10^{11} cm^{-2}$ was comparable to F_p for Au irradiation at $5 \times 10^{10} cm^{-2}$.

[1]Department of Quantum Engineering and Systems Science
[2]Engineering Research Institute
The University of Tokyo.
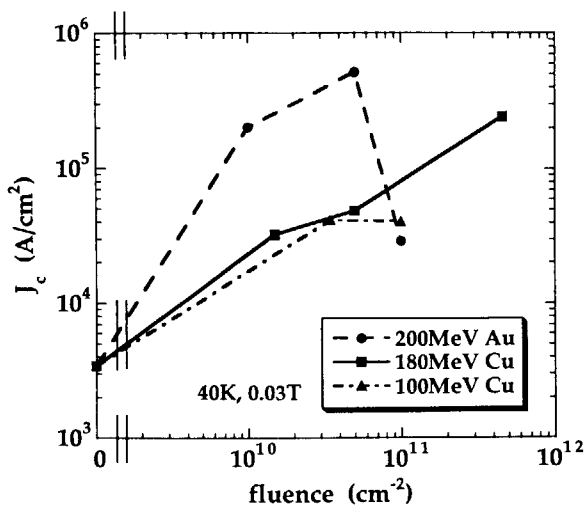
Fig.1 Fluence dependence of J_c
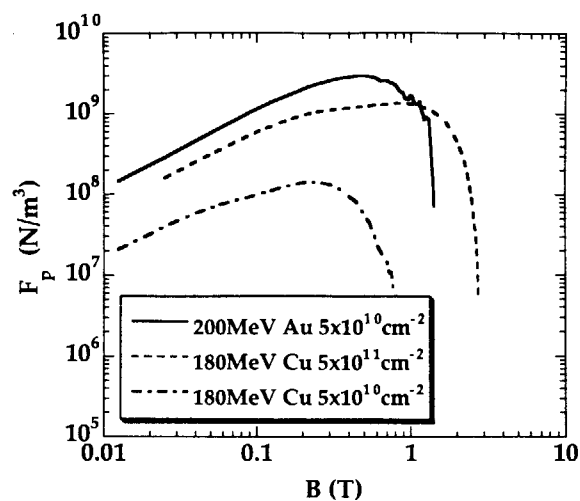
Fig.2 F_p for Au and Cu irradiation

To elucidate the reason of the difference behavior of J_c and F_p between Cu irradiation and Au irradiation, the electronic stopping power S_e of each species in Bi-2212 was calculated using TRIM code. As a result, the maximum value of S_e for Au and Cu irradiation are 30 and 14 keV/nm, respectively. It is expected that the density of columnar defects for Cu irradiation is very little, because the threshold value of the electronic stopping power to produce columnar defects in Bi-2212 seems to be about 16 keV/nm[2]. According to TEM observation on 230MeV Au-irradiated Bi-2212 single crystal[3], however, not only defect clusters along the ion tracks which have less pinning force than columnar defects but also columnar defects are produced around the region where S_e is nearly 14 keV/nm as much as the case of the Cu irradiation. Judging from these results, it is considered that less number of columnar defects and more number of defect clusters are produced by Cu irradiation than by Au irradiation.

References

[1] E.M. Gyorgy et al., *Appl. Phys. Lett.* **55** (1989) 283.
[2] M. Leghissa et al., *Europhys. Lett.* **19** (1992) 323.
[3] D.X. Huang et al., *Phys. Rev.* **B 57** (1998) 13907.

5.8   EFFECTS OF Au²⁴⁺ ION IRRADIATION
ON THE SUPERCONDUCTIVE PROPERTIES AND
MICROSTRUCTURE OF EuBa₂Cu₃Oₓ THIN FILMS

M.SASASE, S. OKAYASU, H. KURATA and K. HOJOU

Large enhancement in critical current density(J_c) has been observed so far in single crystal, thin films and bulk cuprates irradiated with high-energy heavy ions that produced a suitable density and size of columnar defects[1 - 3]. To clarify the relationship between superconductive properties and structures of the irradiated defects, we have investigated the effects of irradiation with energetic Au²⁴⁺ ions using superconducting quantum interface device (SQUID) magnetometer and transmission electron microscopy (TEM).

Specimens used in this study were EuBa₂Cu₃Oₓ thin films (300 nm). The specimens were irradiated with Au²⁴⁺ ions which were accelerated to 300 MeV with the fluence of 2.0 x 10¹⁰ ions/cm² at the room temperature using a tandem accelerator at JAERI. In order to irradiate the specimen with the wide range of ion energies, Au²⁴⁺ ions transmitted through thin Al foils mounted on the specimens were used. By changing the thickness of the Al foil, the irradiation energy was controlled. The ion energies were estimated from the range-energy relations proposed by Ziegler[4]. The range of the EuBa₂Cu₃Oₓ thin films was determined by the stopping powers calculated using TRIM codes[5]. In the present experiment the irradiation energies were varied to be 24, 85, 208 and 300 MeV. Magnetization hysteresis of the specimens before and after irradiation were measured with SQUID magnetometer. Crystalline structures of the EuBa₂Cu₃Oₓ films were measured by X-ray diffraction (XRD). Defects in the specimens were observed with TEM.

The enhancement ratio of J_c depends upon ion energy as shown Fig. 1. J_c was normalized to its initial film value J_{co} (before irradiation) at the magnetic filed of 0.1 T. We found that J_c increased with an increase in the Au²⁴⁺ ion energy and reached a value of 4.8 x 10⁶ A/cm² (5K, 0.1T) at 24 MeV. The irradiations with the higher energy than 85 MeV make the J_c values increase.

Fig. 2 shows the change in the c-axis lattice parameter determined by the diffraction angle of the (007) peak as the function of the ion energy. The peaks (007) position shifted to the lower angle side with increasing ion energy, which means that c-axis lattice parameter increases by ion irradiation. Similar results were also obtained for the other (00l) peaks. We found that C/C_0 increased with an increase in the Au²⁴⁺ ion energy at 24 MeV and C/C_0 decreased with an increase the ion energy.

In Fig. 3, we show TEM image of the EuBa₂Cu₃Oₓ thin films irradiated with 208 MeV Au²⁴⁺ ions. This lattice image was observed along the direction perpendicular to the c-axis. The crystallographic a and c-axis are indicated by the small arrows, while the large arrow identifies the
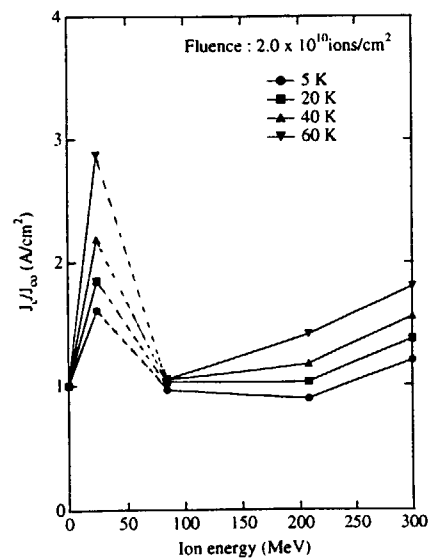
Fig. 1 Ion energy dependence of J_c enhancement ratio on EuBa₂Cu₃Oₓ films.

columnar defect produced by the Au^{24+} ion passing along this direction. The extended defect with an average diameter of about 6 nm appears to be amorphous along the large arrow in fig. 3.

In order to estimate the contribution of energy loss process to the defect formation in the present irradiation experiment, we calculated the energy loss (electronic and nuclear) in a $EuBa_2Cu_3O_x$ specimen for each incident ion energy using the TRIM code[5]. The values of electronic energy loss are increased with an increase in the Au^{24+} ion energy, which means that the electronic energy loss process in damage mechanism becomes important for high energy ions[2]. This is confirmed by the direct observation of columnar defect produced by 208 MeV Au^{24+} ion irradiation. The values of nuclear energy loss are increased with a decrease in the ion energy. The 24 MeV Au^{24+} ion irradiation has a maximum of nuclear energy loss in this experimental condition. Therefore, the increase in the c-axis lattice parameter observed at 24 MeV ion irradiation may be attributed to the expansion of the distance between ab-planes by the knocked-on atoms derived from cascade damages due to nuclear energy loss.

We suggest that the dominant damage mechanism might be changed on the border of incident energy of 85 MeV. The values of electric energy loss is about 20 keV/nm at 85 MeV, which can be regard as the threshold energy loss to produce the columnar defects for $EuBa_2Cu_3O_x$ films. This value is almost same as that reported for YBCO by Hensel[6].

Consequently, the enhancement of J_c observed above 85 MeV irradiation energy is attribute to the existence of columnar defects acting as strong pinning centers. But in order to interpret the enhancement of J_c observed at 24 MeV, it will be necessary to propose the new pinning mechanism based on the aggregation of small defects produced by cascade damage.

Fig. 2 Ion energy dependence of the change in c-axis lattice constant.
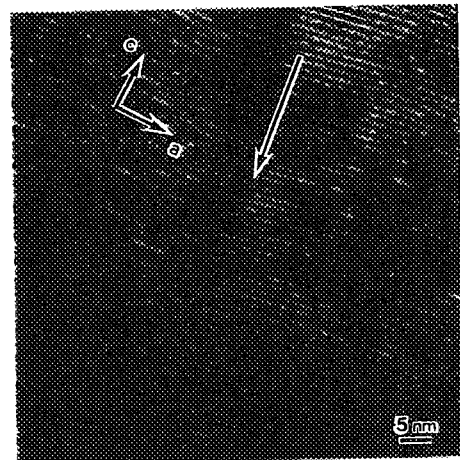
Fig. 3 A cross-sectional TEM micrograph of the defects produced inside the films. The Au^{24+} ions with an energy of 208 MeV were irradiated along the c-axis.

REFERENCE
[1] Y. Zhu, M. Suenaga and D. O. Welch, Phys.Rev.B, 48(1993)pp. 6436-6450.
[2] Y. Zhu, Z. X. Cai, R. C. Budhani, M. Suenaga and D. O. Welch, Phys. Rev., B48(1993)6436.
[3] L. Cival, A. D. Marwick, T. K. Worthington, M. A. Kirk, J. R. Thompson, L. Krusin-Elbaum, Y. Sun, J. R. Clem and F. Holtzberg, Phys. Rev. Lett., 67(1991)p. 648.
[4] J. F. Ziegler : Handbook of Stopping cross Section for Energetic Ions in All Element (Pergamon Press, New York, 1980).
[5] J. P. Biersack and L. G. Haggmark, Nucl. Instr. and Meth., 174(1980)p/ 257.
[6] B. Hensel, B.Roas, S. Henke, R. Hopfengarther, M. Lippert, J. P. Strobel, M. Vildic, G. Saemann-Ischenko and S. Klaumunzer, Phys. Rev. B42(1990)4135.

5.9 SINGLE EVENT BURNOUT OF BIPOLAR TRANSISTORS BY INCIDENT OF HIGH-ENERGY IONS

S. KUBOYAMA[1], T. HIRAO, S. MATSUDA[1], I. NASHIYAMA
S. SHUGYO[1], K. SUGIMOTO[1], T. SUZUKI [1]
T. HIROSE[2], H. OHIRA[2], Y. YOSHIOKA[2], H. OTOMO[2]

Single Event Burnout (SEB) was identified as a possible catastrophic failure mode for Power MOSFETs with double-diffused MOS (DMOS) structure. Up to date, a lot of tests of SEB of Power MOSFETs have been performed, and its mechanism is getting clear. The SEB mechanism of MOSFETs is known that the parasitic bipolar junction transistor (BJT) inherent to the DMOS structure is turned on by incident of high-energy ions. Because the vertical structure of BJTs are similar to the DMOS structure, it is possible to observe SEB of BJTs. Titus et.al. reported on SEB of Power BJTs for the first time[1]. But they distinguished SEB if the sample devices destroy or not. So their experiment was a destructive test, and they did not separate the actual burnout pulses. In our study, Energetic Particle Induced Charge Spectroscopy(EPICS) system[2] usually used to observe SEB of MOSFETs is applied to observe SEB of BJTs. Using EPICS system, SEB of BJTs was observed non-destructively[3].

Figure 1 shows the block diagram of EPICS used this experiment. We used the Ni ion 250MeV from the TANDEM accelerator in JAERI. Its ion beam was scattered by Au foil. Figure 2 shows a typical EPICS spectra of the collected charge by incidence of Ni ion for 2SD854(bipolar transistor for space application). The vertical axis is the number of counts, the horizontal axis is the collected charge.

Increasing V_{CE}(collector-emitter voltage), the second peak disappeared, and the SEB signal appeared. This means that the second peak becomes the SEB signal. So when the high-energy ion induced the emitter-base junction region, SEB of BJTs occurred at higher V_{CE}.
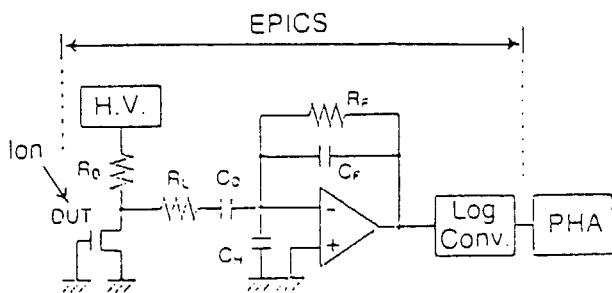
Fig.1 block diagram of EPICS
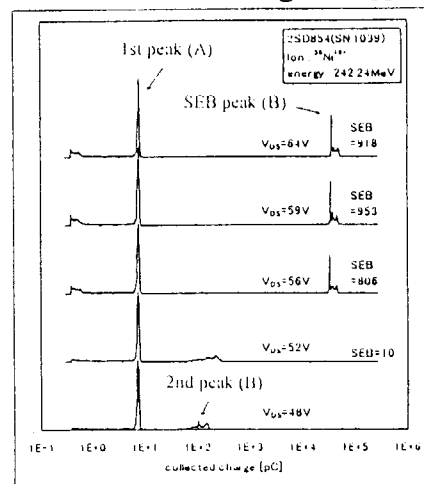
Fig.2 typical EPICS spectra for 2SD854
1st peak:collected charge on the base-collector junction
2nd peak:collected charge on the emitter-base junction

[1]Electronic and Information Technology Laboratory, Office of Research and Development, National Space Development Agency of Japan.
[2]Components Engineering Section, Engineering Dept., RYOEI TECHNICA Corporation.

In Figure 2, A and B is called the total counts of the first peak and the second peak (include the SEB peak). We define the spectra ratio of A to B as C, the diffusion area ratio of the base region to the emitter region as D. Figure 3 shows the fundamentals of the BJT structure. Basically, C will correspond to D. In Figure 4, the spectra ratio for 2SD854 are plotted, and the solid line shows the diffusion area ratio. The spectra ratio and the diffusion area ratio have a good agreement. Therefore, EPICS system is applicable to the SEB evaluation of BJTs.
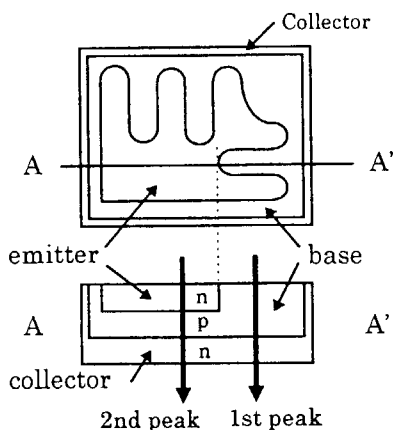
Fig.3 typical BJT structure   Fig.4 emitter/base ratio
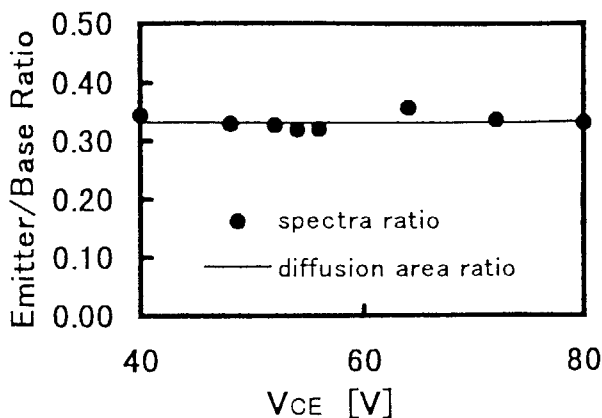
The various BJTs were evaluated. Table 1 shows the summary of the result. In table 1, SEB occurred at about $50\sim60\%$ of rated V_{CEO}(absolute maximum rating voltage) in the devices with a epitaxial layer. On the other hand, SEB did not occurred under rated V_{CEO} in the non-epitaxial layer devices.

Table 1   the summary of this experiment result.

Device Type	Rated V_{CEO} [V]	Epi*	LET [MeV/(mg/cm^2)]	Range [μm]	Pass V_{CE} [V]	Fail V_{CE} [V]
2SD854	80	○	28.0	37.7	48	52
2SD2822	50	○	27.8	38.7	25	30
2SC4339	100	○	27.8	38.6	60	65
2SC4553	100	○	28.1	36.8	50	55
2SC4814	100	○	28.3	36.0	60	65
2SC4136	120	×	29.0	32.9	120	—
2SC4534	300	×	28.3	36.0	300	—
2SC4832	400	×	28.0	37.4	400	—

*)   ○:epitaxial planer structure,   ×:non-epitaxial planer structure

The SEB testing of BJTs was performed non-destructively by using EPICS system. And it was cleared that SEB occured in case of the epitaxial planer structure. But its mechanism was not cleared. So, more experiments are needed to make it clear the SEB mechanism of BJTs.

References
1)J.L.Titus, G.H.Johnson, R.D.Schrimpf and K.F.Galloway, IEEE. Trans.Nucl.Sci., Vol.NS-38,No.6,pp.1315-1322,(1991)
2)S.Kuboyama, S.Matsuda, T.Kanno and T.Ishii, IEEE. Trans.Nucl.Sci. Vol.NS-39,No.6, pp.1698-1703(1992)
3)T.Suzuki,K.Sugimoto,S.Shugyo,S.Kuboyama,S.Matsuda,T.Hirao,I.Nashiyama,T.Hirose, H.Ohira, Inst. Electro, Informat. Communicat Eng.Vol.97,No.600,pp.25-29(1998)

5.10 LIGHT EMISSION CHARACTERISTICS OF PHOTO-STIMULATED LUMINESCENCE PHOSPHOR BY HEAVY CHARGED PARTICLE IRRADIATION

C.MORI[1], M.YOSHIDA, T.SUZUKI[1], A.URITANI[1], F.TAKAHASHI, T.OISHI

The purpose of this research is to clarify the previous argument that the difference in the intensity ratios of photo-stimulated luminescence (PSL) to prompt scintillation between β-ray and α-ray incidences into Imaging Plate (IP) phosphor (so-called photostimulated luminescence phosphor) comes from the difference of specific energy loss (-dE/dx) of the incident particles and not mainly from the difference of the penetration ranges.

In the earlier experiments, we found that the characteristics of the decreasing of PSL intensities in the iterative readings for the same latent image are different depending on the kind of radiations, e.g. β-rays or α-rays, and also on the energy of beta-rays as shown in Fig.1[1]. We also found the intensity ratio of PSL to the prompt scintillation depends on the radiation kinds[2]. We gave the explanation for these phenomena that the specific energy loss -dE/dx determines the densities of F-centers and holes as latent image and the densities determine the probability of electron hole recombination of electrons excited from F-centers to the conduction band by laser beam irradiation for the image reading. However, there was the argument that such phenomena come from the difference of the penetration ranges of incident particles in the the phosphor plate.

If the phenomena are still observed when we use different incident particles whose penetration ranges are sufficiently enough to pass through the whole thickness of the phosphor and their specific energy losses are different, it would be concluded that the phenomena mainly come from the difference of the specific energy loss. Then we irradiated IP with various kinds of particles from the TANDEM accelerator in JAERI.

Table 1 shows the average deposited-energy (E) in the IP phosphor with a thickness of 150 μ m, penetration range or maximum thickness to lose the energy of the particle (R, the maximum value is the phosphor thickness) in the phosphor, and the ratio E/R(MeV/μ m) for various radiations. Li^{3+}(50MeV) has larger penetration range than the phosphor thickness and nearly the same specific energy loss E/R to α particles. And O^{7+}(120MeV) has almost the same penetration range to the phosphor thickness and very large specific energy loss.

Fig. 2(a) shows the ratio of PSL(n) intensity at n-th reading to the first reading PSL(1) vs. number of reading times n for Li3+ and α-ray incidence. Since the both specific energy losses are nearly the same, the decreasing characteristics of the ratio are almost the same.
Fig. 2(b) shows the larger decreasing of the characteristics is shown for larger specific energy loss. The difference between the characteristics for α-rays in (a) and (b) comes from different experimental set-up in different experimental days. Fig.3 shows the ratio of PSL intensity to prompt scintillation (PL) intensity vs. specific energy loss.

From the results, it would be possible to explain that the recombination probability of electrons excited from F-center to conduction band is larger, which leads to larger probability of prompt emission, for particle with larger specific energy loss.

References
[1] C.Mori, A. Matsumura, T.Suzuki, H.Miyahara. T.Aoyama, and K.Nishizawa, Nucl. Instrum. Methods A339(1994)278
[2] T.Suzuki, C.Mori, K.Yanagida, A.Uritani, H.Miyahara, K.Takahashi, J.Miyahara, M.Yoshida, and F.Takahashi, Nucl. Instrum. Methods A390(1997)155

---

[1]School of Engineering, Nagoya University.
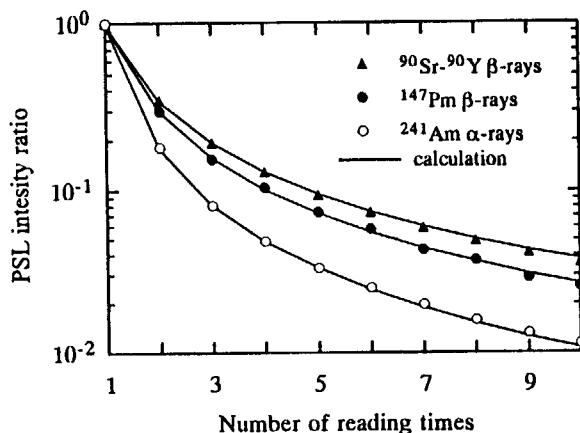
Fig. 1 PSL intensity ratio vs. reading
times of iterative readings

Table 1 Various kinds of radiations and
their characteristics

	^{90}Sr-^{90}Y, β-rays	^{147}Pm, β-rays	^{241}Am, α-rays	Li^{3+}, 50MeV	O^{7+}, 120MeV
E(MeV)	0.2	0.05	3.0	18	90
R(μm)	150	10	20	150	100
E/R(MeV/μm)	0.0013	0.005	0.15	0.12	0.9
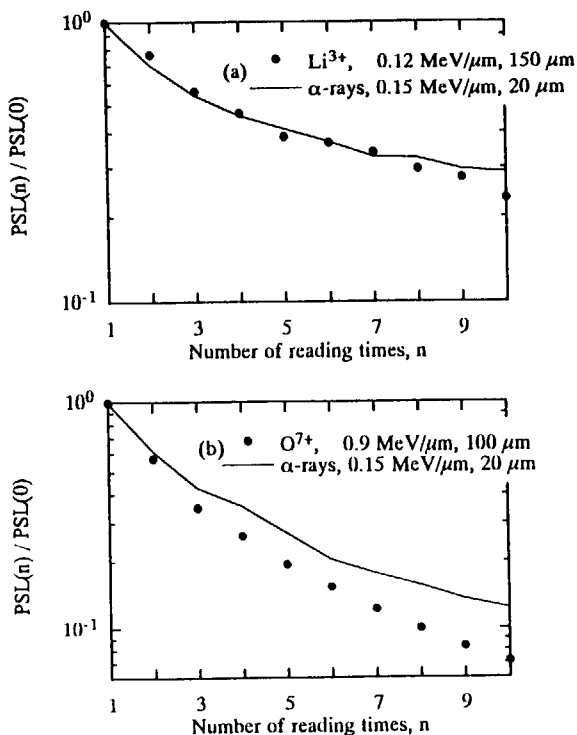
Fig. 2 (a) PSL intensity ratio vs.
reading times for α and Li^{3+} and
(b) for α and O^{7+}
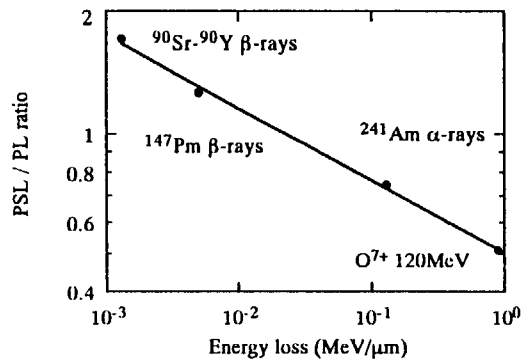
Fig. 3 Ratio of PSL intensity to prompt
scintillation (PL) vs. specific energy
loss

5.11 X-RAY DIFFUSE SCATTERING STUDY OF DEFECT CLUSTER BY HEAVY ION-IRRADIATED Ni CRYSTALS AT LOW TEMPERATURE

H. MAETA, T. KATO, H. OHTSUKA, H.YUYA, H. SUGAI
H.MOTOHASHI, K.YAMAKAWA[1] and F. ONO[2]

Energetic heavy ions produces point defects such as vacancy-interstitial pairs and also displacement cascades[1] containing high local concentrations of these in materials. In the study of radiation damage of solids, it was recognized that some radiation-induced defects might be mobile even below liquid hydrogen temperature. In order to retain the defects in the original configuration, in which they were introduced, irradiation facilities at liquid helium (LHe) temperature are now in use in many laboratories. Various experimental techniques to study various defect properties require measurements outside the irradiation facility as well as in situ and these can only be done after transfer of irradiated specimens to a measuring cryostat without any warming up.

Fundamental study of radiation damage is necessary to irradiate such as at low temperature that the defects can not migrate and measure the specimens at the low temperature at which the specimens were irradiated. Especially, to study of the cascade zones in the atomic energy materials is one of the most important problems. There are many studies of the cascade zones in these materials, exactly these information about the cascades by the transmission electron microscopy. However, the observations have been carried out at the temperatures after the defect moved to change its original structure and also the size. And such a cascade may be small size below the visibility limit of the TEM.

This is a very important thing for study of the cascade in ion irradiated materials. On the other hand, the X-ray diffuse scattering method[2] is powerful method to observe such a small defect studied nondestructively in bulk specimen[3].

The purpose of this paper is to report a reliable method of transferring specimens at LHe temperature without any warming up after the ion irradiation using the Jaeri Tandem Accelerator. We have reported preliminary results of the defects in the heavy ion irradiated Ni specimens by measurements of x-ray diffuse measurements using the synchrotoron radiation source (SR) at the KEK in Tsukuba for study of the cascade in heavy ion-irradiated nickel single crystals.

The irradiated specimen was settled at the end of the cryostat in the ion irradiation chamber as shown in the fig .1. The cryostat was connected to cool down at below 10 K with a refrigerator and also with a liquid helium container to flow the LHe into the specimen cell during ion irradiation. After ion irradiation, the radio- activated specimen by ion irradiation was cooled down for about one mouth. Then, a cap to maintain vacuum in the cryostat with the specimen covered the end of the

[1] Faculty of Engineering, Ehime University
[2] Department of Science, Okayama University

cryostat.   The cryostat with the irradiated specimen was removed from the irradiation chamber to retain the specimen at the liquid helium temperature, during the specimen cell of the cryostat following by the liquid helium from the LHe container.   To measure x-ray diffuse scattering using SR , the chamber with the specimen was transported by a car to the KEK in Tsukuba, during the cryostat with the LHe container flowing the LHe into the specimen cell to cool down the specimen   as shown in fig.1 (c). The cryostat was set up to a four-circle diffractometer installed at the beam line BL-27B at the KEK, maintaining the specimen at the low temperature as shown in fig. 1 (d). The specimens with <111> orientation were irradiated below 18K with 90 MeV iodine (I^{+7}) ions using the jaeri tandem accelerator to   fluence of 8.3 x 10^{14} ions/cm^2. Diffuse scattering experiments of the irradiated specimens were performed on the four-circle diffractometor.   The diffuse scattering near the 111 reflection was measured at 18 K.   The measured diffuse scattering for I ion irradiated nickels is shown in the fig. 2.   The specimen was also   carried out   the diffuse   measurements for isochronal annealing   from   65 K to 300 K for ten minutes, the results is also shown in fig.2. Some troubles had happened to exchange the cooling system from the refrigerator to flowing system of the LHe for the cryostat. The temperature of the specimen raised up to about 65 K for a few minutes .

We   are now developing the cooling system of the specimen cell of the cryostat flowing LHe into the specimen cell from the LHe container.

References
1) for example ,R.S.Averback , J. Nucl. Mater. 216, (1994) 49-62.
2) P.Ehrhart , J. Nucl. Mater. 216, (1994) 170-198.
3) H. Maeta et al., JAERI-Review   97-010 , (1997) 67.

Refrigerator

Cryostat

Specimen cell

Specimen

Ion beam

Cap for seal of vacuum

LHe

Ion irradiation chamber

(a)

(b)

The specimen and end of cryostat are covered by the cap .

cryostat

about 70 km

Goniometor

refrigerator

(d)

(c)
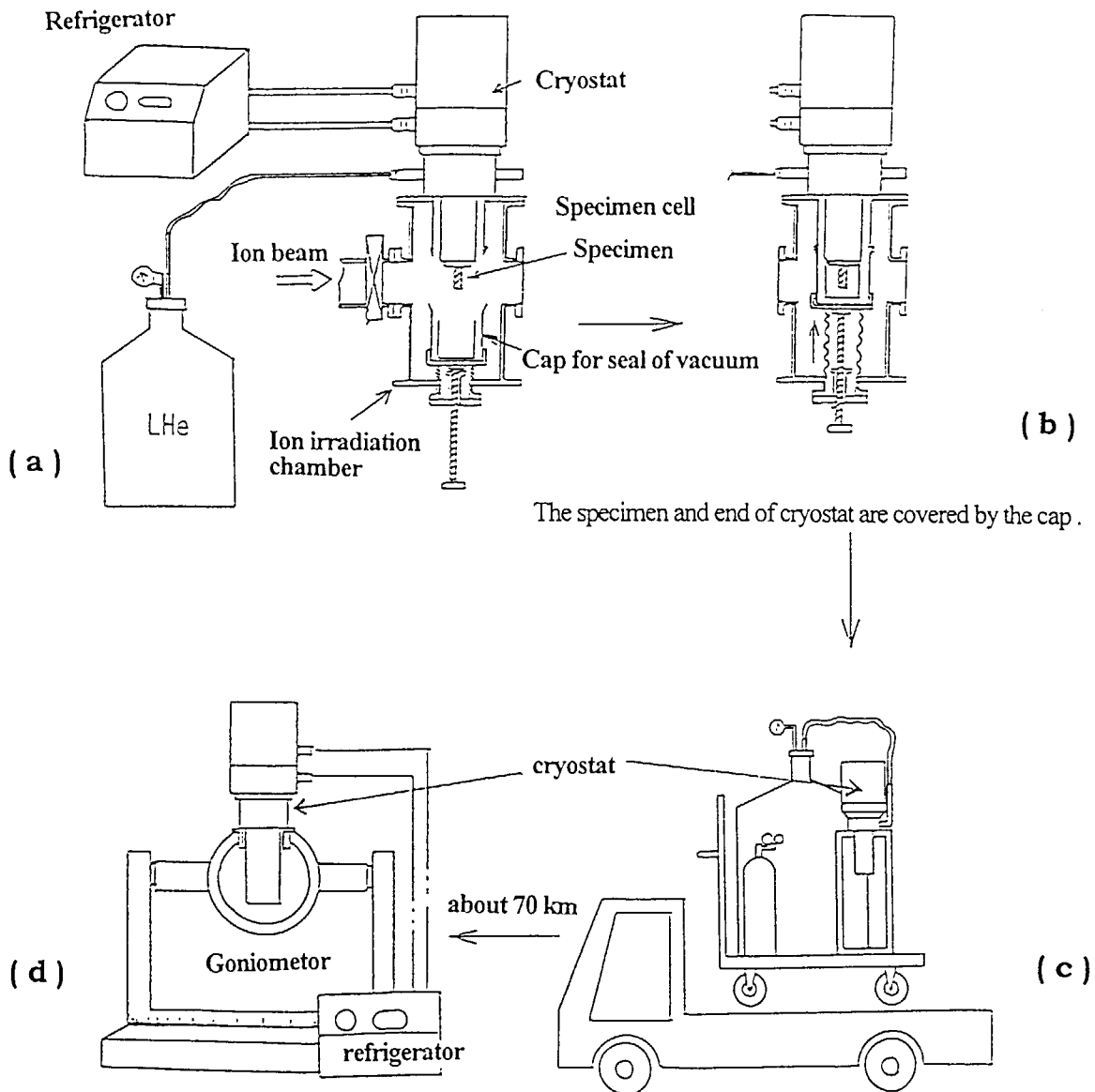
Figs. 1. Schematic drawing of ion irradiation and transport system of the specimen at low temperature.

Fig. 2. X-diffuse scattering of the I ion
Irradiated Ni single crystal
at low temperature .

10^4

o irrad. up
to 69 K
+ un irrad.

Intensity (a.u)

10^2

10^0

10^{-2}

40

50

2 theta

This is a blank page.

- 91 -
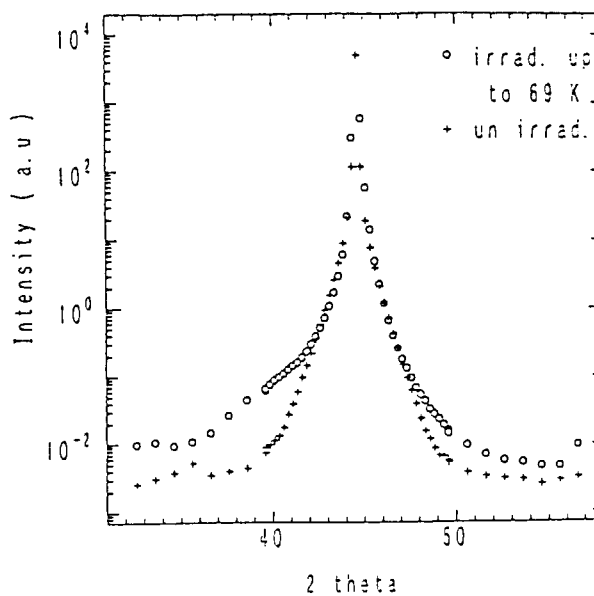
6. Publication in Journal and Proceedings, and Contribution to Scientific Meetings

This is a blank page.

ACCELERATOR OPERATION AND DEVELOPMENT
Journal/Proceedings

Hanashima, S.
Status Report of Concurrent Control System for the JAERI Tandem Accelerator.
Annual Report of NIES(National Institute of Environmental Studies)-TERRA.
(Proc. of the 10th Workshop on Tandem Accelerator and Associated Technology)F-
113-'98/NIES(1998)pp.64-67.

Hanashima, S.
Status of Control System for the JAERI Tandem Accelerator.
Proc. of the 11th Symposium on Accelerator Science and Technology, Spring-8, Harima,
Japan(October 21-23, 1997) pp.519-521.

Matsuda, M., Takeuchi, S., and Kobayashi, C.
Development of the Terminal ECR Ion Source for the JAERI Tandem Accelerator.
(Proc. of the 10th Workshop on Tandem Accelerator and Associated Technology)F-
113-'98/NIES(1998)pp.109-111.

Matsuda, M., Takeuchi, S., and Kobayashi, C.
Application of an ECR Ion Source to the JAERI Tandem Accelerator.
Proc. of the 11th Symposium on Accelerator Science and Technology, Spring-8, Harima,
Japan(October 21-23, 1997) pp.165-167.

Takeuchi, S.
Possibility of Heavy Ion Acceleration at Unusually Low Injection Velocity in a Tandem
Booster.
Annual Report of NIES(National Institute of Environmental Studies)-TERRA.
(Proc. of the 10th Workshop on Tandem Accelerator and Associated Technology)F-
113-'98/NIES(1998)pp.97-100.

Takeuchi, S.
Acceleration of Unusually Slow Heavy Ions in an Independently Phased Linac.
Proc. of the 22nd Linear Accelerator Meeting in Japan (Sept. 9-11, 1997)pp.311-313

Yoshida, T., Kanda, S., Takeuchi, S., Hanashima, S., Shouji, T., Ohuchi, I., Horie, K.,

Tsukihashi, Y., Abe, S., Ishizaki, N., Tayama, H., and Matsuda, M.
The status of the JAERI Tandem Accelerator.
Proc. of the 10th Workshop of the Tandem Accelerator and their Associated
Technologies.(NIES-TERRA Tsukuba, July 7-8, 1997)pp.32-34.

Meetings

Hanashima, S.
Status Report of Concurrent Control System for the JAERI Tandem Accelerator.
The 10th Workshop on Tandem Accelerator and Associated Technologies, Tsukuba,
Japan(July 7-8,1997).

Hanashima, S.
Status of Control System for the JAERI Tandem Accelerator.
Proc. of the 11th Symposium on Accelerator Science and Technology, Spring-8, Harima,
Japan(October 21-23, 1997).

Matsuda, M., Takeuchi, S., and Kobayashi, C.
Development of the Terminal ECR Ion Source for the JAERI Tandem Accelerator.
The 10th Workshop on Tandem Accelerator and Associated Technologies, Tsukuba,
Japan(July 7-8,1997).

Matsuda, M., Takeuchi, S., and Kobayashi, C.
Application of an ECR Ion Source to the JAERI Tandem Accelerator.
The 11th Symposium on Accelerator Science and Technology, Spring-8, Harima,
Japan(October 21-23, 1997).

Takeuchi, S.
Possibility of Heavy Ion Acceleration at Unusually Low Injection Velocity in a Tandem
Booster.
The 10th Workshop on Tandem Accelerator and Associated Technologies, Tsukuba,
Japan(July 7-8, 1997)

Takeuchi, S.
Acceleration of Unusually Slow Heavy Ions in an Independently Phased Linac.

The 22 nd Linear Accelerator Meeting in Sendai, Japan (Sept. 9-11, 1997).

Takeuchi, S.
Superconducting RF Activities at JAERI.
The 8 th Workshop on RF Superconductivity, Abano Terme(Padva), Italy(Oct., 6-10, 1997).

Takeuchi. S., and Matsuda, M.
First Three Year Operational Experience with the JAERI Tandem Booster.
The 8 th Workshop on RF Superconductivity, Abano Terme(Padva), Italy(Oct., 6-10, 1997).

Yoshida, T., Kanda, S., Takeuchi, S., Hanashima, S., Shouji, T., Ohuchi, I., Horie, K., Tsukihashi, Y., Abe, S., Ishizaki, N., Tayama, H., and Matsuda, M.
The status of the JAERI Tandem Accelerator.
The 10 th Workshop of the Tandem Accelerator and their Associated Technologies, Tsukuba, Japan(July 7-8, 1997)

NUCLEAR STRUCTURE

Journal/proceedings

Furutaka, K., Hayakawa, T., Nakada, H., Hatsukawa, Y., Kidera, M., Oshima, M.,
Mitarai, S., Komatsubara, T., Matsuda, M., and Furuno, K.
High Spin States in ^{62,64}Zn.
Z. Phys. A358(1997)279.

Hatsukawa, Y., Hayakawa, T., Furutaka, K., Nakada, H., Kidera, M., Ishii, T.,
Oshima, M., Mitarai, S., Sugawara, M., Kusakari, H., Komatsubara, T., and Furuno, K.
High Spin States in ^{61}Cu.
Z. Phys. A359(1997)3.

Hayakawa, T., Lu, J., Furuno, K., Komatsubara, T., Shizuma, T., Hashimoto, N.,
Saitoh,T., Matsuda, M., Hatsukawa, Y., and Oshima, M.
High Spin States of ^{132}Cs.
Z. Phys. A357 (1997)349.

Ichikawa, S., Tsukada, K., Asai, M., Osa, A., Oura, Y., Iimura, H., Kojima, Y., Hirose, T.,
Nishinaka, I., Hatsukawa, Y., Nagame, Y., Kawada, K., Ohyama, T., and Sueki, K.
Search for Unknown Isotopes Using the JAERI-ISOL.
Nucl. Instrum. Method B126(1997)205.

Iimura, H., Ichikawa, S., Oshima, M., Katakura, J., Shinohara, N., Magara, M., Osa, A.,
Tamura, T., Asai, M., and Yamamoto, H.
Level Scheme of ^{127}La Fed by the ^{127}Ce Beta-decay.
Proc. of the 9th International Symposium on Capture Gamma-ray Spectroscopy and
Related Topics, Springer, 1997, p.297.

Ishida, Y., Iimura, H., Ichikawa, S., and Horiguchi, T.
Isotope Shifts of Optical Transitions in Cell by Collinear Laser-ion Beam Spectroscopy.
J. Phys. B30(1997)2569

Ishii, T., Itoh, M., Ishii, M., Makishima, A., Ogawa, M., Hossain, I., Hayakawa, T., and
Kohno, T.
Isomer-scope: A New Instrument for In-beam γ-ray Spectroscopy through Deep

Inelastic Collisions.
Nucl. Instrum. Methods Phys. Res. A395(1997)210.

Kidera, M., Katagiri, M., Oshima, M., Hatsukawa, Y., and Morikawa, T.
Development of a Compact Umulti-electron Detector Array for In-beam Spectroscopy.
Nucl. Instrum. and Moth. A397(1997)304.

Odahara, A., Gono, Y., Mitarai, S., Morikawa, T., Shizuma, T., Kidera, M., Shibata, M.,
Kishida, T., Ideguchi, E., Morita, K., Yoshida, A., Kumagai, H., Zhang, Y.H., Ferragut, A.,
Murakami, T., Oshima, M., Iimura, H., Shibata, M., Hamada, S., Kusakari, H.,
Sugawara, M., Ogawa, M., Nakajima, M., Min, B.J., Kim, J.C., Chae, S.J., and
Sagawa, H.
High-spin Isomer and Level Structure of ^{145}Sm.
Nucl. Phys. A620(1997)363.

Sugawara, M., Kusakari, H., Igari, Y., Terui, K., Myojin, K., Nishiyama, D., Mitarai, S.,
Oshima, M., Hayakawa, T., Kidera, M., Furutaka, K., and Hatsukawa, Y.
Dipole Bands in ^{142}Gd.
Z. Phys. A358(1997)1.

Sugawara, M., Kusakari, H., Igari, Y., Myojin, K., Nishiyama, D., Mitarai, S.,
Oshima, M., Hayakawa, T., Kidera, M., Furutaka, K., and Hatsukawa, Y.
Dipole and Quadrupole Cascades in the Yrast Region of ^{143}Gd.
Eur. Phys. J. A1(1998) 123.

Zhou, X.H., Ideguchi, E., Gono, Y., Kishida, T., Mitarai, S., Odahara, A., Morikawa, T.,
Tsuchida, H., Shibata, M., Watanabe, H., Miyake, M., Oshima, M., Hatsukawa, Y.,
Hamada, S., Iimura, H., Ishii, T., and Ishihara, M.
Study of High-lying States in ^{147}Eu.
Z. Phys. A358(1997)285.

Meetings

Asai, M., Ishii, T., Hossain, I., Sinchi, S., Makishima, A., Ishii, M., Itoh, M., and
Ogawa, M.

In-beam γ-ray Spectroscopy of ^{67}Cu through Deep-inelastic Collision.
Spring Meeting of the Physical Society of Japan, Chiba(April 1, 1998).

Hayakawa, T., Lu, J., Furuno, K., Furutaka, K., Komatsubara, T., Shizuma, T., Hashimoto, N., Saitoh, T., Matsuda, M., Hatsukawa, Y., and Oshima, M.
High-spin States in Odd-odd ^{132}Cs.
The Workshop on Gamma-ray Spectroscopy Utilizing Heavy-ion, Photon and RI Beams, JAERI(July, 15, 1997). JAERI-conf 98-008(1998)p.14.

Ichikawa, S., Tsukada, K., Asai, M., Osa, A., Oura, Y., Iimura, H. Kojima, Y., Hirose, T., Shibata, M., Nishinaka, I., Hatsukawa, Y., Nagame, Y., and
Kawada, K.
Identification of New Neutron-rich Rare-earth Isotopes produced in Proton-induced Fission of ^{238}U.
1997 Asia-Pacific Symposium on Radiochemistry, Kumamoto, Japan (Oct., 6-9, 1997).

Iimura, H., Ichikawa, S., Oshima, M., Sekine, T., Katakura, J., Shinohara, N., Magara, M., Osa, A., Asai, M., Miyaji, M., and Yamamoto, H.
Conversion electron Measurements in the ^{127}Ce and ^{127}La Beta-decay.
Spring Meeting of the Physical Society of Japan, Funabashi(April 1, 1998).

Ishida, Y. Iimura, H., Ichikawa, S., and Horiguchi, T.
Laser Spectroscopy of Radioactive ^{144}Ce.
Fall Meeting of the Physical Society of Japan, Tokyo(Sept., 21, 1997).

Ishii, T., Asai, M., Sinichi, S., Hossain, I., Ishii, M., Itoh, M., Ogawa, M., and
Makishima, A.
Nuclear Structure of Neutron-rich Nuclei in the Vicinity of ^{68}Ni.
Fall Meeting of the Physical Society of Japan, Tokyo(Sept. 21, 1997).

Nakada, H., Furutaka, K., Hatsukawa, Y., Hayakawa, T., Matsuda, M., Ishii, T., Oshima, M., Kidera, M., Mitarai. S., Komatsubara, T., Furuno, K., Kusakari, H., and Sugawara, M.
Sturucture of High-spin States in the Region of A~60.
The Workshop on Gamma-ray Spectroscopy Utilizing Heavy-ion, Photon and RI Beams, JAERI(July, 15, 1997). JAERI-conf 98-008(1998)p.97.

Oshima, M., Hayakawa, T., Hatsukawa, Y. Furutaka, K., Kidera, M., Katakura, J., Matsuda, M., Kusakari, H. Terui, K. Myojin, K., Nishiyama, D., Sugawara, M., and Shizuma, T.
Stimulated Side Band Populations in Coulomb Excitation of ^{155}Gd.
Sixth Int. Conf. On Nucleus-Nucleus Collisions, Gatlinberg, Tennessee, U.S.A.(June 2-6, 1997).

Oshima, M.
JAERI Gamma-ray Spectroscopy project.
The Workshop on Gamma-ray Spectroscopy Utilizing Heavy-ion, Photon and RI Beams, JAERI(July, 15, 1997). JAERI-conf 98-008(1998)p.1.

Oshima, M., Hayakawa, T., Hatsukawa, Y., Sugita, M., Furutaka, K., Kidera, M., Katakura, J., Matsuda, M., Kusakari, H., Terui, K., Myojin, K., Nishiyama, D., Sugawara, M., and Shizuma, T.
Enhanced Population of Side-band in Coulomb Excitation of ^{155}Gd.
The Workshop on Gamma-ray Spectroscopy Utilizing Heavy-ion, Photon and RI Beams, JAERI(July, 15, 1997). JAERI-conf 98-008(1998)p.4.

Sekine, T., Osa, A., Koizumi, M., Ichikawa, S., Iimura, H., Tsukada, K., Nishinaka, I., Hatsukawa, Y., Nagame, Y., Asai, M., Kojima, Y., Hirose, T., Shibata, M., Yamamoto, H., and Kawade, K.
Recent studies of Unstable Nuclei far from Stability with the On-line Isotope Separators of JAERI.
1997 Asia-Pacific Symposium on Radiochemistry, Kumamoto, Japan (Oct., 6-9, 1997).

Sugawara, M., Kusakari, H., Igari, Y., Terui, K., Myojin, K., Nishiyama, D., Mitarai, S., Oshima, M., Hatsukawa, T., Kidera, M., Furutaka, K., and Hatsukawa, Y.
M1 Bands in A~130 and 80 Regions.
The Workshop on Gamma-ray Spectroscopy Utilizing Heavy-ion, Photon and RI Beams, JAERI(July, 15, 1997). JAERI-conf 98-008(1998)p.17.

Tsukada, K., Sakama, M., Asai, M., Ichikawa, S., Oura, Y., Nagame, Y., Nishinaka, I., Hata, K., Hatsukawa, Y., Shinohara, N., Qin, Z., Zhao, Y.L., Sueki, I., Ohyama, T., Nakahara, H., Hirose, T., Kojima, Y., Yamamoto, H., and Kawade, K.
Mass Separation of Neutron Deficient Americium Isotopes Using the Gas-jet Coupled

JAERI-ISOL.

1997 Asia-Pacific Symposium on Radiochemistry, Kumamoto, Japan (Oct., 6-9, 1997).

NUCLEAR REACTIONS
Journal/Proceedings

Baba, H., Saito, T., Takahashi, N., Yokoyama, A., Miyauchi, T., Mori, S., Yano, D.,
Hakoda, T., Takamiya, K., Nakanishi, K., and Nakagome, Y.
Role of Effective Distance in the Fission Mechanism Study by the Double-energy
Measurement for Uranium Isotopes.
J. Nucl. Sci. Technol. (Tokyo) 34(1997)871.

Hamada, S., Yasue, M., Kubono, S., Tanaka, M., and Peterson, R J.
Cluster Structure in ^{10}Be from the ^{7}Li(α,p)^{10}Be Reaction.
Phys. Rev. C49(1997)3192.

Hamada, S., Yasue, M., and Ogino, K.
Results of DWBA Analysis for ^{24}Mg(^{6}Li,d)^{28}Si and ^{28}Si(d,^{6}Li)^{24}Mg Reactions.
Proc. of ENMA95. International Conference on Exotic Nuclei and Atomic Masses. p.137.

Hamada, S., Ikuta, T., Sugiyama, Y., and Yamazaki, A.
On the Cluster Structure Study by ^{6}Li Induced Transfer Reaction on ^{9}Be Nucleus.
AIP Conference Proceedings, "Similarities and Differences between Atomic Nuclei and
Clusters" Tsukuba, Japan 1997. p.415.

Harada, M., Yamamoto, A., Yoshioka, S., Sato, K., Nakashima, T., Ijiri, H., Watanabe, Y.,
Yoshida, H., Uozumi, Y., Chiba, S., Fukahori, T., Meigo, S., and Iwamoto, O.
Study of the p + ^{12}C Reaction at Energies up to 30 MeV.
Proc. of the 1997 Symposium on Nuclear Data(Nov. 27-28, 1997, JAERI, Tokai), JAERI-
Conf 98-003(1998)p.273.

Ikezoe, H., Ikuta, T., Mitsuoka, S., Kuzumaki, T., Lu, J., Nagame, Y., Nishinaka, I., and
Tsukada, K.
Fusion Reactions of Deformed Nuclei near Coulomb Barrier.
Tour Symposium on Nuclear Physics III, Tour, France 1997. AIP 425(1997)249.

Ikuta, T., Ikezoe, H., Mitsuoka, S., Nishinaka, I., Tsukada, K., Nagame, Y., Lu, J., and
Kuzumaki, T.
Observation of a New Isometric State in ^{217}Pa.

Phys. Rev. C57(1998)1.

Nagame, Y.
Production of Neutron-rich Isotopes in Fission of Actinides (in Japanese).
Isotope News, no.522(1997)16.

Nagame, Y., Nishinaka, I., Tsukada, K., Ichikawa, S., Ikezoe, H., Zhao, Y.L., Oura, Y.,
Sueki, K., Nakahara, H., Tanikawa, M., Ohtsuki, T., Takamiya, K., Nakanishi, K., Kudo,
H., Hanajima, Y., and Chung, Y.H.
Bimodal Nature in Low-Energy Fission of Light Actinides.
Radiochim. Acta   78(1997)3.

Nishinaka, I., Nagame, Y., Tsukada, K., Ikezoe, H., Sueki, K., Nakahara, H.,
Tanikawa, M., and Ohtsuki, T.
Nuclear Fission of Neutron-deficient Protactinium Nuclides.
Phys. Rev. C56(1997)891.

Tsukada, K., Shinohara, N., Nishinaka, I., Ichikawa, S., Nagame, Y., Sueki, K.,
Kobayashi, T., Nakahara, H., Tanikawa, M., and Ohtsuki, T.
Highly Asymmetric Mass Division in Low-Energy Proton-induced Fission of ^{232}Th and
^{244}Pu.
Radiochim. Acta   76(1997)173.

Tsukada, K., Ichikawa, S., Hatsukawa, Y., Nishinaka, I., Hata, K., Nagame, Y., Oura, T.,
Ohyama, T., Sueki, K., Nakahara, H., Asai, M., Kojima, Y., Hirose, T., Yamamoto, H.,
and Kawade, K.
Half-life of the Electron Capture Decaying Isotope ^{236}Am.
Phys. Rev. C57(1998)2057.

Sugiyama, Y., Hamada, S., Ikuta, T., and Yamazaki, A.
Elastic Two-Neutron Transfer Reaction of ^{58}Ni+^{60}Ni and ^{62}Ni+^{64}Ni around the Coulomb
Barrier
J. Phys. G: Nucl. Part. Phys. 23(1997)1393.

Watanabe, Y., Yoshioka, S., Harada, M., Sato, K., Nakao, Y., Kuwata, R., Ijiri, H., Chiba,
S., Fukahori, T., Meigo, S., Iwamoto, O., and Koori, N.

Continuum (p,xp) Spectra at 14.1 and 26 MeV

Proc. of International Conference on Nuclear Data for Xcience and Technology, Trieste, Italy(May 19-24, 1997) SIF, Bologna, 1997, p.580.

Meetings

Baba, H.

Thirty Six Years on Nuclear Fission.

Specialists' Meeting on the Chemistry and Technology of Actinide Elements, Kumatori, Osaka, Japan(Dec. 15, 1997).

Hamada, S., Ikuta, T., Sugiyama, Y., and Yamazaki, A.

$\sigma \cdot \pi$ Mixing Excitation via Cluster States of ^{9}Be-^{10}Be/^{10}Be-^{11}Be Nuclei.

Fall Meeting of the Physical Society of Japan, Tokyo(Sept., 21, 1997).

Harada, M., Yamamoto, A., Yoshioka, S., Sato, K., Nakashima, T., Ijiri, H., and Watanabe, Y.

Study of the p + ^{12}C Reacrion at Energies up to 30 MeV(II).

Fall Meeting of the Atomic Energy Society of Japan, Okinawa(Oct. 14-17, 1997).

Ikezoe, H., Ikuta, T., Mitsuoka, S., Kuzumaki, T., Lu, J., Nagame, Y., Nishinaka, I., Tsukada, K., and Ohtsuki, T.

Fusion Reactions of Deformed Nuclei near Coulomb Barriers.

RIKEN Symposium on Dynamics in Hot Nuclei(March 13-14, 1998).

Nagame, Y., Nishinaka, I., Zhao, Y.L., Tsukada, K., Ichikawa, S., Ikezoe, H., Tanikawa, M., Ohtsuki, T., Oura, Y., Sueki, K., Nakahara, H., Kudo, H., Hamajima, Y., Takamiya, K., Nakanishi, K., and Baba. H.

Systematics of Bimodal Nature in Actinide Fission.

Asia-Pacific Symposium on Radiochemistry 1997, kumamoto, Japan(Oct. 7, 1997).

Nakanishi, K., Takamiya, K., Inoue, T., Yokoyama, A., Saito, T., Baba, H., Nishinaka, I., Tsukada, K., Nagame, Y., Zhao, Y., and Tanikawa, K.

Dependence of Excitation Energy of ^{238}U(p,f).

Annual Meeting of the Chemical Society of Japan, Tokyo(March 27, 1997).

Nishinaka, I., Zhao, Y., Nagame, Y., Tsukada, K., Ichikawa, S., Ikezoe, H.,
Tanikawa, M., and Nakahara, H.
Correlation between Mass Division Modes and Neutron Multiplicity in Fission of
Actinides.
1997 Asia-Pacific Symposium on Radiochemistry, Kumamoto, Japan(Oct., 7, 1997)

Qin, Z., Tsukada, K., Shinohara, N., Zhao, Y.L., Hatsukawa, Y., Nishinaka, I.,
Ichikawa, S., Hata, K., and Nagame, Y.
Mass Yield Distributions in Proton-Induced Fission of ^{248}Cm.
Asia-Pacific Symposium on Radiochemistry 1997, Kumamoto, Japan(Oct. 7, 1997).

Sugiyama, Y.
Molecular Resonance Observed through the Measurement of the m-substate Population
in ^{12}C+^{12}C Inelastic Scattering.
Workshop on Molecular Resonance in Heavy-ion Collision, Sapporo, Japan(Feb. 12,
1998).

Zhao, Y.L., Nishinaka, I., Nagame, Y., Tsukada, K., Tanikawa, M., Qin, Z., Nakahara, S.,
Ichikawa, Y., Hatsukawa, Y., Hata, K., Ikezoe, H., Oura, Y., Sueki, K., Ohtsuki, T.,
Goto, S., and Kudo, H.
Characteristics of Shell-governed Scission State in Proton Induced Fission of ^{244}Pu.
APSORC '97, Kumamoto, Japan(Oct. 6-9, 1997).

Zhao, Y.L., Nishinaka, I., Nagame, Y., Tsukada, K., Tanikawa, M., Sueki, K., Oura, Y.,
Ichikawa, S., Ikezoe, H., Ohtsuki, T., Kudo, H., and Nakahara, H.
Experimental Verification of Two Deformation Paths in the Mass Division Process of
Actinides.
ACTINIDES '97, Baden-Baden, Germany(Sept. 21-26, 1997).

NULCLEAR THEORY
Journal/Proceedings

Bonasera, A., and Iwamoto, A.
Bonasera and Iwamoto Reply
Phys. Rev. Lett. 79(1997)3540.

Bonasera, A., Kondratyev, V.N., and Iwamoto, A.
Nuclear dynamics below the Coulomb barrier.
J. Phys. G 23(1997)1297.

Bonasera, A., and Iwamoto, A.
Spontaneous Fission: A Many-body Approach.
Proc. International Conference on Large-scale Collective Motion of Atomic Nuclei,
World Scientific, ISBN 981-02-3045-1 (1997)p.285.

Iwamoto, A., Kondratyev, V.N., and Bonasera, A.
Vlasov Treatment of Spontaneous Fission and Sub-barrier Fusion Reactions.
Proc. Tour Symposium on Nuclear Physics III, AIP Proc. 425(1998)222.

Iwamoto, A.
Overview of the QMD Calculations on Nucleon-induced Multistep Process.
Proc. International Conference on Nuclear Data for Science and Technology,
Italian Physical Society (1997)pp.221-225.

Kondratyev, V.N., and Iwamoto, A.
Nonlocality and Polarizability in the Fusion of Fermi Droplets.
Phys. Lett. B423(1998)1.

Maruyama, Toshiki, Niita, K., Maruyama, Tomoyuki, and Iwamoto, A.
On the IMF Multiplicity in Au+Au Reactions.
Prog. Theor. Phys. 98(1997)87.

Maruyama, Toshiki, Niita, K., Oyamatsu, K., Maruyama, Tomoyuki, Chiba, S., and
Iwamoto, A.
Quantum Molecular Dynamics Approach to the Nuclear Matter below the Saturation

Density.
Phys. Rev. C57(1998)655.

Sugita, M.
Application of IBM-3 to the Z~N~40 Nuclei.
Phys. Lett. B394(1997)235.

Uchiyama, K., Furuno, K., Shizuma, T., Sugita, M., Tokita, Y., Murasaki, M.,
Hashimoto, N., Takahashi, H., Komatsubara, T., Matsuura, K., Tanaka, T., and
Sasaki, Y.
Measurements of the Lifetime of the First 2+ State in ^{124}Ba.
Euro. Phys. J.　A2(1998)13.

Meetings

Chiba, S., Fukahori, T., Niita, K., Maruyama, Tomoyuki, Maruyama, Toshiki, and
Iwamoto, A.
Study of Intermediate-energy Total Reaction Cross Section of Light- and Heavy-ion
Induced Reactions by an Improved QMD Framework.
International Conference on Nuclear Data for Science and Technology, Trieste,
Italy(May 22, 1997).

Iwamoto, A.
Overview of the QMD Calculation on Nucleon-induced Multistep Process.
International Conference on Nuclear Data for Science and Technology, Trieste,
Italy(May 22, 1997).

Iwamoto, A., Kondratyev, V.N., and Bonasera, A.
Vlasov Treatment of Spontaneous Fission and Subbarrier Fusion.
Tours Symposium on Nuclear Physics III, Tours, France(Sept. 3, 1997).

Iwamoto, A., Kondratyev, V.N., and Bonasera, A.
Effect of the Exchange of Particles in Heavy-ion Fusion and Fission.
Fall Meeting of the Physical Society of Japan, Hachiouji(Sept. 23, 1997).

Iwamoto, A.

QMD Calculation on Nucleon-induced Multistep Process.

Kyoto Meeting on Nuclear Collision Dynamics, Kyoto(Nov. 16-17, 1997).

Iwamoto, A., Maruyama, Toshiki, Niita, K., Oyamatsu, K., and Maruyama, Tomoyuki.

QMD analysis of Subsaturated Nuclear Matter and Surface Structure of Neutron Star.

International Symposium on "nuclear Structure under Extreme Conditions", Xian, China(March 23, 1998)

Maruyama, Tomoyuki, Niita, K., Chiba, S., Maruyama, Toshiki, and Iwamoto, A.

QMD Study of (g,p pi) Reaction.

Fall Meeting of the Physical Society of Japan, Hachiouji(Sept. 23, 1997).

Sugita, M.

New Scissors-type Excitation of Octupole-Quadrupole Deformed Nuclei.

Kiken workshop "Nuclear Structure Theory in the Extremes", Kyoto(January 20, 1998).

Sugita, M.

New Scissors-type Excitation of Octupole-Quadrupole Deformed Nuclei.

Spring Meeting of the Physical society of Japan, Chiba(March 30, 1998).

ATOMIC PHYSICS, SOLID STATE PHYSICS AND IRRADIATION EFFECTS IN MATERIALS
Journal/proceedings

Huang, D.H., Sasaki, Y., Okayasu, S., Aruga, T., Hojou, K., and Ikuhara, Y.
Defect Study along Au-ion Traces in $Bi_2Sr_2CaCu_2O_x$ Single Crystal.
Proc. of the 10th International Symposium on Superconductivity (ISS'97), Gifu, Japan(Oct. 27-30, 1997), vol.1(1998)p.429.

Huang, D.H., Sasaki, Y., Okayasu, S., Aruga, T., Hojou, K., and Ikuhara, Y.
Damage Morphology along Ion Traces in Au-irradiated $Bi_2Sr_2CaCu_2O_x$
Phys. Rev. B57(1998)13907.

Imai, M., Sataka, M., Yamazaki, Y., Komaki, K., Kawatsura, K., and Kanai, Y.
Electron Spectra from Highly Excited Si Ions.
Phys. Scr. T73(1997)93.

Kawatsura, K., Sataka, M., Imai, M., Komaki, K., Yamazaki, Y., Kuroi, K., Kanai, Y., and Stolterfoht, N.
Charge State Dependence of Very Low Projectile Autoionizing Transitions from 2 Mev/u S+He collisions.
Phys. Scr. T73(1997)145.

Kazumata, Y., Okayasu, S., Sataka, M., and Kumakura, H.
Parallel and Crossed Columnar Defects aligned at 45° to the C-axis in $Bi_2Sr_2CaCu_2O_x$ tapes.
Phys. Rev. B58(1998)5839.

Mori, C., and Suzuki, T.
Measurement of Extremely Low Level Radioactivity Distribution with Image Plate.
Hohshasen 23(1997)89.

Okayasu, S., and Kazumata, Y.
Proton Irradiation Effects on Effective Activation Energies of QMG-YBCO
Advances in Superconductivity IX (Proc. of the 9 th International Symposium on Superconductivity, October 21-24, 1996, Sapporo)p.507.

Sekioka, T., Terasawa, M., Sataka, M., and Kitazawa, S.
Emission of Secondary Ions from a Foil Bombarded with High Energy Heavy Ios.
Physica Scripta, Vol. T73(1997)335.

Suzuki, T., Mori, C., Yanagida, K., Uritani, A., Miyahara, Hiroshi, Takahashi, Kenji,
Miyahara, Junji, Yoshida, M., and Takahashi, Fumiaki.
Characteristics of Prompt Scintilation from Image Plate.
Nucl. Instrum. Methods A390(1997)155.

Suzuki, T., Mori, C., Yanagida, K., Uritani, A., Miyahara, H., Yoshida, M., and
Takahashi, F.
Characteristics and Correction of the Fading of Imaging Plate.
J. Nucl. Sci. Technol. 34(1997)461.

Suzuki, T., Mori, C., Miyahara, H., Uritani, A., Yoshida, M., and Takahashi, F.
Improvement of Precision in Quantitative Measurement of Radioactivity with
an Imaging Plate.
Appl. Radiat. Isotopes 49(1998) 1127.

Meetings

Chimi, Y., Iwase, A., and Ishikawa, N.
Effect of Electronic Excitation on High-energy Heavy Ion Irradiation in Fe.
Fall Meeting of the Physical Society of Japan, Kobe(Oct. 5, 1997).

Chimi, Y., Iwase, A., and Ishikawa, N.
Defect Accumulation Behavior in Fe Irradiated with Energetic Ions at ~80K.
The 8 th International Conference on Fusion Reactor Materials, Sendai, Japan(Oct. 29,
1997).

Chimi, Y., Iwase, A., and Ishikawa, N.
Electronic Excitation Effect on Radiation Annealing in Fe Irradiated at ~80K with
Energetic Ions.
Fall Meeting of Material Research Society, Boston, U.S.A.(Dec. 2, 1997).

Ishikawa, N., Chimi, Y., Iwase, A., Tsuru, K., and Michikami, O.

Defect Production and Annealing in High-T$_c$ Superconductor EuBa$_2$Cu$_3$O$_x$ Irradiated with Energetic Ions at Low Temperature.

Fall Meeting of Material Research Society, Boston, U.S.A.(Nov. 27. 1997).

Ishikawa, N., Chimi, Y., Iwase, A., Tsuru, K., and Michikami, O.

Columnar Defect Structure and Electrical Resistivity in High-T$_c$ superconductors Irradiated with Heavy Ions.

Spring Meeting of the Physical society of Japan, Chiba(April 2, 1997).

Iwase, A.

Electron Excitation and Atomic Displacement by GeV Ions.

RIKEN Symp. on "Materials Science Using RIKEN RI Beam Factory"(Dec. 22, 1997).

Iwase, A.

High Density Electron Excitation Effects on Atomic Displacement in Solids.

RIKEN Symp. on "Research on Materials Science, Atomic Physics, Nuclear Chemistry and Biology Using RIKEN RI Beam Factory"(January 26, 1998).

Iwase, A.

Current Studies on Materials Science Using Ion irradiation.

KUR Workshop, Kumatori, Japan(January 9, 1998).

Iwase, A.

Electron Excitation and Atomic Displacement in Metals and Oxide Superconductors.

International Symposium on Highly Charged Ions and Clusters, Himeji, Japan (March 24, 1998).

Iwase, A.

Electron Excitation Effects on Radiation Damage in Metals and Oxide Superconductors.

Universitaet Stuttgart/Max-Plank-Institut, Diplomanden- und

Doktorandensemianr, Stuttgart, Germany(May 19, 1998).

Kato, T., Maeta, H., Ohtsuka, H., Matsumoto, N., Yuya, H., and Sugai, H.

X-ray Diffraction Cryostat for Heavy Ion Irradiation(Ⅱ).

Fall Meeting of Cryogenics Engineering, Osaka(Nov. 8, 1997).

Kawatsura, K., Sataka, M., Kitazawa, S., Komaki, K., Yamazaki, Y., Azuma, T.,
Kanai, Y., Imai, M., Shibata, H., Tawara, H., Hansen, J.E., Kadar, I., and Stolterfoht, N.
High Lesolution L Auger Electron Spectra from Fast Projectile Ions Studied by Zero-
degree Electron Spectroscopy.
The VIIth International Conference on Electron Spectroscopy, Chiba, Japan(Sept. 9,
1998)

Kawatsura, K., Imai, M., Sataka, M., Kitazawa, S., Komaki, K., Yamazaki, Y.,
Azuma, T., Shibata, H., Kanai, Y., Tawara, H., and Stolterfoht, N.
Electron Spectra from Fast Projectile Si and S Ions Studied by Zero-degree Electron
Spectroscopy.
The VIIth International Conference on Electron Spectroscopy, Chiba, Japan(Sept. 9,
1998)

Matsumoto, N., Ohtsuka, H., Maeta, H., Sugai, T., Kato, T., Yuya, H., and Motohashi, H.
X-ray Diffuse Scattering from Radiation Defects in FCC Metals.
Spring meeting of Japan Physical Society, Yamaguchi(April 3, 1997).

Ogikubo, K., Kobayashi, T., Terai, T., Tanaka, S., Kishio, K., and Shimoyama, J.
Effect of High-energy Heavy-ion Irradiation on the Critical Current Density of Bi-2212
Single Crystals.
The 10th International Symposium on Superconductivity, Nagaragawa, Japan(Oct. 27-
30, 1997).

Ogikubo, K., Kobayashi, T., Terai, T., Tanaka, S., Shimoyama, J., and Kishio, K.
Effect of High-energy Heavy-ion Irradiation on the Critical Current Density of Bi-2212
Single Crystals.
Spring Meeting of the Japan Society of Applied Physics and related Societies,
Tokyo(March 28-31, 1998).

Sasaki, Y., Huang, D.H., Ikuhara, Y., Hojou, K., and Okayasu, S.
Structure of Irradiation Defects and Effects on the Magnetic Property in Bi-2212
Superconducor Irradiated with High Energy Ions.
Spring Meeting of the Ceramics Society of Japan, Osaka(May 31, 1997).

Sasaki, Y., Huang, D.H., Ikuhara, Y., Hojou, K., and Okayasu, S.

Structure Analysis of Irradiation Defects Generated with Au-240 MeV in Bi-2212 Superconductor.
Fall Meeting of the Ceramics Society of Japan, Kanazawa(Oct. 2, 1997).

Sasase, M., Okayasu, S., and Hojou, K.
Effect of Au^{24+} Ion Irradiation on the Superconductive Properties and Microstructure of EBCO Thin Films.
Spring Meeting of the Japan Society of Applied Physics, Chiba(March 30, 1997).

Sasase, M., Okayasu, S., Kurata, H., and Hojou, K.
Effect of Au^{24+} Ion Irradiation on the Superconductive Properties and Microstructure of $EuBa_2Cu_3O_x$ Thin Films.
The 10th International Conference on Surface Modification of Metals by Ion Beams(SMMIB '97), Gatlinburg, U.S.A. (Sept. 21, 1997).

Sasase, M., Okayasu, S., Kurata, H., and Hojou, K.
Effect of Au^{24+} Ion Irradiation on J_c of $EuBa_2Cu_3O_x$ Thin Films.
Spring Meeting of the Japan Society of Applied Physics, Tokyo(March 31, 1998).

Sataka, M., Kitazawa, S., Komaki, K., Yamazaki, Y., Azuma, T., Shibata, H., Kawatsura, K., Kanai, Y., and Tawara, H.
Electron Capture Differential Cross Section for 5-MeV Proton-Rare Gas Collisions.
The XXth International Conference on the Physics of Electronic and Atomic Collisions, Vienna, Austria(July 25, 1997).

Sataka, M.
Binary Encounter Electron Production by Highly Charged Ions.
International Symposium on Atomic processes of Highly Charged Heavy Ions and Clusters, Himeji, Japan(March 23, 1997).

Sueyoshi, T., Ishikawa, N., Iwase, A., Chimi, Y., Tsuru, K., Michikami, O., Kisu, T., Fujiyoshi, T., and Miyahara, K.
Magnetic Field Direction Dependence of Critical Current Density in Heavy-ion Irradiated $EuBa_2Cu_3O_x$ Thin Films
Fall Meeting of the Physical society of Japan, Kobe(Oct. 7, 1997).

Sueyoshi, T., Ishikawa, N., Iwase, A., Chimi, Y., Kisu, T., Fujiyoshi, T., and Miyahara, K.
Magnetic Field Direction Dependence of Critical Current Density in $YBa_2Cu_3O_y$ Thin
Films Irradiated by Heavy Ions.
Fall Meeting of the Physical society of Japan, Chiba(March 30, 1997).

Suzuki, T., Sugimoto, K., Shugyo, S., Kuboyama, S., Matsuda, S., Hirao, T.,
Nashiyama, I., Hirose, T., and Ohira, H.
Tolerance for Single-event Effect of Bipolar Transistors for Space and Commercial
System Apllication.
The Institute of Electronics, Information and Communication Engineers(March 13,
1998).

This is a blank page.

7. Personnel and Committees

This is a blank page.

(1) Personnel (FY 1997)

Department of Reactor Engineering

Masayuki	Nakagawa	Director
Hiroshi	Maekawa	Deputy Director
Takashi	Okabe	Administrative Manager

Accelerator Division
Scientific Staff

Tadashi	Yoshida*
Suehiro	Takeuchi
Susumu	Hanashima
Makoto	Matsuda

Technical Staff

Susumu	Kanda
Isao	Ohuchi
Tokio	Shoji
Katsuzo	Horie
Yoshihiro	Tsukihashi
Shinichi	Abe
Shuhei	Kanazawa
Nobuhiro	Ishizaki
Hidekazu	Tayama

Nuclear Data Center

Akira	Hasegawa*
Satoshi	Chiba
Tokio	Fukahori
Osamu	Iwamoto

Fusion Neutron Center

Yujiro	Ikeda*
Yoshitomo	Uno
Yoshimi	Kasugai

Advanced Science Research Center
Research Group for Exotic Heavy Nuclei

Hiroshi	Ikezoe*

* Head

Yasuharu Sugiyama
Masumi Oshima
Yoshiaki Tomita
· Yoshimaro Yamanouchi
Michiaki Sugita
Tetsuro Ishii
Shingo Hamada
Shin-ichi Mitsuoka
Tomohiko Ikuta
Kazuyoshi Furutaka
Takehito Hayakawa

Research Group for Hadron Transport Theory
Akira Iwamoto*
Toshiki Maruyama
Tomoyuki Maruyama

Research Group for Low-temperature Radiation Effects
Akihiro Iwase*
Norito Ishikawa
Yasuhiro Chimi
Naoshi Kuroda
Tetsuro Sueyoshi

Department of Health Physics
Radiation Control Division II
Masayuki Ueno
Katsuya Kawasaki
Tohru Tayama

Radiation Dosimetry Laboratory
Makoto Yoshida*
Fumiaki Takahashi

* Head

Department of Materials Science and Engineering
Material Innovation Laboratory

Kenji	Noda*
Tetsuya	Nakazawa
Daijyu	Yamaki

Solid State Physics Laboratory

Kiichi	Hojou*
Masao	Sataka
Satoru	Okayasu
Sin-iti	Kitazawa
Masato	Sasase

Synchrotron Radiation and Solid State Laboratory

Hiroshi	Maeta*
Hideo	Ohtsuka
Teruo	Kato

Department of Chemistry and Fuel Research
Nuclear Chemistry Laboratory

Toshiaki	Sekine*
Nobuo	Shinohara
Yuichiro	Nagame
Shin-ichi	Ichikawa
Yuichi	Hatsukawa
Kazuaki	Tsukada
Hideki	Iimura
Ichiro	Nishinaka
Kentaro	Hata

Department of Radioisotopes
Isotope Research and Development Division

Hiroyuki	Sugai

* Head

(2)Tandem Steering Committee

(Chairman)	Kunihisa	Soda	(Deputy Director General, Tokai Research Establishment)
	Muneyuki	Date	(Director, Advanced Science Research Center)
	Hiroshi	Katsuta	(Director, Department of Materials Science and Engineering)
	Masayuki	Nakagawa	(Director, Department of Reactor Engineering)
	Michio	Hoshi	(Director, Department of Chemistry and Fuel Research)
	Hisamichi	Yamabayashi	(Director, Department of Radioisotopes)
(Secretary)	Tadashi	Yoshida	(Head, Accelerator Division)
(Secretary)	Takashi	Okabe	(Administrative Manager, Department of Reactor Engineering)

(3)Tandem Consultative Committee

(Chairman)	Shinzo	Saito	(Director General, Tokai Research Establishment)
(Vice Chairman)	Kunihisa	Soda	(Deputy Director General, Tokai Research Establishment)
(Vice Chairman)	Masayuki	Nakagawa	(Director, Department of Reactor Engineering)
	Hiroyasu	Ejiri	(Professor, Osaka University)
	Kohei	Furuno	(Professor, Tsukuba University)
	Naohiro	Hirakawa	(Professor, Tohoku University)
	Jun	Imasato	(Professor, National Laboratory for High Energy Physics)
	Masayasu	Ishihara	(Professor, The University of Tokyo, Research Scientist, Institute of Physics and Chemical Research)
	Yasuo	Ito	(Associate professor, The University of Tokyo)
	Kenji	Katori	(Professor, Osaka University)
	Hisaaki	Kudo	(Associate professor, Niigata University)

	Kohzoh	Masuda	(Professor emeritus, University of Tsukuba)
	Shunpei	Morinobu	(Professor, Kyushu University)
	Kenji	Morita	(Professor, Nagoya University)
	Hiroshi	Nakahara	(Professor, Tokyo Metropolitan University)
	Masaharu	Nakazawa	(Professor, The University of Tokyo)
	Naoto	Sekimura	(Associate professor, The University of Tokyo)
	Akito	Takakahashi	(Professor, Osaka University)
	Hiroyuki	Tawara	(Professor, Institute of Plasma Physics, Nagoya University)
	Sadae	Yamaguchi	(Professor, The Research Institute for Ion Steel and Other Metals, Tohoku University)
	Hiroshi	Maekawa	(Deputy Director, Department of Reactor Engineering)
	Hiroshi	Ikezoe	(Head, Research Group for Exotic Heavy Nuclei, Advanced Science Research Center)
	Akira	Iwamoto	(Head, Research Group for Hadron Transport Theory)
	Akihiro	Iwase	(Head, Research Group for Low-temperature Radiation Effects, Advanced Science Research Center)
	Kiichi	Hojou	(Head, Solid State Physics Laboratory, Department of Materials Science and Engineering)
	Kenji	Noda	(Head, Material Innovation Laboratory, Department of Materials Science and Engineering)
	Toshiaki	Sekine	(Nuclear Chemistry Laboratory, Department of Chemistry and Fuel Research)
(Secretary)	Takashi	Okabe	(Administrative Manager, Department of Reactor Engineering)

(Secretary)   Suehiro   Takeuchi   (Department of Reactor Engineering)
(Secretary)   Tadashi   Yoshida   (Head, Accelerator Division)

8. Cooperative Researches

This is a blank page.

	Title	Contact person Organization
1.	Study on Decay Properties of Heavy Nuclei using JAERI Recoil Mass Separator	Jirota KASAGI Laboratory of Nuclear Science, Tohoku University
2.	Study of Electromagnetic Properties of Nuclear High-spin State through Crystal Ball (II)	Kohei FURUNO Tandem Accelerator Center, Tsukuba University
3.	Study of Multipole Deformed State in Heavy Nuclei	Hideshige KUSAKARI Faculty of Education Chiba University
4.	Nuclear Structure of Neutron-rich Nuclei through Deep Inelastic Collisions	Masao OGAWA Department of Energy Science, Tokyo Institute of Technology
5.	Dependence of Bimodal Fission on Excitation Energy	Hiromichi NAKAHARA Faculty of Science, Tokyo Metropolitan University
6.	Search for Large Nuclear Deformation near N=Z Region	Yasuyuki GONO Faculty of Science, Kyushu University
7.	α-cluster Structure in Heavy Nuclei	Takemi NAKAGAWA Faculty of Science, Tohoku University
8.	Correlation between Fragment Deformation and Mass Division Modes in Actinide Fission	Hiroshi BABA Faculty of Science, Osaka University

9. Study of Single-events Induced by   Sumio MATSUDA
   High Energy Ions   NASDA

10. High-energy Ion Beam Irradiation of   Takayuki TERAI
    Functional Electronic Materials   Engineering Research Institute,
                                          School of Engineering,
                                          University of Tokyo

11. Research of Coulomb Explosion by   Mititaka TERASAWA
    Heavy Ions Irradiation   Faculty of Engineering,
                                          Himeji Institute of Technology

12. Atomic Collision Research using   Ken-ichiro KOMAKI
    Highly Charged Ions   Graduate School of Arts and Science,
                                          University of Tokyo

13. Study of the Property and   Yukichi SASAKI
    Microstructure on the Oxide   Japan Fine Ceramics Center
    Superconductors Irradiated with High
    Energy Ions

14. Study of Luminescence   Chizuo MORI
    Characteristics of Photostimulable   School of Engineering,
    Phoser with Heavy Charged Particles   Nagoya University

国際単位系 (SI) と換算表

表1　SI基本単位および補助単位

量	名　称	記号
長　　さ	メ ー ト ル	m
質　　量	キ ロ グ ラ ム	kg
時　　間	秒	s
電　　流	ア ン ペ ア	A
熱力学温度	ケ ル ビ ン	K
物 質 量	モ ー ル	mol
光　　度	カ ン デ ラ	cd
平 面 角	ラ ジ ア ン	rad
立 体 角	ステラジアン	sr

表3　固有の名称をもつSI組立単位

量	名　称	記号	他のSI単位による表現
周 波 数	ヘ ル ツ	Hz	s^{-1}
力	ニ ュ ー ト ン	N	$m\cdot kg/s^2$
圧力，応力	パ ス カ ル	Pa	N/m^2
エネルギー,仕事,熱量	ジ ュ ー ル	J	$N\cdot m$
工率，放射束	ワ ッ ト	W	J/s
電気量，電荷	ク ー ロ ン	C	$A\cdot s$
電位,電圧,起電力	ボ ル ト	V	W/A
静 電 容 量	フ ァ ラ ド	F	C/V
電 気 抵 抗	オ ー ム	Ω	V/A
コンダクタンス	ジ ー メ ン ス	S	A/V
磁 束	ウ ェ ー バ	Wb	$V\cdot s$
磁 束 密 度	テ ス ラ	T	Wb/m^2
インダクタンス	ヘ ン リ ー	H	Wb/A
セルシウス温度	セルシウス度	℃	
光 束	ル ー メ ン	lm	$cd\cdot sr$
照 度	ル ク ス	lx	lm/m^2
放 射 能	ベ ク レ ル	Bq	s^{-1}
吸 収 線 量	グ レ イ	Gy	J/kg
線 量 当 量	シ ー ベ ル ト	Sv	J/kg

表2　SIと併用される単位

名　称	記　号
分，時，日	min, h, d
度，分，秒	°, ′, ″
リ ッ ト ル	l, L
ト ン	t
電 子 ボ ル ト	eV
原子質量単位	u

$1 \text{eV} = 1.60218 \times 10^{-19} \text{J}$

$1 \text{u} = 1.66054 \times 10^{-27} \text{kg}$

表4　SIと共に暫定的に維持される単位

名　称	記　号
オングストローム	Å
バ ー ン	b
バ ー ル	bar
ガ ル	Gal
キ ュ リ ー	Ci
レ ン ト ゲ ン	R
ラ ド	rad
レ ム	rem

$1 \text{Å} = 0.1 \text{nm} = 10^{-10} \text{m}$

$1 \text{b} = 100 \text{fm}^2 = 10^{-28} \text{m}^2$

$1 \text{bar} = 0.1 \text{MPa} = 10^5 \text{Pa}$

$1 \text{Gal} = 1 \text{cm/s}^2 = 10^{-2} \text{m/s}^2$

$1 \text{Ci} = 3.7 \times 10^{10} \text{Bq}$

$1 \text{R} = 2.58 \times 10^{-4} \text{C/kg}$

$1 \text{rad} = 1 \text{cGy} = 10^{-2} \text{Gy}$

$1 \text{rem} = 1 \text{cSv} = 10^{-2} \text{Sv}$

表5　SI接頭語

倍数	接頭語	記 号
10^{18}	エ ク サ	E
10^{15}	ペ タ	P
10^{12}	テ ラ	T
10^{9}	ギ ガ	G
10^{6}	メ ガ	M
10^{3}	キ ロ	k
10^{2}	ヘ ク ト	h
10^{1}	デ カ	da
10^{-1}	デ シ	d
10^{-2}	セ ン チ	c
10^{-3}	ミ リ	m
10^{-6}	マ イ ク ロ	μ
10^{-9}	ナ ノ	n
10^{-12}	ピ コ	p
10^{-15}	フ ェ ム ト	f
10^{-18}	ア ト	a

(注)

1. 表1－5は「国際単位系」第5版．国際度量衡局　1985年刊行による．ただし，1 eVおよび1 uの値はCODATAの1986年推奨値によった．
2. 表4には海里，ノット，アール，ヘクタールも含まれているが日常の単位なのでここでは省略した．
3. barは，JISでは流体の圧力を表わす場合に限り表2のカテゴリーに分類されている．
4. EC閣僚理事会指令ではbar，barnおよび「血圧の単位」mmHgを表2のカテゴリーに入れている．

換　算　表

力	N($=10^5$dyn)	kgf	lbf
	1	0.101972	0.224809
	9.80665	1	2.20462
	4.44822	0.453592	1

粘　度　$1 \text{Pa·s}(\text{N·s/m}^2) = 10 \text{P}(\text{ポアズ})(\text{g/(cm·s)})$

動粘度　$1 \text{m}^2/\text{s} = 10^4 \text{St}(\text{ストークス})(\text{cm}^2/\text{s})$

圧	MPa($=10$bar)	kgf/cm²	atm	mmHg(Torr)	lbf/in²(psi)
力	1	10.1972	9.86923	7.50062×10^3	145.038
	0.0980665	1	0.967841	735.559	14.2233
	0.101325	1.03323	1	760	14.6959
	1.33322×10^{-4}	1.35951×10^{-3}	1.31579×10^{-3}	1	1.93368×10^{-2}
	6.89476×10^{-3}	7.03070×10^{-2}	6.80460×10^{-2}	51.7149	1

エネルギー・仕事・熱量	J($=10^7$erg)	kgf·m	kW·h	cal(計量法)	Btu	ft·lbf	eV
	1	0.101972	2.77778×10^{-7}	0.238889	9.47813×10^{-4}	0.737562	6.24150×10^{18}
	9.80665	1	2.72407×10^{-6}	2.34270	9.29487×10^{-3}	7.23301	6.12082×10^{19}
	3.6×10^6	3.67098×10^5	1	8.59999×10^5	3412.13	2.65522×10^6	2.24694×10^{25}
	4.18605	0.426858	1.16279×10^{-6}	1	3.96759×10^{-3}	3.08747	2.61272×10^{19}
	1055.06	107.586	2.93072×10^{-4}	252.042	1	778.172	6.58515×10^{21}
	1.35582	0.138255	3.76616×10^{-7}	0.323890	1.28506×10^{-3}	1	8.46233×10^{18}
	1.60218×10^{-19}	1.63377×10^{-20}	4.45050×10^{-26}	3.82743×10^{-20}	1.51857×10^{-22}	1.18171×10^{-19}	1

$1 \text{cal} = 4.18605 \text{J}$ (計量法)

$= 4.184 \text{J}$ （熱化学）

$= 4.1855 \text{J}$ （15 ℃）

$= 4.1868 \text{J}$ （国際蒸気表）

仕事率　1 PS（仏馬力）

$= 75 \text{kgf·m/s}$

$= 735.499 \text{W}$

放射能	Bq	Ci
	1	2.70270×10^{-11}
	3.7×10^{10}	1

吸収線量	Gy	rad
	1	100
	0.01	1

照射線量	C/kg	R
	1	3876
	2.58×10^{-4}	1

線量当量	Sv	rem
	1	100
	0.01	1